

## ABSTRACT

Title of dissertation: PROBLEMS IN SELECTIVE MODAL  
ANALYSIS AND CONTROL

Mohamed S. Saad, Doctor of Philosophy, 2007

Dissertation directed by: Professor Eyad H. Abed  
Department of Electrical and Computer Engineering

In this dissertation, we develop monitoring and control systems for improving the performance of systems that are required to operate at the edge of their stability envelopes. The concept of modal participation factors, which is an essential construct in the theory of Selective Modal Analysis, is used extensively in this work. The basic definition of modal participation factors that was originally given for unforced linear time-invariant systems is revisited, and related notions of output participation factors and input-to-output participation factors are introduced, studied and applied to models of electrical power systems.

A signal-based approach for real-time detection of impending instability in nonlinear systems is considered. The main idea pursued involves using a small additive white Gaussian noise as a probe signal and monitoring the spectral density of one or more measured states or outputs for certain signatures of impending instability. Input-to-state and input-to-output participation factors are used as tools to aid in selection of locations for probe inputs and states or outputs to be mon-

itored, respectively. Since these participation factors are model-based, the work presented combines signal-based and model-based ideas toward achieving a robust methodology for instability monitoring. Case studies from power systems are used to illustrate the developed monitoring system, one of which involves the WSCC 3-generator, 9-bus network.

Feedback algorithms are developed for assigning modal participation factors in general linear time-invariant systems using eigenvector assignment-based techniques. The goal is to reduce the interaction between a selected group of states (the *high-value group*) and an undesirable mode (for example a *critical mode*, i.e., one corresponding to an eigenvalue or pair of eigenvalues approaching the imaginary axis in the complex plane). In particular, we address two cases, one in which the mode of interest corresponds to a real eigenvalue approaching zero, and the other in which the mode involves a complex conjugate pair of eigenvalues that may be approaching the imaginary axis. A novel procedure for computing the desired closed-loop right eigenvector(s) associated with the critical mode (based on given constraints on the desired closed-loop participation factors) is presented. An example from power systems is presented to demonstrate the effectiveness of the controller. The example used is the WSCC 3-generator, 9-bus network.

PROBLEMS IN SELECTIVE MODAL ANALYSIS AND  
CONTROL

by

Mohamed S. Saad

Dissertation submitted to the Faculty of the Graduate School of the  
University of Maryland, College Park in partial fulfillment  
of the requirements for the degree of  
Doctor of Philosophy  
2007

Advisory Committee:

Professor Eyad H. Abed, Chair/Advisor

Professor William S. Levine

Professor Gilmer L. Blankenship

Professor Amr Baz

Assistant Professor Richard J. La

© Copyright by  
MOHAMED S. SAAD  
2007

# DEDICATION

*To my parents, brothers*

*To my wife Maha and my kids Karim and Malak*

## ACKNOWLEDGMENTS

First and foremost I'd like to thank my advisor, Professor Eyad H. Abed for his endless support and advise throughout my graduate studies at the University of Maryland. He has been a great source of inspiration throughout the years.

I would also like to thank Professors William Levine, Gilmer Blankenship, Amr Baz and Richard La for agreeing to serve on my thesis committee and for sparing their invaluable time reviewing the manuscript.

I would like to thank Professor Andre Tits for the helpful discussions on my research. I would also like to thank Professor Robert Israel of the University of British Columbia for the help with my research questions. Thanks are due to Professor David Elliott for his advice on research. Thanks are also due to Dr. Monther Hasouneh for the great time we spent on discussing research and other general life topics.

I owe my deepest thanks to my family - my mother and father who have always stood by me, gave me endless patience and love and guided me through my career. Words cannot express the gratitude I owe them. Deep thanks are also due to my dear brothers Ahmed and Maged.

Special and deep thanks to my wife Maha. She has always been surrounding

me with care and love. I will never forget her nice encouraging words throughout the time of my PhD. Also, I would like to thank my lovely twins, Karim and Malak for the joy they have been filling my life with.

I am grateful to all my colleagues at the University of Maryland; Chao Wu, Amirali Sharifi, Maben Rabi, Nassir BenAmmar and Guojian Lin. I will never forget our nice discussions on every aspect of life.

I am also grateful to my close friends during this whole PhD journey; Mohamed Abdallah, Mohamed Zahran, Abdel-hameed Badawy, Ahmed Elsaid, Mostafa Arafa, Tarek Massoud and Mohamed Fahmi. I hope that our friendship will remain forever.

It is impossible to remember all, and I apologize to those I've inadvertently left out.

# Contents

<b>List of Tables</b>	<b>ix</b>
<b>List of Figures</b>	<b>xi</b>
<b>1 Introduction</b>	<b>1</b>
1.1 Thesis Outline . . . . .	10
<b>2 Mathematical Background</b>	<b>12</b>
2.1 Modal Participation Factors . . . . .	12
2.1.1 Conventional participation factors . . . . .	13
2.1.2 Generalized participation factors . . . . .	16
2.2 Bifurcation Theory . . . . .	18
2.2.1 Stationary bifurcation . . . . .	19
2.2.2 Hopf bifurcation . . . . .	22
2.3 Eigenstructure Assignment for Control System Design . . . . .	25
2.3.1 Eigenstructure assignment using state feedback . . . . .	26

<b>3</b>	<b>Output Participation Factors</b>	<b>32</b>
3.1	Introduction . . . . .	33
3.2	Output Participation Factors . . . . .	35
3.3	Input-to-Output Modal Participation Factors . . . . .	45
<b>4</b>	<b>Detecting Impending Instability in Nonlinear Systems</b>	<b>47</b>
4.1	Precursor-Based Monitoring . . . . .	48
4.1.1	Developed monitoring system . . . . .	49
4.1.2	Instability proximity index . . . . .	53
4.2	Power System Examples . . . . .	55
4.2.1	Single generator with dynamic load . . . . .	55
4.2.2	Single generator connected to an infinite bus . . . . .	57
4.2.3	Three-generator nine-bus power system . . . . .	63
<b>5</b>	<b>Participation Factor Assignment Using Eigenvector Assignment- Based Feedback Control</b>	<b>74</b>
5.1	Introduction . . . . .	75
5.2	Participation Factor Assignment: Case of Real Eigenvalue Approaching Zero . . . . .	77
5.2.1	Computing desired closed-loop right eigenvector $r^{i/d}$ . . . . .	78
5.2.2	Feedback control design: exactly assignable case . . . . .	80
5.2.3	Feedback control design: not exactly assignable case . . . . .	84

5.2.4	Feedback control design: “sacrificial” case . . . . .	85
5.3	Participation Factor Assignment: Case of Eigenvalue Pair Approaching Imaginary Axis . . . . .	90
5.3.1	Computing desired closed-loop right eigenvectors $\{r^{i'd}, r^{i+1'd} = r^{i'd*}\}$ . . . . .	91
5.3.2	Feedback control design: exactly assignable case . . . . .	95
5.3.3	Feedback control design: not exactly assignable case . . . . .	98
<b>6</b>	<b>Application to Electric Power Networks</b>	<b>101</b>
6.1	Introduction . . . . .	102
6.2	Three-Generator Nine-Bus Power System . . . . .	102
6.2.1	Feedback control design . . . . .	107
6.3	Remarks on Use of State Feedback in Power Networks . . . . .	112
<b>7</b>	<b>Conclusions and Future Directions</b>	<b>114</b>
7.1	Conclusions . . . . .	114
7.2	Future Directions . . . . .	116
<b>A</b>	<b>Proof of Propositions 5.1 and 5.2</b>	<b>118</b>
A.1	Proof of Proposition 5.1 . . . . .	118
A.2	Proof of Proposition 5.2 . . . . .	120
<b>B</b>	<b>Table of Symbols</b>	<b>122</b>



# List of Tables

4.1	Input-to-state participation factors and spectral peaks at $\omega_c$ . . . . .	60
4.2	Parameter values for the single generator connected to an infinite bus model. . . . .	61
4.3	Input-to-state participation factors and spectral peaks at $\omega_c \approx 7.8$ for the single generator connected to an infinite bus system. . . . .	63
4.4	Three-generator nine-bus power system: machine data. . . . .	68
4.5	Three-generator nine-bus power system: exciter data. . . . .	68
4.6	Input-to-state participation factors for the 3-machine nine-bus system (partial listing). The load at bus 5 is 4.4 pu. . . . .	68
4.7	Input-to-output participation factors for the 3-machine nine-bus system (partial listing). The load at bus 5 is 4.4 pu. . . . .	69
5.1	Closed-loop ratios $\{z_1, z_2\}$ for coefficient vectors $\{k^1, k^2, k_{cad}\}$ . The desired closed-loop ratios are $\{z_1^d = 1.2, z_2^d = 2.24\}$ . . . . .	100

6.1	The states with the highest norms of open-loop participation factors in the critical mode associated with $\lambda_{\{i,i+1\}} = -0.04602 \pm j2.1151$ . The load at bus 5 is 4.4 pu. . . . .	105
6.2	Closed-loop ratios $\{z_{13}, z_{23}\}$ for coefficient vectors $\{k^1, k^2, k_{cad}\}$ . The desired closed-loop ratios are $\{z_{13} = 2.92, z_{23} = 2.03\}$ . . . . .	108
6.3	The states with the highest norms of closed-loop participation factors in the critical mode associated with $\lambda_{\{i,i+1\}} = -0.04602 \pm j2.1151$ . The load at bus 5 is 4.4 pu. . . . .	109

# List of Figures

2.1	Transcritical bifurcation. . . . .	21
2.2	Pitchfork bifurcation. (a) supercritical, (b) subcritical . . . . .	22
2.3	Andronov-Hopf bifurcation. (a) supercritical, (b) subcritical . . . . .	24
3.1	Illustrating diagonal transformation $T$ in two dimensions, (a) Elliptic original uncertainty set $\Psi$ , (b) Rectangular original uncertainty set $\Psi$ .	43
4.1	Precursor-based instability monitor with external probe signal. . . . .	49
4.2	Power spectral densities of the states of the model given in (4.5)-(4.8). The bifurcation parameter was set to $Q_1 = 2.9$ . Band-limited AWGN of zero mean and $(0.001)^2$ power was added to $P_m$ . . . . .	58
4.3	Variation of the peak value of the power spectral density of $\omega$ as a function of the bifurcation parameter $Q_1$ . Band-limited AWGN of zero mean and $(0.001)^2$ power was added to $P_m$ . . . . .	59

4.4	Power spectral densities of the states of the single generator connected to an infinite bus system. The bifurcation parameter was set to $K_A = 185$ . Band-limited AWGN of zero mean and $(0.000032)^2$ power was added to $P_m$ . . . . .	64
4.5	Power spectral densities of the states of the single generator connected to an infinite bus system. The bifurcation parameter was set to $K_A = 185$ . Band-limited AWGN of zero mean and $(0.000032)^2$ power was added to $V_{ref}$ . . . . .	65
4.6	Variation of the peak value of the power spectral density of $V_R$ as a function of the bifurcation parameter $K_A$ . Band-limited AWGN of zero mean and $(0.000032)^2$ power was added to $P_m$ . . . . .	66
4.7	Plot of the inverse of the power spectral density index of $\omega$ versus the bifurcation parameter $K_A$ . The threshold value is equal to 5. . . . .	67
4.8	WSCC 3-machine, 9-bus system. . . . .	69
4.9	Power spectral densities of the states $E_{fd_1}$ , $E_{fd_2}$ and $E_{fd_3}$ . The load on bus 5 was used as a bifurcation parameter. The load value is 4.0 pu. Band-limited AWGN of zero mean and 0.05 power was added to $P_{m_3}$ , the mechanical power of generator number 3. . . . .	70

4.10	Power spectral densities of the states $E_{fd_1}$ , $E_{fd_2}$ and $E_{fd_3}$ . The load on bus 5 was used as a bifurcation parameter. The load value is 4.4 pu. Band-limited AWGN of zero mean and 0.05 power was added to $P_{m_3}$ , the mechanical power of generator number 3. . . . .	71
4.11	Power spectral density of $E_{fd_1}$ for three values of $P_{L_5}$ (the load on bus 5): $P_{L_5} = 4.0$ pu (dash-dotted line), $P_{L_5} = 4.25$ pu (dashed line) and $P_{L_5} = 4.4$ pu (solid line). Band-limited AWGN of zero mean and 0.05 power was added to $P_{m_3}$ , the mechanical power of generator number 3. . . . .	72
4.12	Power spectral densities of the state $E_{fd_1}$ and outputs $Q_{14}$ and $Q_{27}$ . The load on bus 5 was used as a bifurcation parameter. The load value is 4.4 pu. Band-limited AWGN of zero mean and 0.05 power was added to $P_{m_3}$ , the mechanical power of generator number 3. . . . .	73
6.1	Exciter for the three-generator, nine-bus system. . . . .	104
6.2	Open-loop response for a perturbation of 2% in the initial condition of the $q$ -axis transient voltage of generator 2 ( $e_{q_2}^0$ ) of the WSCC 3-gen., 9-bus power system. (a) $e'_{q_3}$ , (b) $e'_{q_2}$ and (c) $e'_{q_1}$ . . . . .	107
6.3	Plot of $q$ -axis transient voltage of generator 1 ( $e'_{q_1}$ ) versus time for a perturbation of 2% in the initial condition of the $q$ -axis transient voltage of generator 2 ( $e_{q_2}^0$ ) before and after control. . . . .	110

6.4	Plot of $q$ -axis transient voltage of generator 2 ( $e'_{q2}$ ) versus time for a perturbation of 2% in the initial condition of the $q$ -axis transient voltage of generator 2 ( $e'^0_{q2}$ ) before and after control. . . . .	111
6.5	Plot of $q$ -axis transient voltage of generator 3 ( $e'_{q3}$ ) versus time for a perturbation of 2% in the initial condition of the $q$ -axis transient voltage of generator 2 ( $e'^0_{q2}$ ) before and after control. . . . .	112

# Chapter 1

## Introduction

This dissertation focuses on development of monitoring and feedback control systems for managing the relative impact of certain critical modes on the states of a dynamical system. The work begins with a review of modal participation factors, which are quantities measuring the relative impact of a system mode in system states. Participation factors provide a convenient tool for determining which states should be monitored in order to detect that a critical mode is approaching the imaginary axis, which would lead to instability of the system. They can also be used to determine which inputs should be used in state feedback control to mitigate the effect of a critical mode on system states that may correspond to equipment that must be protected. We find that the conventional notion of participation factors is insufficient for monitoring and control when we have access not to system states, but to system output variables. This motivates us to introduce several new concepts extending the traditional notion of participation factors. These include output

participation factors and input-to-output participation factors. We use these new concepts to develop a signal-based approach for real-time detection of impending instability in nonlinear systems. The main idea pursued involves using a small additive white Gaussian noise as a probe signal and monitoring the spectral density of one or more measured states or outputs for certain signatures of impending instability. Input-to-state and input-to-output participation factors are used as tools to aid in selection of locations for probe inputs and states or outputs to be monitored. We also apply eigenstructure assignment techniques to develop procedures for assignment of participation factors. We provide examples from the field of electric power systems demonstrating the concepts introduced in this thesis, both for modal monitoring and control.

The conventional definition of participation factors was introduced in the framework of Selective Modal Analysis (SMA) in [2, 34]. SMA is a methodology for the modal analysis of linear time-invariant systems that emphasizes scale-independent notions that facilitate modal analysis, control design, and order reduction. The number of modes involved in a phenomenon of interest is usually only a small fraction of those appearing in the dynamics of a system, usually confined to a single mode. Participation factors are non-dimensional scalars that measure the interaction between modes and the state variables of a linear system. Since their introduction, participation factors have been used for stability analysis, order reduction, actuator placement and controller design in a variety of fields, especially

electric power systems [9, 10, 11]. Participation factors have recently also been used in coherency and clustering studies in electrical power systems [31, 32].

In [15], a new approach to defining modal participation factors for unforced systems was presented. This approach involves taking an average or a probabilistic expectation of a quantitative measure of relative modal participation. The average is performed with respect to all possible values of the initial state vector, assumed to be unknown but to lie in a known set or satisfy a known probability density. The definitions found in [15] were shown to reduce to the original definition of participation factors of [2, 34] if the uncertainty in the initial condition satisfies a symmetry condition.

There is a need to extend the participation factors definitions referred to above in several directions. Two extensions that are pursued in this thesis are output participation factors and input-to-output participation factors. The need for these extensions becomes apparent when we consider systems for which the states may not be readily available for measurement or as feedback signals, while other variables (namely certain system output variables) are readily available. In such cases, it is useful to have a criterion for determining which output signal carries the most information about a critical mode of interest. In some applications, for example, clustering in power system studies, participation of modes in variables that are not state variables (e.g., bus voltages) are needed.

The concept of participation of modes in output variables has not previously

been considered in the literature. Such a concept can be useful in many applications such as clustering studies and in stability monitoring and detection of closeness to instability. In clustering in power systems, for example, development of output participation factors will facilitate studies and understanding of intracluster oscillations (i.e., oscillations resulting from modes within the cluster) and intercluster oscillations (i.e., oscillations resulting from modes common to more than one cluster [31, 32]). It will be also useful for local and coordinated control design. For example, in control design to dampen intercluster oscillations, coordinated control (distributed control) must be used. While local controls guarantee stable operation within a cluster, poor choices of local controls might lead to instabilities caused by the coupled operations of the clusters.

Recently, Canizares and co-workers have proposed some extensions to the participation factors notions available in the literature, also targeting the incorporation of output variables in the definitions. In [35], a concept of “extended eigenvector” was introduced and used to identify the dominant output variable associated with a critical mode. In [36] an observability index was used to determine the preferred output signal for observing a critical mode. They have used their new definitions in a modal-based analysis technique for monitoring and control of electric power systems [35, 36].

The concept of “mode observability factor,” introduced by [26], has been used to determine the best output for either monitoring a mode, or possibly as a

good candidate feedback signal to control a mode of interest. In particular, the mode observability factor was used for determining the most suitable buses in a power system for placing static VAR compensators in order to dampen the critical modes of oscillation.

A drawback to using the definitions referred to above is that it is scale-dependent, i.e., for a change in the units of system outputs, the factors values will change. Another drawback to using these definitions is that they do not reduce to the conventional state participation factors when the output is simply a state variable.

The thesis then focuses on using the newly introduced concept of input-to-output participation factors and the concept of input-to-state participation factors given in [40] to develop a signal-based approach for real-time detection of impending instability in nonlinear systems with examples from power systems. Kim and Abed [25] developed monitoring systems for detecting impending instability in nonlinear systems that builds on Wiesenfeld's research on "noisy precursors of bifurcations". Wiesenfeld's research was originally introduced to characterize and employ the noise amplification properties of nonlinear systems near bifurcations of various types [37, 38]. Noisy precursors are features of the power spectral density (PSD) of a measured output of a system nearing instability that is excited by additive white Gaussian noise (AWGN). In [25], the noisy precursors concept was extended from systems operating at limit cycles to systems operating near equilibria, and

closed-loop monitoring systems were developed to facilitate use of noisy precursors in revealing impending loss of stability for such systems. It was shown in [25] that systems driven by white Gaussian noise and operating near an equilibrium point exhibit sharply growing peaks near certain frequencies as the system nears a bifurcation. In particular, it was shown that for stationary bifurcation where an eigenvalue passes through the origin (as in the case of pitchfork or transcritical bifurcation), the peak in the PSD occurs at zero frequency. Analogously, for the case of Hopf bifurcation (complex conjugate pair of eigenvalues crossing the imaginary axis transversely), the peak in the PSD occurs near  $\omega_c$ , the critical frequency of the Hopf bifurcation.

As noted by Hauer [19], the recurring problems of system oscillations and voltage collapse in power systems are due in part to system behavior not well captured by the models used in planning and operation studies. In the face of component failures, system models quickly become mismatched to the physical network, and are only accurate if they are updated using a powerful and accurate failure detection system. Therefore, it is important to employ nonparametric techniques for instability monitoring.

The use of probe signals is shown to help reveal an impending loss of stability. This is because probe signals propagate in the power system and give certain signatures near an instability that can be used as a warning signals for possible impending voltage collapse. Such warning signals are needed to alert system opera-

tors of a situation that may require preventive control, and to provide the operators with valuable additional time to take necessary preventive (rather than corrective) measures.

The focus of the thesis then shifts to addressing possible actions to be taken to counter the possible effects of the impending instability on the system. The need to carry such actions can be attributed to the fact that in many systems composed of smaller subsystems, it may be desirable to assign the magnitudes of participation factors corresponding to various subsystems to desired values. This would ensure that the energy corresponding to a critical mode minimally affects subsystems of high value, directing the energy of this mode to other, possibly purposefully introduced, subsystems of lesser value to the system operator. This idea is based on the fact that the higher the magnitude of participation factor, the higher the tendency of a subsystem to be affected in a serious way by an impending (or true) instability. Power systems are a good example for this discussion. In power systems operation, nuclear units, for example, are regarded as high-value subsystems. Reducing participation factors of these units in some critical mechanical mode would reduce the risk of premature tripping, as well as alleviate the effect on these units of a troublesome mode being excited.

The goal of the control effort will not be to alter the position of the eigenvalue(s) (associated with the critical mode), but rather to reduce the participation factors of a *high-value group* of states in that mode. This means that the closed-loop

eigenvalues will be kept the same as the open-loop ones. Similarly, all open-loop right eigenvectors will be kept unchanged except for those eigenvector(s) associated with the critical mode. This is possible using the freedom offered by state feedback in multivariable systems beyond closed-loop eigenvalue assignment [17]. Moreover, and as noted in the seminal paper of Moore [17], “One advantage of eigenstructure assignment is that you can still assign eigenvectors associated with uncontrollable eigenvalues.” This is important in participation factor assignment where it is desired that open-loop eigenvalues are kept unchanged.

A state feedback control system is given for assigning modal participation factors using eigenvector assignment-based techniques. The idea of using eigenvector assignment-based techniques to assign participation factors has not previously been addressed. Some work has addressed the problem of assigning right eigenvector(s) associated with a mode of interest (usually the critical mode). In [4], the author alerted the power systems community to the possible use of eigenvector assignment to make a target area participate highly in an unstable mode. This could be done by an unscrupulous provider of power to hurt the operation of a competing provider. In [13], a control scheme was proposed to assign eigenvalues and eigenvectors to improve system damping and dynamic behavior, respectively. Since right and left eigenstructure problems are strongly interdependent, assigning participation factors is not an easy task. Indeed, if the required objective is not exactly attainable, participation factor assignment may require solving an optimization problem for

achieving an objective as close as possible to the desired one.

Inspired by vibration absorbers in mechanical and civil engineering, in this work we desire to design controllers that reduce participation of certain, “high-value” system states in a particular mode at the expense of other “low-value” states. Those low-value states can be viewed as taking a role akin to that of vibration absorbers in mechanical systems. In power systems for instance, an isolated remote generator station or flywheel could be regarded as a vibration absorber that protects heavily loaded high-capacity generating stations. We will refer to the aforementioned problem as the participation factor assignment problem.

Reducing the participation factors of a high-value group of states in the critical mode implies that some other groups of states will be burdened with higher magnitudes of their participation factors in the critical mode. Deciding which group of states will be seen as “low-value” is based on system conditions and operator experience.

Control systems that assign participation factors should work in unison with monitoring systems that detect closeness to instability. The control becomes active when the monitoring system provides an alert that instability is near. The objective of participation factor assignment in this setting is as described above: to lessen the impact of a critical mode on high-value states by a trade with impact on low-value states.

## 1.1 Thesis Outline

The dissertation proceeds as follows. In Chapter 2, theoretical background material used throughout the thesis is collected. The topics include bifurcation theory, modal participation factors and eigenstructure assignment-based feedback control algorithms.

In Chapter 3, a study is given on extending the uncertain initial condition approach to defining state participation factors in [15] to facilitate finding a general measure of output participation. The new proposed definition has the desirable property that it reduces to the original state participation definition when the outputs are simply the system states. Also, this new definition is unit independent, i.e., the output participation factors do not depend on the units of system states or outputs. Another notion of modal participation is presented in this chapter. This new definition is one of input-output participation factors. It involves probe input signals as well as modes and outputs, and is applicable to a large set of systems.

In Chapter 4, a signal-based approach for real-time detection of impending instability in nonlinear systems is considered. The developed monitoring system is based on using a small additive white Gaussian noise as a probe signal and monitoring the spectral density of one or more measured states or outputs for certain signatures of impending instability. Input-to-output participation factors (introduced in Chapter 3), and input-to-state participation factors [40] (discussed in Chapter 2) are used as tools to aid in selection of locations for probe inputs and outputs or

states to be monitored. Examples from power systems are given to demonstrate the performance of the monitoring system.

In Chapter 5, state feedback control is presented for assigning modal participation factors for systems nearing instability using eigenvector assignment-based techniques. The focus is on assigning participation factors for state variables within a predefined group of state variables, where the group can be any subvector of the state vector, or could consist of all system states. A procedure for computing the desired closed-loop right eigenvector(s) (based on a given desired closed-loop participation factors) is given. Two cases are addressed, first the case of systems with a mode associated with a single real eigenvalue approaching zero, and second the case of systems with a mode associated with a pair of conjugate complex eigenvalues approaching the imaginary axis.

In Chapter 6, the results obtained in Chapter 5 are applied to a sample power system operating close to its stability limits. The considered power system is the WSCC 3-generator, 9-bus network. As expected, participation factor assignment has a clear effect on the relative time domain responses of system states.

Finally, we collect concluding remarks in Chapter 7, along with possible directions for future research. Some of the results reported in this thesis were published in a conference paper and a book chapter [22, 21].

## Chapter 2

# Mathematical Background

In this chapter, the theoretical and algorithmic background materials employed throughout this dissertation are reviewed. Section 2.1 focuses on modal participation factors, a basic construct in the theory of Selective Modal Analysis [2, 34]. In Section 2.2 a summary on bifurcation theory is provided, and various types of continuous-time local bifurcations are reviewed. In section 2.3, background material on eigenstructure assignment for control system design is reviewed.

## 2.1 Modal Participation Factors

In the theory of Selective Modal Analysis [2, 34], participation factors are non-dimensional scalars that measure the interaction between the modes and the state variables of a linear time-invariant system. The notion of participation factors provides a tool for modal participation analysis where an efficient method is required to single out a selected portion of the model related to the dynamics of interest. The

conventional definition of participation factors has been used as a tool for stability analysis, modal reduction, actuator placement and controller design in a variety of fields, especially electric power systems [9, 11, 10]. The number of modes involved in the phenomenon of interest is usually only a small fraction of those governing the dynamics of the system, mostly restricted to only one mode. Participation factors have also recently been used in coherency and clustering studies in electrical power systems [31, 32].

Another potential use of modal participation factors is in the area of stability monitoring of nonlinear systems close to instability. Such systems are also known to be close to a bifurcation in their dynamics. Input-to-state participation factors (given in [40]) and input-to-output participation factors (introduced in Chapter 3) will be employed in Chapter 4 to design stability monitoring systems for detecting impending instability in nonlinear systems.

### 2.1.1 Conventional participation factors

Consider a general continuous linear time-invariant system

$$\dot{x}(t) = Ax(t) \tag{2.1}$$

where  $x(t) \in \mathbb{R}^n$ , and  $A$  is a real  $(n \times n)$  matrix. Suppose that  $A$  has a set of  $n$  distinct eigenvalues  $\{\lambda_1, \lambda_2, \dots, \lambda_n\}$ . Let  $\{r^1, r^2, \dots, r^n\}$  be right eigenvectors of the matrix  $A$  associated with the eigenvalues  $\{\lambda_1, \lambda_2, \dots, \lambda_n\}$ , respectively. Let  $\{l^1, l^2, \dots, l^n\}$  denote left (row) eigenvectors of the matrix  $A$  associated with the

eigenvalues  $\{\lambda_1, \lambda_2, \dots, \lambda_n\}$ , respectively. The right and left eigenvectors are taken to satisfy the normalization

$$l^i r^j = \delta_{ij} \quad (2.2)$$

where  $\delta_{ij}$  is the Kronecker delta:

$$\delta_{ij} = \begin{cases} 1 & i = j \\ 0 & i \neq j \end{cases}$$

The participation factor of the  $i$ -th mode in the  $k$ -th state is defined to be the complex number [2, 34, 15]

$$p_{ki} := l_k^i r_k^i \quad (2.3)$$

This formula also gives the participation of the  $k$ -th state in the  $i$ -th mode. Participation factors is a measure of the relative participation of modes in states and the relative participation of states in modes. Since  $r_k^i$  measures the *activity* of  $x_k$  in the  $i$ -th mode and  $l_k^i$  *weighs* the contribution of this activity to the mode, the product  $p_{ki}$  measures the *net participation*.

### Properties of participation factors

The following properties of participation factors are recalled from [1, 3] and can be easily proved through appropriate consideration of the Definition in (2.3) and the normalization assumption in (2.2).

1. Participation factors are dimensionless quantities that are independent of the units in which state variables are measured.

2. In view of the eigenvector normalization (2.2), the sum of the participation factors associated with any mode ( $\sum_{i=1}^n p_{ki}$ ) or with any state variable ( $\sum_{k=1}^n p_{ki}$ ) is equal to 1.
3. The participation factor  $p_{ki}$  represents the sensitivity of the eigenvalue  $\lambda_i$  to the diagonal element  $a_{kk}$  of the state matrix  $A$

$$p_{ki} = \frac{\partial \lambda_i}{\partial a_{kk}}.$$

The solution to system dynamic equations in (2.1) for an initial condition  $x^0$  is given by:

$$x(t) = e^{At} x^0 \quad (2.4)$$

Since the state matrix  $A$  is assumed to have distinct eigenvalues, then  $A$  could be written in terms of right and left modal matrices as well as a diagonal matrix of its eigenvalues. Then  $x(t)$  in (2.4) is

$$x(t) = \sum_{i=1}^n (l^i x^0) e^{\lambda_i t} r^i \quad (2.5)$$

Now suppose the initial condition  $x^0$  is  $e^k$ , the unit vector along the  $k$ -th coordinate axis. Then the evolution of the  $k$ -th state becomes

$$x_k(t) = \sum_{i=1}^n (l_k^i r_k^i) e^{\lambda_i t} \quad (2.6)$$

$$= \sum_{i=1}^n p_{ki} e^{\lambda_i t}. \quad (2.7)$$

Equation (2.7) indicates that  $p_{ki}$  can be viewed as the relative participation of the  $i$ -th mode in the  $k$ -th state at time  $t = 0$ <sup>1</sup>.

### 2.1.2 Generalized participation factors

The concept of participation factors of modes in states and vice versa has been extended to linear time-invariant systems with inputs [40]

$$\dot{x}(t) = Ax(t) + Bu(t) \quad (2.8)$$

$$y(t) = Cx(t). \quad (2.9)$$

In [40], the case where the input is applied to one component, say the  $q$ -th component, of the right side of (2.8) and only one state, say the  $k$ -th state, is measured is considered. That is, in equations (2.8)-(2.9),  $B$  and  $C$  take the form

$$B = e^q = [0 \ \dots \ 0 \ \underbrace{1}_{q\text{-th}} \ 0 \ \dots \ 0]^T,$$

$$C = e^{kT} = [0 \ \dots \ 0 \ \underbrace{1}_{k\text{-th}} \ 0 \ \dots \ 0].$$

---

<sup>1</sup>In [15], a new approach to defining modal participation factors was presented. The new approach involved taking an average or a probabilistic expectation of a quantitative measure of relative modal participation over an uncertain initial state vector. The new definitions were shown to reduce to the original definition of participation factors of [2, 34] if the initial state obeys a symmetry condition.

With this choice of  $C$  and  $B$ , in steady state the output in (2.9) (in the frequency domain) is given by

$$\begin{aligned} y(s) = x_k(s) &= C(sI - A)^{-1}Bu \\ &= \sum_{i=1}^n \frac{Cr^i l^i B}{s - \lambda_i} u(s) \\ &= \sum_{i=1}^n \frac{r_k^i l_q^i}{s - \lambda_i} u(s) \end{aligned}$$

The generalized participation factor, *participation factor of mode  $i$  in state  $k$  when excitation is applied to state  $q$* , is defined as follows:

$$p_{qk}^i := \frac{r_k^i l_q^i}{\|H^k\|} \quad (2.10)$$

Here  $\|H^k\| := |r_k^i r_q^i|$  is the normalization factor where

$$(\tilde{k}, \tilde{q}) = \arg \max_{p,q} (|r_k^i l_q^i|)$$

attains maximum participation of norm 1. The above normalization makes the participation factors to be bounded by zero and one in amplitude and independent of system scaling. In [1], the quantity  $p_{qk}^i = r_k^i l_q^i$  is called a generalized participation. We will call this quantity the *input-to-state participation factor (ISPF)* for mode  $i$ , with measurement at state  $k$  and input applied to state  $q$ . The input-to-state participation factor (ISPF) will be employed in designing monitoring systems of impending instabilities in nonlinear systems in Chapter 4.

## 2.2 Bifurcation Theory

The term *bifurcation* is commonly used to describe a qualitative change in steady state behavior as the parameters on which the dynamical system depends are varied through certain values [6, 7, 5]. The parameter being varied is referred to as the bifurcation parameter. In other words, a bifurcation is a change in the number of candidate operating conditions of a nonlinear dynamical system that occurs as a parameter is quasi-statically varied. A value of the bifurcation parameter at which a bifurcation occurs is called a critical value of the bifurcation parameter. A nonlinear system operating at an equilibrium point undergoes a bifurcation when a quasistatic change in parameters causes the equilibrium to lose stability. Typically, new equilibria and/or limit cycles appear from the nominal equilibrium at a bifurcation. When these so-called bifurcated solutions are stable, the bifurcation is said to be supercritical or soft. When they are unstable, the bifurcation is said to be subcritical or hard. The implication of these concepts for operation of real systems is easy to describe (see [5] for a detailed exposition). For a subcritical bifurcation, the system trajectory escapes from a local neighborhood of the nominal equilibrium and can diverge to a distant (unacceptable) steady state. Therefore, detecting an impending subcritical bifurcation is highly desirable. For a supercritical bifurcation, on the other hand, the motion is likely to settle on the nearby bifurcated steady state, which is stable and does not represent a major departure from the nominal operation.

To fix ideas, consider a general one-parameter family of ordinary differential equation systems

$$\dot{x} = F_\mu(x, \mu) \tag{2.11}$$

where  $x \in \mathbb{R}^n$  is the system state,  $\mu \in \mathbb{R}$  denotes the bifurcation parameter, and  $F_\mu$  is smooth in  $x$  and  $\mu$ . For any value of  $\mu$ , the equilibrium points of (2.11) are given by the solutions for  $x$  of the algebraic equations  $F_\mu(x, \mu) = 0$ . Local bifurcations are those that occur in the vicinity of an equilibrium point. Local bifurcations of equilibrium points consist of stationary bifurcations and the Andronov-Hopf bifurcation (Hopf bifurcation for short). Stationary bifurcation is any bifurcation of one or more equilibrium points from a nominal equilibrium point. Saddle-node, transcritical, and pitchfork bifurcations are some examples of stationary bifurcation. Unlike the stationary bifurcation, in Hopf bifurcation a branch of periodic orbits bifurcates from an equilibrium point. Stationary and Hopf bifurcation of equilibrium points can be also categorized on the basis of the critical eigenvalues at the corresponding bifurcation points. Next, a brief summary of various types of continuous-time local bifurcations is given.

### 2.2.1 Stationary bifurcation

Stationary bifurcation occurs when a single real eigenvalue goes from being negative to being positive as the bifurcation parameter  $\mu$  passes through a critical value  $\mu_c$ . Precisely, the origin of (2.11) undergoes a stationary bifurcation at the critical

parameter value  $\mu = 0$  if assumptions, (L1), (L2) and (L3) hold.

**(L1)**  $F_\mu$  of system (2.11) is sufficiently smooth in  $x$ ,  $\mu$ , and  $F_\mu(0) = 0$  for all  $\mu$  in a neighborhood of 0 (i.e., 0 is an equilibrium for all values of  $\mu$  in the neighborhood);

**(L2)** The Jacobian  $A(\mu) := D_x F_\mu(0)$  possesses a simple real eigenvalue  $\lambda(\mu)$  such that at the critical parameter value  $\mu_c = 0$ ,  $\lambda(0) = 0$  and

$$\lambda'(0) := \left. \frac{\partial \lambda}{\partial \mu} \right|_{\mu=0} \neq 0;$$

**(L3)** All eigenvalues of the critical Jacobian  $A(0)$  besides 0 have negative real parts.

Under assumptions (L1), (L2) and (L3), two new equilibrium points of (2.11) emerge from the origin at  $\mu = 0$ . Bifurcation stability coefficients are quantities that determine the direction of bifurcation, and in particular the stability of the bifurcated solutions. Locally, the new equilibrium points occur for parameter values given by a smooth function of an auxiliary small parameter  $\epsilon$  ( $\epsilon$  can be positive or negative):

$$\mu(\epsilon) = \mu_1 \epsilon + \mu_2 \epsilon^2 + O(\epsilon^3) \tag{2.12}$$

One of the new equilibrium points occurs for  $\epsilon > 0$  and the other for  $\epsilon < 0$ . Also, the stability of the new equilibrium points is determined by the sign of an eigenvalue  $\beta(\epsilon)$  of the system linearization at the new equilibrium points. This eigenvalue is near 0 and is also given by a smooth function of the parameter  $\epsilon$ :

$$\beta(\epsilon) = \beta_1 \epsilon + \beta_2 \epsilon^2 + O(\epsilon^3) \tag{2.13}$$

Stability of the bifurcated equilibrium points is determined by the sign of  $\beta(\epsilon)$ . If  $\beta(\epsilon) < 0$  the corresponding equilibrium point is stable, while if  $\beta(\epsilon) > 0$  the equilibrium point is unstable. The coefficients  $\beta_i$ ,  $i = 1, 2, \dots$  in the expansion above are the bifurcation stability coefficients mentioned earlier, for the case of stationary bifurcation. The values of these coefficients determine the local nature of the bifurcation, as explained next.

Since  $\epsilon$  can be positive or negative, it follows that if  $\beta_1 \neq 0$  the bifurcation is neither subcritical nor supercritical. (This is equivalent to the condition  $\mu_1 \neq 0$ .) The bifurcation is therefore generically transcritical. Figure 2.1 shows the corresponding bifurcation diagram. If  $\beta_1 = 0$  and  $\beta_2 \neq 0$ , a stationary bifurcation is known as a *pitchfork bifurcation*. The pitchfork bifurcation is subcritical if  $\beta_2 > 0$ ; it is supercritical if  $\beta_2 < 0$ . Figure 2.2 shows the corresponding bifurcation diagram.

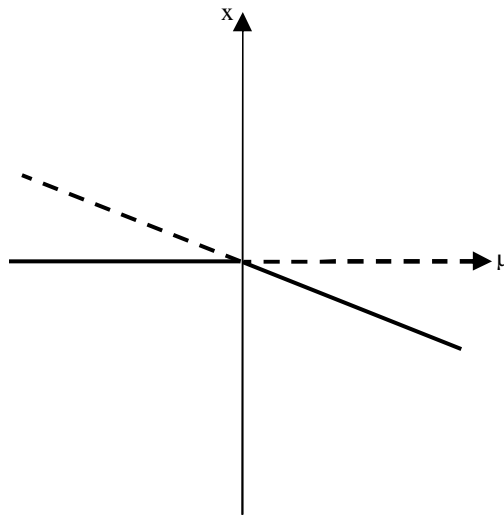


Figure 2.1: Transcritical bifurcation.

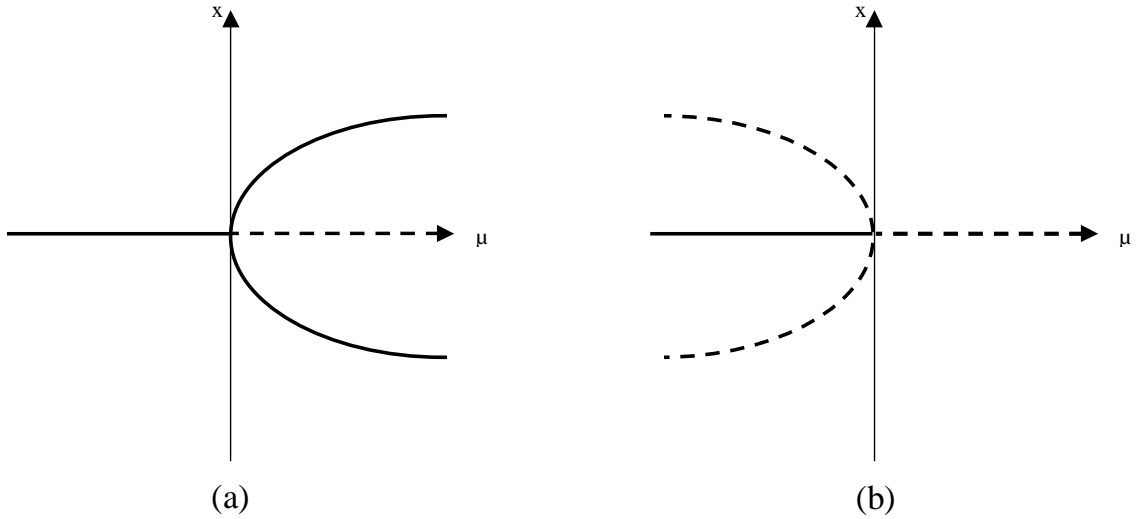


Figure 2.2: Pitchfork bifurcation. (a) supercritical, (b) subcritical

### 2.2.2 Hopf bifurcation

Suppose that the origin of (2.11) loses stability as the result of a complex conjugate pair of eigenvalues of  $A(\mu)$  crossing the imaginary axis. All other eigenvalues are assumed to remain stable, i.e., their real parts are negative for all values of  $\mu$ . Under this simple condition on the linearization of a nonlinear system, the nonlinear system typically undergoes a bifurcation. To be more precise, assume the following conditions are satisfied (the critical parameter value is taken to be  $\mu_c = 0$  without loss of generality).

**(H1)**  $F_\mu$  of system (2.11) is sufficiently smooth in  $x$ ,  $\mu$ , and  $F_\mu(0, \mu) = 0$  for all  $\mu$  in a neighborhood of 0. The Jacobian  $A(\mu)$  possesses a complex-conjugate pair of (algebraically) simple eigenvalues  $\lambda_{1,2}(\mu) = \alpha(\mu) \pm i\omega(\mu)$ , such that  $\alpha(0) = 0$ ,

$\alpha'(0) \neq 0$  and  $\omega_c := \omega(0) > 0$ .

**(H2)** All eigenvalues of the critical Jacobian  $A(0)$  besides  $\pm i\omega_c$  have negative real parts.

The Hopf Bifurcation theorem asserts that, under conditions (H1) and (H2), a small-amplitude non constant limit cycle (i.e., periodic solution) of (2.11) emerges from the origin at  $\mu = 0$ . Locally, the limit cycles occur for parameter values given by a smooth and even function of the amplitude  $\epsilon$  of the limit cycles:

$$\mu(\epsilon) = \mu_2\epsilon^2 + \mu_4\epsilon^4 + \dots \quad (2.14)$$

where the ellipsis denotes higher order terms. The stability of the limit cycle resulting from a Hopf bifurcation is determined by the sign of a particular characteristic exponent  $\beta(\epsilon)$ . This characteristic exponent is real and vanishes in the limit as the bifurcation point is approached. It is given by a smooth and even function of the amplitude  $\epsilon$  of the limit cycles:

$$\beta(\epsilon) = \beta_2\epsilon^2 + \beta_4\epsilon^4 + \dots \quad (2.15)$$

The coefficients  $\mu_2$  and  $\beta_2$  in the expansions above are related by the exchange of stability formula

$$\beta_2 = -2\alpha'(0)\mu_2.$$

Generically, these coefficients do not vanish. Their signs determine the direction of bifurcation. The coefficients  $\beta_2, \beta_4, \dots$  in the expansion (2.15) are the bifurcation

stability coefficients for the case of Hopf bifurcation. If  $\beta_2 > 0$ , then locally the bifurcated limit cycle is unstable and the bifurcation is subcritical. If  $\beta_2 < 0$ , then locally the bifurcated limit cycle is stable (more precisely, one says that it is orbitally asymptotically stable). This is the case of supercritical Hopf bifurcation. If it happens that  $\beta_2$  vanishes, then stability is determined by the first non vanishing bifurcation stability coefficient (if one exists). Figure 2.3 shows a typical Hopf-bifurcation diagram.

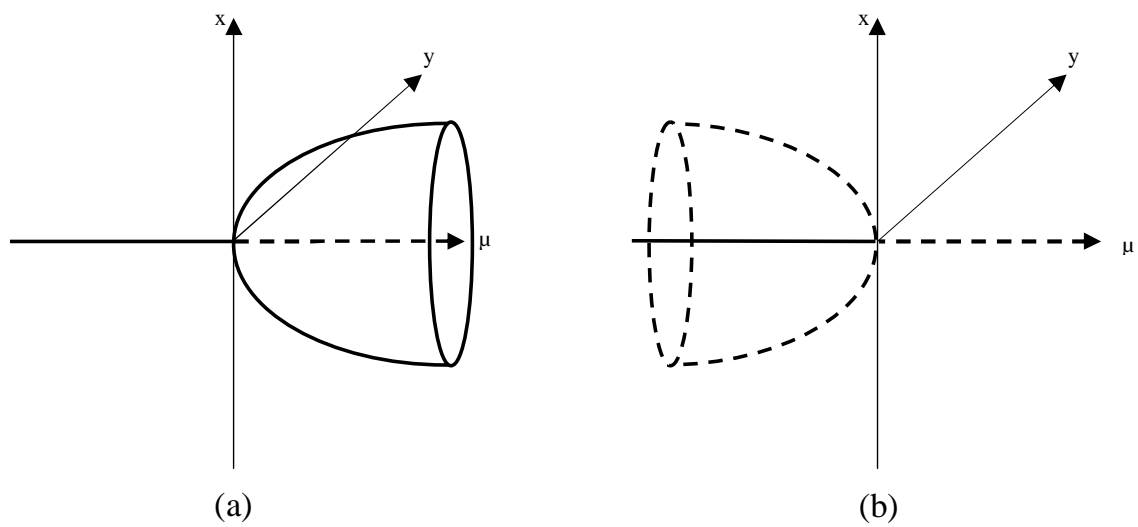


Figure 2.3: Andronov-Hopf bifurcation. (a) supercritical, (b) subcritical

## 2.3 Eigenstructure Assignment for Control System Design

Eigenstructure assignment problem is considered the general extension to the well known eigenvalue assignment problem [23, 17]. This general notion is attributed to the fact that, apart from the case of single-input single-output (SISO) systems, the specification of closed-loop eigenvalues does not uniquely define the feedback structure of a closed-loop system. The source of nonuniqueness can be identified as that coming from the freedom offered by state or output feedback in multi-input multi-output (MIMO) systems, beyond eigenvalue assignment, in selecting the associated eigenvectors and generalized eigenvectors from allowable spaces. Most of the work on eigenstructure assignment has been purely eigenvalue assignment (pole placement) up to late 60's. Later, Moore found that degrees of freedom are available over and above eigenvalue assignment using state feedback control for linear time-invariant multi-input multi-output (MIMO) systems [17]. Since then, numerous methods and algorithms have been developed to exercise those extra degrees of freedom to give the system some good performance characteristics. Good performance characteristics span the areas of low sensitivity, robust, multi-objective and fault detection [23]. In this section, background material on eigenstructure assignment that is needed in the dissertation is recalled.

### 2.3.1 Eigenstructure assignment using state feedback

Consider the closed-loop *LTI* system

$$\dot{x}(t) = (A + BF)x(t) \quad (2.16)$$

associated with an open-loop system

$$\dot{x}(t) = Ax(t) + Bu(t) \quad (2.17)$$

to which a state feedback  $u(t) = Fx(t)$  is applied. Here  $x(t) \in \mathbb{R}^n$ ;  $u(t) \in \mathbb{R}^m$ ;  $A \in \mathbb{R}^{(n \times n)}$ ;  $F \in \mathbb{R}^{(m \times n)}$ . For a given complex scalar  $\lambda$ , which may be viewed as a closed-loop eigenvalue, define the Hautus matrix [4]:

$$S_\lambda := \begin{bmatrix} (\lambda I - A) & B \end{bmatrix}, \quad S_\lambda \in \mathbb{C}^{n \times (n+m)}$$

Also define the matrix  $K_\lambda$ , with its row partitions along the same boundary as the partitions of columns in  $S_\lambda$ .  $K_\lambda$  is given by:

$$K_\lambda := \begin{bmatrix} N_\lambda \\ M_\lambda \end{bmatrix}, \quad K_\lambda \in \mathbb{C}^{(n+m) \times m}, \quad (2.18)$$

and is composed of columns that constitute a basis for null space (or kernel) of  $S_\lambda$ .

The matrix  $K_\lambda$  can be calculated by performing the singular value decomposition (SVD) or orthogonal triangular decomposition (OTD) on  $S_\lambda$  [23]. To compute  $K_\lambda$  through SVD, apply singular value decomposition to  $S_\lambda$  to yield:

$$S_\lambda = U\Sigma V^H, \quad (2.19)$$

where  $U$  is an  $(n \times n)$  unitary matrix over the field of complex numbers, the matrix  $\Sigma$  is  $(n \times (n + m))$  with nonnegative numbers (singular values of  $S_\lambda$ ) on the diagonal and zeros off the diagonal, and  $V^H$  denotes the conjugate transpose of  $V$ , an  $((n + m) \times (n + m))$  unitary matrix over the field of complex numbers. The matrix  $K_\lambda$  is given by the last  $m$  columns of the unitary matrix  $V$ . Knowing  $K_\lambda$  means that for any  $z \in \mathbb{C}^{(m+n)}$  such that

$$S_\lambda z = 0, \tag{2.20}$$

there exists a  $k \in \mathbb{C}^m$  such that

$$z = K_\lambda k. \tag{2.21}$$

It is clear that the columns of  $N_\lambda$  are linearly independent if  $B$  has linearly independent columns, and that  $N_{\lambda^*} = N_\lambda^*$ . It is known that  $F$  may be chosen to yield any self-conjugate set of closed-loop eigenvalues provided that the pair  $(A, B)$  is controllable, i.e.,

$$\text{rank } [B \ AB \ \dots \ A^{n-1}B] = n$$

Moore in [17] described the available freedom for assigning eigenvectors for an arbitrary self-conjugate set of eigenvalues using state feedback in the case  $m > 1$ . He gave both necessary and sufficient conditions for a state feedback to exist that achieves a desired set of eigenvalues and eigenvectors.

**Proposition 2.1** [17] *Consider  $\{ \lambda_1, \lambda_2, \dots, \lambda_n \}$  a set of self-conjugate distinct complex numbers, and a set of complex vectors  $\{v^1, v^2, \dots, v^n\}$ . There exists a matrix  $F$*

of real numbers such that  $\lambda_i v^i = (A + BF)v^i$  for all  $i \in \{1, 2, \dots, n\}$  if and only if the following three conditions are satisfied:

1. The vectors  $\{v^1, v^2, \dots, v^n\}$  form a linearly independent set within  $\mathbb{C}^n$  (over the field of complex scalars),
2.  $v^i = v^{j^*}$  whenever  $\lambda_i = \lambda_j^*$ , and
3.  $v^i \in \text{span} \{N_{\lambda_i}\}$ ,

where  $N_{\lambda_i}$  is defined as given in (2.18). Furthermore, if such a feedback gain matrix  $F$  exists and  $\text{rank } B = m$ , then  $F$  is unique.

A proof of this proposition, along with a procedure for computing the feedback gain matrix  $F$ , is given in [17]. Next, we recall Moore's procedure for computing the feedback gain matrix  $F$  [17].

## Computing feedback gain matrix $F$

Suppose that  $v^i$ ,  $i \in \{1, 2, \dots, n\}$  are chosen to satisfy the three conditions of Proposition 2.1. Since  $v^i \in \text{span} \{N_{\lambda_i}\}$  for  $i \in \{1, 2, \dots, n\}$ , then  $v^i$  can be expressed as

$$v^i = N_{\lambda_i} k^i. \tag{2.22}$$

for some vector  $k^i \in \mathbb{R}^m(\mathbb{C}^m)$  (based on whether  $\lambda_i$  is real (complex)), which implies that

$$\begin{bmatrix} (\lambda I - A) & B \end{bmatrix} \begin{bmatrix} v^i \\ M_{\lambda_i} k^i \end{bmatrix} = 0,$$

i.e.,

$$(\lambda_i I - A)v^i + BM_{\lambda_i}k^i = 0.$$

If  $F$  is chosen such that  $-M_{\lambda_i}k^i = Fv^i$ , then  $[\lambda_i I - (A + BF)]v^i = 0$ . Let

$$w^i = -M_{\lambda_i} k^i.$$

If all  $n$  eigenvalues are real numbers, then  $v^i$ ,  $w^i$  are vectors of real numbers. Also the first condition of Proposition 2.1 implies that the matrix  $[v^1 \ v^2 \ \dots \ v^n]$  is always nonsingular. For this case,

$$F = \begin{bmatrix} w^1 & w^2 & \dots & w^n \end{bmatrix} \begin{bmatrix} v^1 & v^2 & \dots & v^n \end{bmatrix}^{-1} \quad (2.23)$$

For the case where there are complex eigenvalues, assume that  $\lambda_1 = \lambda_2^*$ . The second condition of Proposition 2.1 states that  $v^1 = v^{2*}$  which implies that  $w^1 = w^{2*}$ . The equation which must be solved is then:

$$F \begin{bmatrix} v_R^1 + jv_I^1 & v_R^1 - jv_I^1 & V \end{bmatrix} = \begin{bmatrix} w_R^1 + jw_I^1 & w_R^1 - jw_I^1 & W \end{bmatrix} \quad (2.24)$$

where the columns of  $V$  and  $W$  are  $v^i$ ,  $i = 3, \dots, n$  and  $w^i$ ,  $i = 3, \dots, n$ , respectively.

Multiplying both sides of (2.24) from the right by the nonsingular matrix

$$\left[ \begin{array}{cc|c} \frac{1}{2} & -j\frac{1}{2} & 0 \\ \frac{1}{2} & +j\frac{1}{2} & \\ \hline & 0 & I \end{array} \right]$$

yields the equivalent equation

$$F \begin{bmatrix} v_R^1 & v_I^1 & V \end{bmatrix} = \begin{bmatrix} w_R^1 & w_I^1 & W \end{bmatrix}.$$

As  $v^i$ ,  $i \in \{1, 2, \dots, n\}$  are independent, the columns of  $[v_R^1 \ v_I^1 \ V]$  are linearly independent. Then  $F$  is given by:

$$F = \begin{bmatrix} w_R^1 & w_I^1 & W \end{bmatrix} \begin{bmatrix} v_R^1 & v_I^1 & V \end{bmatrix}^{-1}. \quad (2.25)$$

The third condition of Proposition 2.1 implies that the eigenvector  $v^i$  must be in the subspace spanned by the columns of  $N_{\lambda_i}$ . This subspace is of dimension  $m$  which is equal to the rank of  $B$ , or equivalently the number of independent control variables. Therefore, the number of control variables available determines how large (dimension) the subspace in which achievable eigenvectors must reside. The orientation of the subspace is determined by the open-loop quantities  $A$ ,  $B$  and the desired closed-loop eigenvalue  $\lambda_i$ . In general, however, a desired eigenvector  $v^{id}$  will not reside in the prescribed subspace and hence cannot be achieved. Instead a “best possible” choice for an achievable eigenvector is made. Next, we recall the analysis to compute the best possible achievable eigenvector  $v^{ia}$  associated with a desired eigenvector  $v^{id}$  [8].

### “Best possible $v^{i^a}$ ”

This best possible achievable eigenvector  $v^{i^a}$  is the projection of  $v^{i^d}$  onto the subspace spanned by the columns of  $N_{\lambda_i}$ . To compute  $v^{i^a}$  associated with a real eigenvalue  $\lambda_i$ , recall from (2.22) that

$$v^{i^a} = N_{\lambda_i} k^i; \quad k^i \in \mathbb{R}^m.$$

To find the value of  $k^i$  corresponding to the projection of  $v^{i^d}$  onto the “achievable subspace,”  $k^i$  is chosen to minimize

$$J = \|v^{i^d} - v^{i^a}\|^2 = \|v^{i^d} - N_{\lambda_i} k^i\|^2.$$

Now

$$dJ/dk^i = 2 N_{\lambda_i}^T (N_{\lambda_i} k^i - v^{i^d}).$$

Hence  $dJ/dk^i = 0$  implies

$$k^i = (N_{\lambda_i}^T N_{\lambda_i})^{-1} N_{\lambda_i}^T v^{i^d} \tag{2.26}$$

$$v^{i^a} = N_{\lambda_i} (N_{\lambda_i}^T N_{\lambda_i})^{-1} N_{\lambda_i}^T v^{i^d}. \tag{2.27}$$

For complex eigenvalues/eigenvectors the presentation above is formally correct with minor arithmetic adjustments to accommodate complex quantities [17].

## Chapter 3

# Output Participation Factors

In this chapter, the basic definition of modal participation factors that was originally given for LTI systems without input or output signals [2, 34] is revisited, along with an extension proposed in [15], and then several new extensions are proposed. The first such extension is a concept of output participation factors that measure the participation of modes in output variables that are not necessarily system states. The definition is based on computing an average relative contribution of a mode in an output relative to uncertainty in the system initial condition. This follows the approach proposed in [15] for defining state participation factors. The new definition proposed here has the desirable property that it reduces to the original state participation definition when the outputs are simply the system states. Also, this new definition is unit independent, i.e., the output participation factors do not depend on the units of system states or outputs. It is also found that the proposed output participation factors depend on the set to which the uncertain

initial condition belongs.

Another notion of modal participation is presented in this chapter. This new definition is one of input-output participation factors. It involves probe input signals as well as modes and outputs, and is applicable to a large set of systems. This chapter proceeds as follows. In Section 3.1, we recall the work of [15] on defining participation factors using averaging over an uncertain initial condition. In Section 3.2, development of a notion of output participation factors is presented. In Section 3.3, input-to-output participation factors are introduced and studied.

### 3.1 Introduction

Consider a continuous linear time-invariant system described as given in (2.1). The system solution for a general initial condition  $x^0$  (given in (2.5)), and the solution for the particular initial condition  $x^0 = e^k$  (given in (2.7)) are repeated here for convenience:

$$\dot{x}(t) = Ax(t) \tag{3.1}$$

$$x(t) = \sum_{i=1}^n (l^i x^0) e^{\lambda_i t} r^i \tag{3.2}$$

$$\begin{aligned} x(t) &= \sum_{i=1}^n (l_k^i r_k^i) e^{\lambda_i t} \\ &= \sum_{i=1}^n p_{ki} e^{\lambda_i t}. \end{aligned} \tag{3.3}$$

Abed et al. [15] redefined the participation factors concept of Verghese et al. [2, 34] by considering the effect of uncertainty in the initial condition  $x^0$ . The reconsideration of modal participation in this light was motivated by the following simple observations for the linear system (3.1) and its solution (3.2): If the initial condition  $x^0$  lies along the  $i$ -th eigenvector, then the only mode that participates in the evolution of any state is the  $i$ -th mode. On the other hand, if the initial condition lies along the  $k$ -th coordinate axis, then the evolution of the  $k$ -th state involves all system modes according to (3.3). Clearly, then, the degree to which a mode participates in a state depends on the initial condition. The authors proposed a new definition for state participation factors that reduces to the original definition of participation factors of [2, 34] if the initial condition  $x^0$  is taken to lie in a connected set  $\Psi$  containing the origin and obeys a symmetry condition defined as follows:

**Definition 3.1.** ([15]) The set  $\Psi$  is symmetric with respect to each of the hyperplanes  $x_k = 0$ ,  $k = 1, 2, \dots, n$  if and only if for any  $k \in \{1, \dots, n\}$  and  $z = (z_1, \dots, z_k, \dots, z_n) \in \mathbb{R}^n$ ,  $z \in \Psi$  implies that  $(z_1, \dots, -z_k, \dots, z_n) \in \Psi$ .

The symmetry assumption in Definition 3.1 is reasonable for typical engineering system models although some applications might have restrictions on initial conditions.

The definition of state participation factors proposed in [15] is:

**Definition 3.2.** ([15]) The participation factor for the mode associated with  $\lambda_i$  in

state  $x_k$  with respect to an uncertainty set  $\Psi$  is

$$p_{ki} := \operatorname{avg}_{x^0 \in \Psi} \left\{ \frac{(l^i x^0) r_k^i}{x_k^0} \right\} \quad (3.4)$$

whenever this quantity exists.

Here,  $\operatorname{avg}_{x^0 \in \Psi}$  is an operator that computes the average of a function over the set  $\Psi$ . This quantity measures the *average relative contribution* at time  $t = 0$  of the  $i$ -th mode to state  $x_k$ . In the definition, the  $i$ -th mode is interpreted as the  $e^{\lambda_i t}$  term in (3.2). Also, the denominator on the right-hand side of (3.4) is simply the sum of the contributions of all system modes to  $x_k(t)$  at  $t = 0$ :

$$x_k^0 = \sum_{j=1}^n (l^j x^0) r_k^j. \quad (3.5)$$

In the next section, we consider the natural extension of the definition above to a concept of participation of modes in outputs. The effect of uncertainty in the initial condition  $x^0$  is incorporated in a way similar to that used in [15] for calculation of state participation factors.

## 3.2 Output Participation Factors

Consider a continuous linear time-invariant system with outputs

$$\dot{x}(t) = Ax(t) \quad (3.6)$$

$$y(t) = Cx(t) \quad (3.7)$$

where  $x \in \mathbb{R}^n$ ,  $y \in \mathbb{R}^m$ ,  $A$  is a real  $n \times n$  system matrix and  $C$  is a real  $m \times n$  output matrix. Using the solution for  $x(t)$  in (3.2), the output vector is given by

$$y(t) = C \sum_{i=1}^n (l^i x^0) e^{\lambda_i t} r^i \quad (3.8)$$

The evolution of the  $k$ -th output variable  $y_k$  is given by

$$y_k(t) = C^k \sum_{i=1}^n (l^i x^0) e^{\lambda_i t} r^i \quad (3.9)$$

where  $C^k$  is the  $k$ -th row of  $C$ . It may be tempting to say that the participation of the  $i$ -th mode in the  $k$ -th output is equal to the  $k$ -th row of  $C$  multiplied by the state participation factors, i.e., the sum of the participation of the  $i$ -th mode in all states weighted by the elements of the  $k$ -th row of  $C$ :

$$p_{ik}^y = \sum_{j=1}^n C_j^k p_{ji} \quad (3.10)$$

This temptation is supported by the fact that the expression in (3.10) reduces to the participation of state  $k$  in mode  $i$  when  $C^k = e^k$  (the  $k$ -th unit vector). However, this would lead to a notion that is unit-dependent and hence unacceptable from the point of view of this dissertation.

Next, we give a high-level definition that is the natural extension of the state participation factors definition in [15] to the case of participation of modes in outputs. It is easily verified that this definition is independent of units. Below, the concept is reduced to a simple calculation for systems with initial condition uncertainty known to lie in an  $n$ -ellipsoid or  $n$ -rectangle with main axes parallel to the coordinate axes.

**Definition 3.3.** The participation factor for the mode associated with  $\lambda_i$  in output  $y_k$  with respect to an uncertainty set  $\Psi$  is

$$p_{ik}^y := \operatorname{avg}_{x^0 \in \Psi} \left\{ \frac{(l^i x^0)(C^k r^i)}{y_k^0} \right\} \quad (3.11)$$

whenever this quantity exists.

Here, the expression  $\operatorname{avg}_{x^0 \in \Psi}$  denotes the operator that computes the average of a function over the set  $\Psi$ .

Note that in computing the implied multidimensional volume integral, the argument function is undefined for  $y_k^0 = 0$ , i.e., undefined for  $x^0 \in \{x : C^k x = 0\}$  and the Cauchy principal value of the integral is to be used. The quantity on the right-hand side of Definition 3.3 measures the *average relative contribution* at time  $t = 0$  of the  $i$ -th mode to output  $y_k$ . The denominator of this quantity is simply the sum of the contributions of all modes to  $y_k(t)$  at  $t = 0$ :

$$\begin{aligned} y_k^0 &= \sum_{j=1}^n (l^j x^0) C^k r^j \\ &= C^k x^0. \end{aligned}$$

Writing  $l^i = l_{C^k}^i + l_{C^k}^{i\perp}$ , where  $l_{C^k}^i$  is the projection of  $l^i$  in the direction of  $C^k$  and  $l_{C^k}^{i\perp}$  is the projection of  $l^i$  in the direction orthogonal to  $C^k$ , the expression in (3.11) becomes

$$\begin{aligned} p_{ik}^y &= C^k r^i \operatorname{avg}_{x^0 \in \Psi} \left\{ \frac{(l_{C^k}^i + l_{C^k}^{i\perp}) x^0}{C^k x^0} \right\} \\ &= C^k r^i \operatorname{avg}_{x^0 \in \Psi} \left\{ \frac{l_{C^k}^i x^0}{C^k x^0} + \frac{l_{C^k}^{i\perp} x^0}{C^k x^0} \right\} \end{aligned} \quad (3.12)$$

Writing  $l_{C^k}^i$  in terms of  $l^i$  and  $C^k$ ,

$$\begin{aligned} l_{C^k}^i &= \|l^i\| \cdot \left\{ \frac{l^i C^{kT}}{\|l^i\| \|C^k\|} \right\} \cdot \left\{ \frac{C^k}{\|C^k\|} \right\} \\ &= \left\{ \frac{l^i C^{kT}}{\|C^k\|^2} \right\} \cdot C^k \end{aligned} \quad (3.13)$$

Using (3.13),  $p_{ik}^y$  reduces to

$$\begin{aligned} p_{ik}^y &= C^k r^i \operatorname{avg}_{x^0 \in \Psi} \left\{ \frac{l^i C^{kT}}{\|C^k\|^2} + \frac{l_{C^k}^i x^0}{C^k x^0} \right\} \\ &= \frac{C^k r^i l^i C^{kT}}{\|C^k\|^2} + C^k r^i \operatorname{avg}_{x^0 \in \Psi} \left\{ \frac{l_{C^k}^i x^0}{C^k x^0} \right\} \end{aligned}$$

Let

$$\operatorname{Vol}(\Psi) := \int_{x^0 \in \Psi} dx^0 \quad (3.14)$$

denote the volume of the set  $\Psi$ . The expression on the right-hand side of (3.11) is

$$p_{ik}^y = \frac{C^k r^i l^i C^{kT}}{\|C^k\|^2} + C^k r^i \int_{x^0 \in \Psi} \left\{ \frac{l_{C^k}^i x^0}{C^k x^0} \right\} dx^0 / \operatorname{Vol}(\Psi) \quad (3.15)$$

The orthogonal vectors  $l_{C^k}^i$  and  $C^k$  operate on the initial state vector  $x^0 \in \Psi$  to orthogonally transform it to another set  $\Psi'$ . Generally, even if the set  $\Psi$  is symmetric according to Definition 3.1, the new set  $\Psi'$  is not symmetric with respect to the axes  $x_i^0 = 0$ ,  $i \in \{1, 2, \dots, n\}$ , and the integral term doesn't vanish. Note that in the case where output  $y_k$  is simply the  $k$ -th state (i.e.,  $C^k = e^k$ ), the integral term on the right hand side of (3.15) vanishes. This follows from the observation that the integral term reduces to

$$g \cdot \int_{x^0 \in \Psi} \left\{ \frac{x_j^0}{x_k^0} \right\} dx^0$$

for some  $j \neq k$  and a constant  $g = C^k r^i / \text{Vol}(\Psi)$ . Because  $\Psi$  is symmetric according to Definition 3.1,

$$\int_{x^0 \in \Psi} \left\{ \frac{x_j^0}{x_k^0} \right\} dx^0 = 0$$

where the integral is interpreted in the sense of the Cauchy principal value. The expression in (3.11) is dimensionless, i.e., it does not depend on the units in which state variables are measured or the unit in which the output variable is measured. Also, its simplification (3.15) reduces to the conventional state participation factors when the output is simply a state variable. Thus, it can be used to provide a good measure of the mode that has the highest participation in an output when it is reasonable to assume uncertainty in the system's initial conditions. Also note that the definition in its current form is dependent on the set  $\Psi$  to which  $x^0$  belongs.

Suppose that the initial condition uncertainty set  $\Psi$  is known to be symmetric according to Definition 3.1. This is not enough to ensure that the integral term in (3.15) vanishes. However, this integral vanishes if the initial condition uncertainty set is an  $n$ -cube or an  $n$ -sphere. For instance, the initial state  $z^0$  lies in an  $n$ -sphere if  $\|z^0\| \leq c_0$  where  $c_0$  is a positive constant. Therefore, suppose the initial condition uncertainty set is an  $n$ -ellipsoid or  $n$ -rectangle with main axes parallel to the coordinate axes. Next, consider a change in units ( $x' = Tx$ ),  $T$  is a positive diagonal matrix, such that in the new coordinates the state initial condition  $x'^0$  lies either in an  $n$ -cube or an  $n$ -sphere. In this case, the integral term vanishes (a proof

is given below) and the expression in (3.15) reduces to

$$p_{ik}^y = \frac{C'^k r'^i l^i C'^k T}{\|C'^k\|^2}, \quad (3.16)$$

where

$$C'^k = C^k T^{-1}, \quad r'^i = T r^i \quad \text{and} \quad l'^i = l^i T^{-1}.$$

**Proof:**

Let  $x'^0 = Q z^0$ , where  $Q$  is an  $(n \times n)$  orthonormal matrix, i.e.,

$$Q^{-1} Q^T = I$$

The orthonormal similarity transformation matrix  $Q$  can be written as

$$Q = \begin{bmatrix} \hat{C}'^k \\ Q_1 \end{bmatrix}^T$$

where

$$\hat{C}'^k = \frac{C'^k}{\|C'^k\|},$$

and  $Q_1$  is chosen such that  $C'^k Q_1^T = 0$ . Note that  $\|x'^0\| = \|z^0\|$ ,  $dx'^0 = dz^0$ . Using

the orthonormal similarity transformation  $Q$ , the integral term in (3.15) becomes

$$\begin{aligned} \int_{x'^0 \leq c_0} \left\{ \frac{l'^{i\perp}}{C'^k} \frac{x'^0}{x'^0} \right\} dx'^0 &= \int_{z^0 \leq c_0} \left\{ \frac{l'^{i\perp}}{C'^k} \frac{Q z^0}{Q z^0} \right\} dz^0 \\ &= \int_{z^0 \leq c_0} \left\{ \frac{l'^{i\perp} (\hat{C}'^k)^T z_1^0 + l'^{i\perp} Q_1^T z^{0'}}{C'^k (\hat{C}'^k)^T z_1^0} \right\} dz^0 \\ &= \int_{z^0 \leq c_0} \left\{ \frac{l'^{i\perp} Q_1^T z^{0'}}{C'^k (\hat{C}'^k)^T z_1^0} \right\} dz^0 \\ &= 0, \end{aligned} \quad (3.17)$$

where  $z^0 = [z_1^0 \ z^0]^T$ . The last step in (3.17) follows from the observation that for any  $j \neq 1$ ,

$$\int_{z^0 \leq c_0} \left\{ \frac{z_j^0}{z_1^0} \right\} dz^0 = 0,$$

where the integral above is interpreted in the sense of Cauchy principal value. ■

Eq. (3.16) is taken as the definition of output participation factors, and *is applied to the transformed system in which the initial condition uncertainty set is an  $n$ -cube or  $n$ -sphere.*

The expression in (3.16) is crucial for computing the value of the high-level definition of output participation factors given in Definition 3.3. This value (that depends on the  $n$ -ellipsoid or  $n$ -rectangle set  $\Psi$  with main axes parallel to the coordinate axes) is equal to the value of the definition of output participation factors in (3.16) when a diagonal transformation (equivalent to a change in units of system states) is performed to transfer the set  $\Psi$  into an  $n$ -cube or an  $n$ -sphere.

Next, we summarize the properties of output participation factors (defined in (3.16)). These properties can be easily proved through appropriate consideration of Definition 3.3 and Eq. (3.16).

### **Properties of output participation factors**

1. The value of the high-level definition of output participation factors given in Definition 3.3, and which is a function of  $A$ ,  $C$  and the set  $\Psi$ , is equal to the value of the definition of output participation factors given in (3.16) evaluated

for  $\hat{A}$  and  $\hat{C}$ , where

$$\hat{A} = TAT^{-1}$$

$$\hat{C} = CT^{-1},$$

where  $T$  is the diagonal transformation matrix required to transform the symmetric  $n$ -ellipsoid or  $n$ -rectangle set  $\Psi$  into a an  $n$ -cube or an  $n$ -sphere. Figure 3.1 depicts such a diagonal transformation  $T$  for the case of a two-dimensional system.

2. The sum of output participation factors associated with any mode is equal to 1, i.e.,

$$\sum_{i=1}^n \frac{C^k_r i^i C^k T}{\|C^k\|^2} = 1$$

3. The output participation factors are dimensionless quantities that are independent of the units in which state and/or output variables are measured.

Next, a numerical example is presented to show that the values of the output participation factors computed according to the expression in (3.10) do not agree with the values of output participation factors (defined in (3.16)).

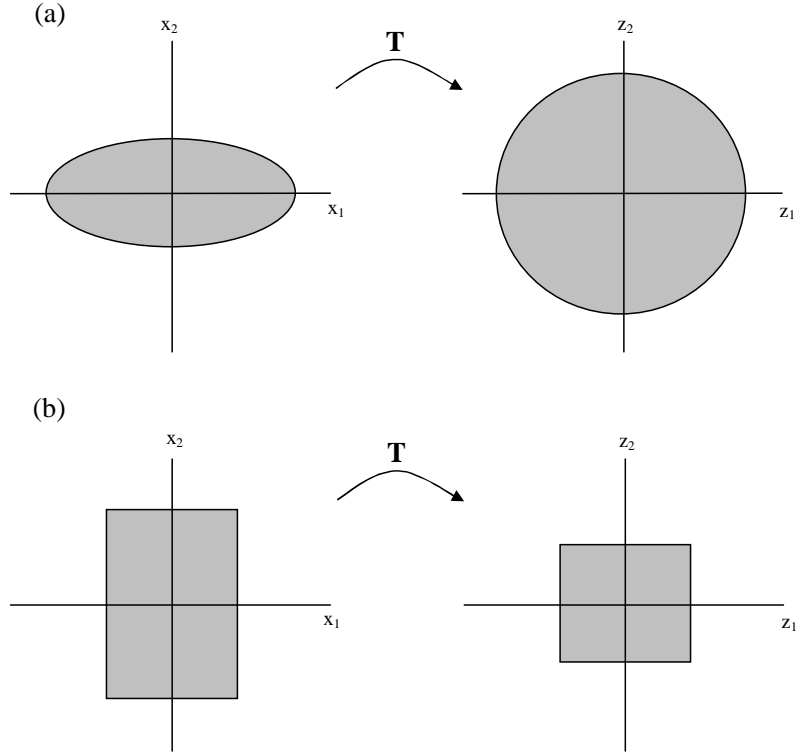


Figure 3.1: Illustrating diagonal transformation  $T$  in two dimensions, (a) Elliptic original uncertainty set  $\Psi$ , (b) Rectangular original uncertainty set  $\Psi$ .

### Numerical example

Consider an LTI system given by (3.6)–(3.7) with

$$A = \begin{pmatrix} 0 & 1 & 0 \\ -1.5 & -0.5 & 1.225 \\ -0.433 & 0 & 0 \end{pmatrix} \text{ and } C = \begin{pmatrix} 0 & 1 & 1 \\ 0 & 2 & 1 \end{pmatrix}$$

The initial conditions of this system are uncertain and lie in a set  $\Psi$ . We assume that  $\Psi$  is an  $n$ -sphere of radius  $c_0$ , i.e.,  $\|x^0\| \leq c_0$  ( $c_0$  is a positive constant). Thus, no transformation is required and the output participation factors can be computed using  $A$  and  $C$  according to the definition in (3.16). The eigenvalues of  $A$  are

$\lambda_{1,2} = -0.0672 \pm j1.2026$ ,  $\lambda_3 = -0.3655$ . We are interested in the participation of the critical mode (corresponding to the complex conjugate pair of eigenvalues  $\lambda_{1,2}$ ) in the states and in the outputs. Right and left eigenvectors corresponding to  $\lambda_1$  that satisfy the normalization condition (2.2) are, respectively,

$$\begin{aligned} r^1 &= \begin{bmatrix} -0.0348 - j0.6216 & 0.7499 & 0.2224 - j0.0249 \end{bmatrix}^T \\ l^1 &= \begin{bmatrix} -0.0078 + j0.8297 & 0.6087 + j0.2255 & 0.1944 - j0.6308 \end{bmatrix}. \end{aligned}$$

The participations of mode 1 in states  $x_i$ ,  $i = 1, 2, 3$  are  $p_{11} = 0.5160 - j0.0240$  ( $|p_{11}| = 0.5166$ ),  $p_{21} = 0.4565 + j0.1691$  ( $|p_{21}| = 0.4868$ ) and  $p_{31} = 0.0275 - j0.1451$  ( $|p_{31}| = 0.1477$ ). The participation of mode 1 in the outputs  $y_1$  and  $y_2$  can be calculated using (3.16):  $p_{11}^y = 0.3854 - j0.2071$  ( $|p_{11}^y| = 0.4375$ ) and  $p_{21}^y = 0.4854 - j0.0690$  ( $|p_{21}^y| = 0.4903$ ). A simple calculation shows that participation of mode 1 in either output is not the weighted sum of the state participations (as suggested by the expression given in (3.10)). Next, we present another notion of modal participation factors. This new definition is one of input-to-output participation factors. It involves probe input signals as well as modes and outputs, and is applicable to a large set of systems.

### 3.3 Input-to-Output Modal Participation Factors

Consider a linear time-invariant system with inputs and outputs:

$$\dot{x}(t) = Ax(t) + Bu(t) \quad (3.18)$$

$$y(t) = Cx(t). \quad (3.19)$$

The sought definition of input-to-output participation factors is considered a natural extension to the definition of input-to-state participation factors [40] given in Section 2.1.2. Recall that the definition of input-to-state participation factors assumes a special form of the input and output matrices  $B$  and  $C$ , respectively. It is assumed that the input is applied to one component, say the  $q$ -th component, of the right side of (3.18) and only one state, say the  $k$ -th state, is measured. For cases of systems where availability of measurements of states is not usually possible, and/or inputs are applied to more than one component of the right side of (3.18), extending the definition in (2.10) to address such cases is needed. We therefore, consider the case of systems with general  $B^q$  and  $C^k$ , where  $B^q$  and  $C^k$  are the  $q$ -th column of input matrix  $B$  and  $k$ -th row of output matrix  $C$ , respectively. This means that the input is applied through the  $q$ -th input channel of the right side of (3.18) and the  $k$ -th output of (3.19) is measured.

With this choice of the input location and the measured output, in steady state the  $k$ -th output in (3.19) (in the frequency domain) is given by

$$\begin{aligned}
y_k(s) &= C^k (sI - A)^{-1} B^q u \\
&= \sum_{i=1}^n \frac{C^k r^i l^i B^q}{s - \lambda_i} u(s) \\
&= \sum_{i=1}^n \frac{R_{ikq}}{s - \lambda_i} u(s)
\end{aligned}$$

Let

$$R_{ikq} := C^k r^i l^i B^q.$$

Take

$$py_{qk}^i = |R_{ikq}| \tag{3.20}$$

as the *participation factor of mode  $i$  in output  $k$  when the input is applied through the  $q$ -th input channel*. We call this quantity the *input-to-output participation factor (IOPF)* for mode  $i$ , with measurement at output  $k$  and input applied through the  $q$ -th input channel. Note that the IOPF, similar to the ISPF, is dimensionless. Also, note that, the quantity  $R_{ikq} = C^k r^i l^i B^q$  is numerically equal to the entry on the  $k$ -th row and  $q$ -th column of the residue matrix associated with mode  $i$ . This definition of input-to-output participation factors is useful in designing monitoring systems to detect impending instability in nonlinear systems as discussed in the next chapter.

## Chapter 4

# Detecting Impending Instability in Nonlinear Systems

In this chapter, a signal-based approach for real-time detection of impending instability in nonlinear systems is considered. The main idea pursued here involves using a small additive white Gaussian noise (AWGN) as a probe signal and monitoring the spectral density of one or more measured states or outputs for certain signatures of impending instability.

Input-to-output participation factors introduced in Chapter 3 along with Input-to-state participation factors given in [40] are used as a tool to aid in selection of locations for probe inputs and outputs or states to be monitored. Since these participation factors are model-based, the chapter combines signal-based and model-based ideas toward achieving a robust methodology for instability monitoring. Power systems will be the main application of this methodology where the detection of impending instabilities is crucial.

The chapter proceeds as follows. In Section 4.1, the sought signal-based approach to instability monitoring using input-to-state and/or input-to-output participation factors is presented. A stability index based on power spectral density measurements is also given. In Section 4.2, three case studies from power systems are given to demonstrate the proposed approach to instability monitoring.

## 4.1 Precursor-Based Monitoring

In this section, we show that noisy precursors can be used as a warning signal indicating that a system is operating dangerously close to instability. We also show that the spectrum of a measured output (state) of the system is proportional to the square of the input-to-output (input-to-state) participation factors. Thus, IOPFs (ISPFs) can be used to determine the best location for applying the probe signal and for choosing which output (state) to measure where the noisy precursor would be most apparent. A stability index based on power spectral density measurements that can be used to aid operators in assessing proximity to the approaching instability is given. Figure 4.1 shows a schematic diagram of our instability monitoring system. The Figure depicts the idea of having the monitoring system to trigger a preventive control action to protect the system against the effects of the approaching instability. One possible preventive action is discussed in Chapter 5.

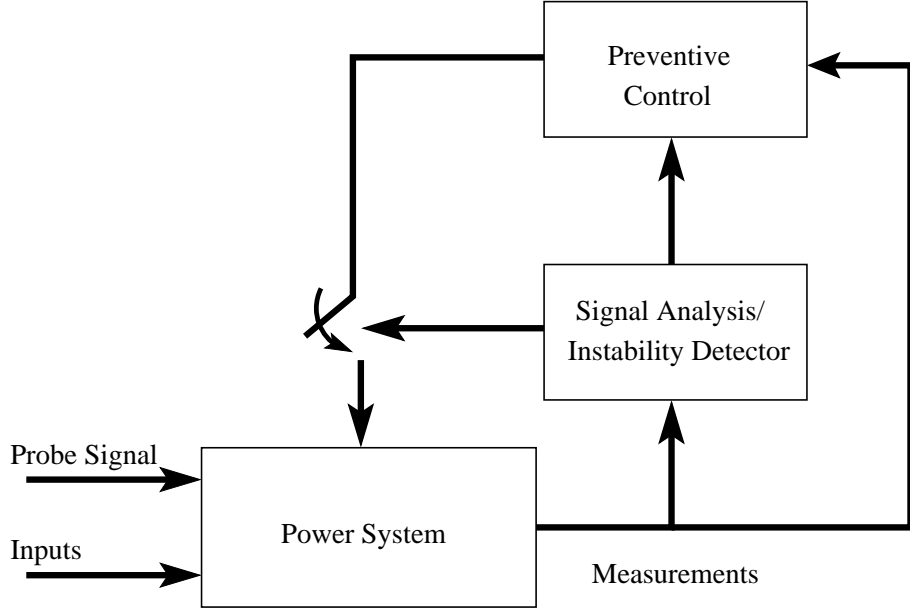


Figure 4.1: Precursor-based instability monitor with external probe signal.

#### 4.1.1 Developed monitoring system

Consider a nonlinear dynamic system (“the plant”)

$$\dot{x} = f(x, \mu) + \xi(t) \quad (4.1)$$

where  $x \in \mathbb{R}^n$ ,  $\mu$  is a bifurcation parameter, and  $\xi(t) \in \mathbb{R}^n$  is a zero-mean vector white Gaussian noise process [25]. Let the system possess an equilibrium point  $x^0$ . For small perturbations and noise, the dynamical behavior of the system can be described by the linearized system in the vicinity of the equilibrium point  $x^0$ . The linearized system corresponding to (4.1) with a small noise forcing  $\xi(t)$  is given by

$$\dot{x} = Df(x^0, \mu)x + \xi(t) \quad (4.2)$$

where  $Df(x^0, \mu)$  represents the gradient of  $f(x, \mu)$  with respect to  $x$  evaluated at  $x = x^0$ . In (4.2),  $x$  now denotes  $x - x^0$  (the state vector referred to  $x^0$ ). For the results of the linearized analysis to have any bearing on the original nonlinear model, we must assume that the noise is of small amplitude.

The noise  $\xi(t)$  can occur naturally or can be injected using available controls. We consider the case where the noise is applied through one input channel and the power spectral density of one output is calculated. That is, we consider the case where  $\xi(t) = B^q \eta(t)$  where  $B^q$  is the  $q$ -th column of the input matrix  $B$ ,  $\eta(t)$  is a scalar white Gaussian noise with zero mean and power  $\sigma^2$ , applied through the  $q$ -th input channel and the output is given by  $y = C^p x$  where  $C^p$  is the  $p$ -th row of the output matrix  $C$ .

In steady state, the  $p$ -th output of system (4.2) forced by a small AWGN is given by

$$\begin{aligned} y_p(s) &= \sum_{i=1}^n \frac{C^p r^i l^i B^q}{s - \lambda_i} \eta(s) \\ &= \sum_{i=1}^n \frac{R_{ipq}}{s - \lambda_i} \eta(s) \\ &= H(s) \eta(s). \end{aligned}$$

The absolute value of  $R_{ipq}$  was defined in Chapter 3 as the participation factor of mode  $i$  in output  $p$  when the input is applied through the  $q$ -th input channel. The power spectral density (PSD) of the output of a linear system with transfer function

$H(j\omega)$  is related to the PSD of the input by [24]

$$S_y(\omega) = H(j\omega)H(-j\omega)S_\eta(\omega)$$

Thus, the power spectrum of the  $p$ -th output is given by

$$\begin{aligned} S_{y_p}(\omega) &= \left( \sum_{i=1}^n \frac{R_{ipq}}{j\omega - \lambda_i} \right) \left( \sum_{k=1}^n \frac{R_{kpq}}{-j\omega - \lambda_k} \right) \sigma^2 \\ &= \sigma^2 \sum_{i=1}^n \sum_{k=1}^n \frac{R_{ipq}}{j\omega - \lambda_i} \frac{R_{kpq}}{-j\omega - \lambda_k} \end{aligned}$$

Suppose that the system is nearing a Hopf bifurcation. Specifically, assume that a complex conjugate pair of eigenvalues is close to the imaginary axis, and has relatively small negative real part in absolute value compared to other system eigenvalues. Denote this pair as  $\lambda_{1,2} = -\epsilon \pm j\omega_c$ , with  $\epsilon > 0$  small and  $\omega_c > 0$ :

$$|\operatorname{Re}(\lambda_i)| \gg \epsilon, \quad i = 3, \dots, n.$$

Under this assumption, and for values of  $\omega$  close to  $\omega_c$ ,  $S_{y_p}(\omega)$  can be approximated as

$$\begin{aligned} S_{y_p}(\omega) &\approx \sigma^2 \sum_{i=1}^2 \sum_{k=1}^2 \frac{R_{ipq}}{j\omega - \lambda_i} \frac{R_{kpq}}{-j\omega - \lambda_k} \\ &= \sigma^2 \left( \frac{|R_{1pq}|^2}{\epsilon^2 + (\omega - \omega_c)^2} + \frac{|R_{1pq}|^2}{\epsilon^2 + (\omega + \omega_c)^2} \right. \\ &\quad \left. + 2\operatorname{Re} \left\{ \frac{1}{\epsilon + j(\omega - \omega_c)} \frac{(R_{1pq})^2}{\epsilon - j(\omega + \omega_c)} \right\} \right). \end{aligned}$$

Note that all terms containing  $\lambda_i$ ,  $i = 3, \dots, n$  have been neglected and only terms containing the critical eigenvalues  $\lambda_1$  and  $\lambda_2$  have been retained. After algebraic manipulation and substituting  $(R_{1pq})^2 = \alpha + j\beta$  where  $\alpha = |R_{1pq}|^2 \cos(2\theta_{pq})$  and

$\beta = |R_{1pq}|^2 \sin(2\theta_{pq})$ , with  $\theta_{pq} = \tan^{-1}\left(\frac{\text{Im}\{R_{1pq}\}}{\text{Re}\{R_{1pq}\}}\right)$ , the PSD of  $y_p$  can be rewritten as

$$\begin{aligned}
S_{y_p}(\omega) &= \sigma^2 |R_{1pq}|^2 \left( \frac{1}{\epsilon^2 + (\omega - \omega_c)^2} + \frac{1}{\epsilon^2 + (\omega + \omega_c)^2} \right) \\
&+ \sigma^2 \frac{(\beta\epsilon + \alpha\omega_c)(\omega - \omega_c) + \epsilon(\epsilon\alpha - \omega_c\beta)}{(\epsilon^2 + \omega_c^2)(\epsilon^2 + (\omega - \omega_c)^2)} \\
&- \sigma^2 \frac{(\beta\epsilon + \alpha\omega_c)(\omega + \omega_c) - \epsilon(\epsilon\alpha - \omega_c\beta)}{(\epsilon^2 + \omega_c^2)(\epsilon^2 + (\omega + \omega_c)^2)} \\
&= \sigma^2 |R_{1pq}|^2 \left[ (1 + G_1(\omega)) \frac{1}{\epsilon^2 + (\omega - \omega_c)^2} \right. \\
&\quad \left. + (1 - G_2(\omega)) \frac{1}{\epsilon^2 + (\omega + \omega_c)^2} \right] \tag{4.3}
\end{aligned}$$

where

$$\begin{aligned}
G_1(\omega) &= \frac{1}{\epsilon^2 + \omega_c^2} [(\epsilon \sin(2\theta_{pq}) + \omega_c \cos(2\theta_{pq}))(\omega - \omega_c) \\
&+ \epsilon(\epsilon \cos(2\theta_{pq}) - \omega_c \sin(2\theta_{pq}))], \\
G_2(\omega) &= \frac{1}{\epsilon^2 + \omega_c^2} [(\epsilon \sin(2\theta_{pq}) + \omega_c \cos(2\theta_{pq}))(\omega + \omega_c) \\
&- \epsilon(\epsilon \cos(2\theta_{pq}) - \omega_c \sin(2\theta_{pq}))].
\end{aligned}$$

For  $\omega = \omega_c$  and sufficiently small  $\epsilon$  ( $\epsilon \ll \omega_c$ ), the power spectral density of  $y_p$  is given by

$$S_{y_p}(\omega_c) = \sigma^2 |R_{1pq}|^2 \left( \frac{1}{\epsilon^2} + O\left(\frac{1}{\epsilon}\right) + O(1) \right).$$

Note that the IOPFs are related to the spectral densities of the outputs of a system driven by small AWGN as in (4.3). The amplitude of the spectrum is proportional to the square of the IOPFs. The input-to-output participation factors can be used

to determine the best location for applying the probe signal and also the output that will have the highest spectral peak.

The special case where only system states are monitored and input is applied to one component of the right side of (4.2) bears similar results [21]. In [21], we show that the ISPFs are related to the spectral densities of the states of a system driven by small AWGN. The amplitude of the spectrum is proportional to the square of the ISPFs. Thus, the input-to-state participation factors can also be used to determine the best location for applying the probe signal and also the state that will have the highest spectral peak.

#### **4.1.2 Instability proximity index**

In this section, an instability proximity index that helps predict closeness to instability based on power spectral density measurements is given. Performance indices have been used to predict proximity to voltage collapse in power systems [44]. Several stability indices have been proposed in the literature, some of these indices are model-based while others rely mainly on online measurements and operators experience. Sensitivity factors, singular values and eigenvalues are among those indices used in the literature [44].

In this paper, a sensitivity-based index is proposed. This index is based on online measurements of power spectral density peaks at certain critical frequencies.

The proposed index is given by

$$PSDI = \frac{d\{PSD_v\}}{d\mu}. \quad (4.4)$$

Here, *PSDI* stands for power spectral density index,  $PSD_v$  is the power spectral density peak value at the critical frequency of the measured variable  $v$  (state or output) corresponding to some value of the bifurcation parameter  $\mu$ . The *PSDI* value at time  $t$  is approximated using  $\Delta\{PSD_v\}/\Delta\{\mu\}$  at time  $t$ , where  $\Delta\{PSD_v\}$  and  $\Delta\{\mu\}$  are the changes in the values of  $PSD_v$  and  $\mu$  between time instances  $t$  and  $t - \Delta t$ , respectively. The sampling time  $\Delta t$  is determined based on operator's experience and system's conditions. The instability index is calculated for the variable  $v$  (state or output) which has the highest ISPF or IOPF, respectively. The instability index grows significantly as the system approaches criticality, where it is theoretically infinity at criticality. The reciprocal of the index is more informative than the index itself as the reciprocal value approaches zero as the system approaches criticality. This index can be used to assist a system operator or an automatic controller in taking a preventive action. For example, a threshold can be used such that if the reciprocal of the index drops below that threshold, a preventive action is triggered. The effectiveness of the proposed instability index in detecting closeness to instability in a single generator power system model is demonstrated in Section 4.2.2.

## 4.2 Power System Examples

In this section, we apply results from the previous section to monitor and detect impending instability of examples from power systems. These examples show how ISPF and IOPF can be used to better monitor an impending instability.

Although white Gaussian noise was used to derive the results presented so far, band-limited white Gaussian noise signals will be used to probe the monitored power system examples. This is because it is practically impossible to generate white noise signals. Band-limited white noise is a useful theoretical approximation when the noise disturbance has a correlation time that is very small relative to the natural bandwidth of the system [43].

### 4.2.1 Single generator with dynamic load

Consider the single generator power system model with induction motor load [12]:

$$\dot{\delta}_m = \omega \quad (4.5)$$

$$M\dot{\omega} = -d_m\omega + P_m - E_m V Y_m \sin(\delta_m - \delta) \quad (4.6)$$

$$K_{q\omega}\dot{\delta} = -K_{qv2}V^2 - K_{qv}V + Q(\delta_m, \delta, V) - Q_0 - Q_1 \quad (4.7)$$

$$\begin{aligned} TK_{q\omega}K_{pv}\dot{V} &= K_{p\omega}K_{qv2}V^2 + (K_{p\omega}K_{pv} - K_{q\omega}K_{pv})V \\ &+ K_{q\omega}(P(\delta_m, \delta, V) - P_0 - P_1) \\ &- K_{p\omega}(Q(\delta_m, \delta, V) - Q_0 - Q_1) \end{aligned} \quad (4.8)$$

The state variables are  $\delta_m$  (the generator phase angle, closely related to the mechanical angle of the generator rotor),  $\omega$  (the rotor speed),  $\delta$  (the load voltage phase angle) and  $V$  (the magnitude of the load voltage). The load includes a constant PQ load in parallel with an induction motor. The real and reactive powers supplied to the load by the network are

$$\begin{aligned} P(\delta_m, \delta, V) &= -E'_0 V Y'_0 \sin(\delta) + E_m V Y_m \sin(\delta_m - \delta), \\ Q(\delta_m, \delta, V) &= E'_0 V Y'_0 \cos(\delta) + E_m V Y_m \cos(\delta_m - \delta) \\ &\quad - (Y'_0 + Y_m) V^2 \end{aligned}$$

where

$$\begin{aligned} E'_0 &= \frac{E_0}{\sqrt{1 + C^2 Y_0^{-2} - 2 C Y_0^{-1} \cos \theta_0}} \\ Y'_0 &= Y_0 \sqrt{1 + C^2 Y_0^{-2} - 2 C Y_0^{-1} \cos \theta_0} \\ \theta'_0 &= \theta_0 + \tan^{-1} \left\{ \frac{C Y_0^{-1} \sin \theta_0}{1 - C Y_0^{-1} \cos \theta_0} \right\} \end{aligned}$$

The values of the parameters for this model are:

$M = 0.01464$ ,  $C = 3.5$ ,  $E_m = 1.05$ ,  $Y_0 = 3.33$ ,  $\theta_0 = 0$ ,  $\theta_m = 0$ ,  $K_{p\omega} = 0.4$ ,  $K_{pv} = 0.3$ ,  $K_{q\omega} = -0.03$ ,  $K_{qv} = -2.8$ ,  $K_{qv2} = 2.1$ ,  $T = 8.5$ ,  $P_0 = 0.6$ ,  $P_1 = 0.0$ ,  $Q_0 = 1.3$ ,  $E_0 = 1.0$ ,  $Y_m = 5.0$ ,  $P_m = 1.0$ ,  $d_m = 0.05$ . All values are in per unit except for angles, which are in degrees.

It has been shown that a supercritical Hopf bifurcation occurs in this power system model as the reactive load  $Q_1$  is increased through the critical value  $Q_1^* = 2.9801438$  [12]. Next, we consider the system operating at loads close to the Hopf

bifurcation, say at  $Q_1 = 2.9$ . The corresponding operating point is  $x^0 = [0.2473, 0, 0.0398, 0.9248]$ . The Jacobian of the system at this operating point is

$$A = \begin{bmatrix} 0 & 1 & 0 & 0 \\ -324.5254 & -3.4153 & 324.5254 & -73.8611 \\ 33.3333 & 0 & -29.2479 & 72.7220 \\ -3.3656 & 0 & 1.5180 & -11.1529 \end{bmatrix}$$

The eigenvalues of  $A$  are  $\{-0.7923 \pm j6.6318, -21.1157 \pm j10.9959\}$ .

To monitor the system, a band-limited AWGN probe signal is applied to the mechanical power  $P_m$ . Figure 4.2 depicts the spectral densities for the four states  $\delta_m, \omega, \delta$  and  $V$  for  $Q_1 = 2.9$  and  $\sigma = 0.001$ . As it is clear from this figure, the state  $\omega$  has a higher peak than all other states. Figure 4.3 demonstrates the variation of the spectral density peak near  $\omega = \omega_c \approx 6.6$  rad/s as a function of the bifurcation parameter  $Q_1$ . The values of the input-to-state participation factors of the critical mode in all states are given in Table 4.1. As predicted by the analysis in Section 4.1, the ordering of the peaks of the spectral densities of all states at  $\omega_c$  can be predicted from the values of the ISPFs.

## 4.2.2 Single generator connected to an infinite bus

Consider a synchronous machine connected to an infinite bus together with excitation control [14]. It was shown in [14] that this system undergoes a Hopf bifurcation as the control gain in the excitation system is increased beyond a critical value. The

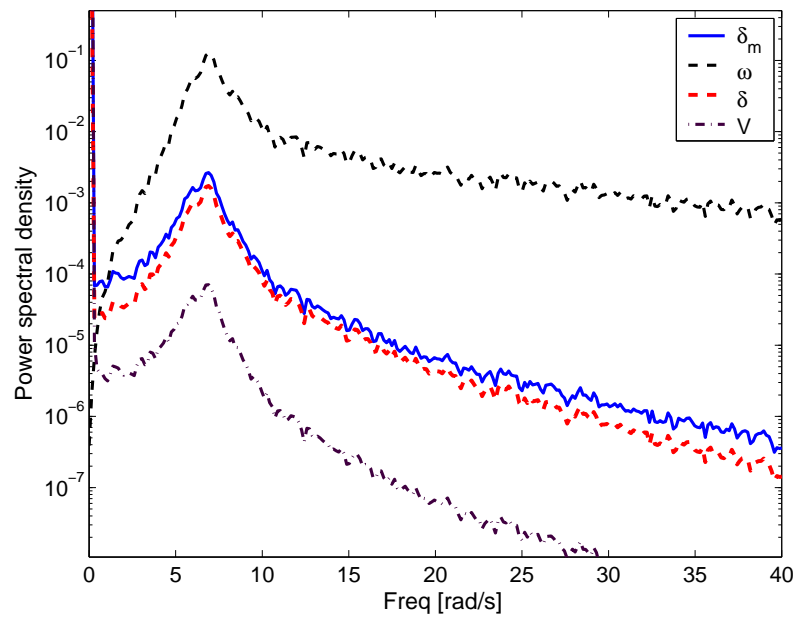


Figure 4.2: Power spectral densities of the states of the model given in (4.5)-(4.8). The bifurcation parameter was set to  $Q_1 = 2.9$ . Band-limited AWGN of zero mean and  $(0.001)^2$  power was added to  $P_m$ .

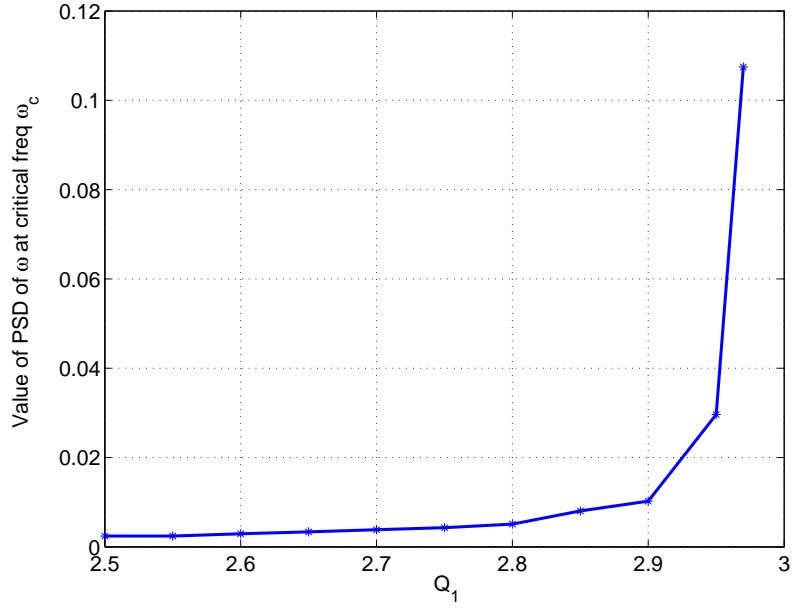


Figure 4.3: Variation of the peak value of the power spectral density of  $\omega$  as a function of the bifurcation parameter  $Q_1$ . Band-limited AWGN of zero mean and  $(0.001)^2$  power was added to  $P_m$ .

dynamics of the generator are given by:

$$\dot{\delta} = \omega \quad (4.9)$$

$$2H\dot{\omega} = -D\omega + \omega_0(P_m - P_e) \quad (4.10)$$

$$\tau'_{d0}\dot{E}'_q = E_{FD} - E'_q - (X_d - X'_d)i_d \quad (4.11)$$

States	Spectral peak at $\omega_c \approx 6.6318$	Input-to-state participation factors (ISPFs)
$\delta_m$	$9.528 \times 10^{-4}$	$p_{21}^1 = 2.8992$
$\omega$	$40.38 \times 10^{-4}$	$p_{22}^1 = 19.364$
$\delta$	$6.616 \times 10^{-4}$	$p_{23}^1 = 2.4013$
$V$	$0.305 \times 10^{-4}$	$p_{24}^1 = 0.4981$

Table 4.1: Input-to-state participation factors and spectral peaks at  $\omega_c$ .

with the following algebraic equations:

$$P_e = E_q i_q$$

$$E_q = E'_q + (X_q - X'_d) i_d$$

$$i_d = x(E_q - E \cos \delta) - r E \sin \delta$$

$$i_q = r(E_q - E \cos \delta) + x E \sin \delta$$

$$x = \frac{X_l + X_q}{R_l^2 + (X_l + X_q)^2}$$

$$r = \frac{R_l}{R_l^2 + (X_l + X_q)^2}$$

The subscripts  $d$  and  $q$  refer to the direct and quadrature axes, respectively. The dynamics of the excitation control are given by

$$\tau_E \dot{E}_{FD} = -K_E E_{FD} + V_R - E_{FD} S_E(E_{FD}) \quad (4.12)$$

$$\tau_F \dot{V}_3 = -V_3 + \frac{K_F}{\tau_E} (-K_E E_{FD} + V_R - E_{FD} S_E(E_{FD})) \quad (4.13)$$

$$\tau_A \dot{V}_R = -V_R + K_A (V_{REF} - V_t - V_3) \quad (4.14)$$

Here  $V_t$  is the terminal voltage and is given by

$$V_t^2 = v_d^2 + v_q^2$$

where

$$-v_d = \psi_q = -X_q i_q$$

$$v_q = \psi_d = E'_q - X'_d i_d.$$

The saturation function  $S_E(E_{FD})$  is usually approximated as

$$S_E(E_{FD}) = A_{EX} \exp(B_{EX} E_{FD}).$$

An equilibrium point of this system is denoted by  $x^0 = (\delta^0, \omega^0, E'_q{}^0, E_{FD}^0, V_3^0, V_R^0)$ .

The values of the parameters that appear in this power system model are given in

Table 4.2.

Synchronous machine	Exciter	Transmission line
$H = 2.37$ s	$K_E = -0.05$	$R_l^0 = 0.02$
$D = 1$ pu	$K_F = 0.02$	$X_l^0 = 0.40$
$X_d = 1.7$	$\tau_E = 0.50$ s	$R_l = \lambda R_l^0$
$X'_d = 0.245$	$\tau_F = 0.60$ s	$X_l = \lambda X_l^0$
$X_q = 1.64$	$\tau_A = 0.10$ s	
$\omega_0 = 377.0$ rad/s	$A_{EX} = 0.09$	
$\tau'_{d0} = 5.9$ s	$B_{EX} = 0.50$	

Table 4.2: Parameter values for the single generator connected to an infinite bus model.

For  $P_m = 0.937$ ,  $V_{REF} = 1.130$ , and  $\lambda = 2$ , it has been shown that a subcritical Hopf bifurcation occurs at  $K_A^* = 193.74$  [14]. Next, we consider the system operating before the Hopf bifurcation, say at  $K_A = 185$ . The corresponding operating point is given by  $x^0 = [1.3515, 0, 1.1039, 2.3150, 0, 0.5472]^T$ . The Jacobian of the system at this operating point is

$$A = \begin{bmatrix} 0 & 1 & 0 & 0 & 0 & 0 \\ -62.2 & -0.2 & -79.7 & 0 & 0 & 0 \\ -0.2 & 0 & -0.4 & 0.2 & 0 & 0 \\ 0 & 0 & 0 & -1.1 & 0 & 2 \\ 0 & 0 & 0 & 0 & -1.7 & 0.1 \\ 125.9 & 0 & -1157.6 & 0 & -1850 & -10 \end{bmatrix}.$$

The eigenvalues of  $A$  are  $\{-0.0139 \pm j7.7707, -4.5832 \pm j12.6178, -2.1029 \pm j0.9417\}$ .

Note that for this model, there are two physically feasible locations for applying the probe signal. The probe signal can be either applied to  $V_{ref}$  or to  $P_m$ . The input-to-state participation factors are used to determine the best location for applying the probe signal. From the values of the ISPFs (see Table 4.3), it is clear that mode 1 has higher participation in other states when the probe signal is applied to  $P_m$  than when applied to  $V_{ref}$ . This can be also seen from the power spectral densities shown in Figures 4.4 and 4.5. Also, the ISPFs give an indication of which state to monitor. The higher the participation factor of the critical mode in a state, the higher the peak of the spectrum for that state. Figure 4.6 shows the variation of the power spectral peak at the critical frequency as a function of the bifurcation parameter when noise is added to  $P_m$ . Figure 4.7 shows the inverse of the PSDI based on measurements from the state  $V_R$  versus the exciter gain  $K_A$ . Note that, for example, a threshold value of 5 can be used such that if the reciprocal of the index drops below that value, a preventive action is triggered.

State	Spect. peak at $\omega_c$ (noise added to $P_m$ )	ISPFs	Spect. peak at $\omega_c$ (noise added to $V_{ref}$ )	ISPFs
$\delta$	0.0226	$p_{21}^1 = 0.0648$	0.0019	$p_{61}^1 = 0.0024$
$\omega$	1.2880	$p_{22}^1 = 0.4923$	0.1084	$p_{62}^1 = 0.0185$
$E'_q$	$0.75938 \times 10^{-4}$	$p_{23}^1 = 0.0038$	$0.68651 \times 10^{-5}$	$p_{63}^1 = 0.0001$
$E_{FD}$	0.2326	$p_{24}^1 = 0.2084$	0.0210	$p_{64}^1 = 0.0078$
$V_3$	$2.4644 \times 10^{-4}$	$p_{25}^1 = 0.0068$	$2.2288 \times 10^{-5}$	$p_{65}^1 = 0.0003$
$V_R$	3.3923	$p_{26}^1 = 0.8006$	0.3064	$p_{66}^1 = 0.0301$

Table 4.3: Input-to-state participation factors and spectral peaks at  $\omega_c \approx 7.8$  for the single generator connected to an infinite bus system.

### 4.2.3 Three-generator nine-bus power system

Below, we consider the Western System Coordinating Council (WSCC) 3-machine, 9-bus power system model, which is widely used in the literature [33, pp. 170–177],[16]. The dynamics of this model includes three identical IEEE-Type I exciters for the three machines. The machines and exciters data are given in Tables 4.4 and 4.5, respectively [33, 16].

In this model, a subcritical Hopf bifurcation occurs as the load on bus 5 is increased beyond 4.5 pu [33]. Our goal in this case study is to detect this impending loss of stability by using a band-limited AWGN probe signal and continuously monitoring the power spectral densities of certain states or outputs. This would give the system operator (or an automatic controller) valuable time to take appropriate preventive measures (e.g., shedding loads at certain buses or trigger a controller

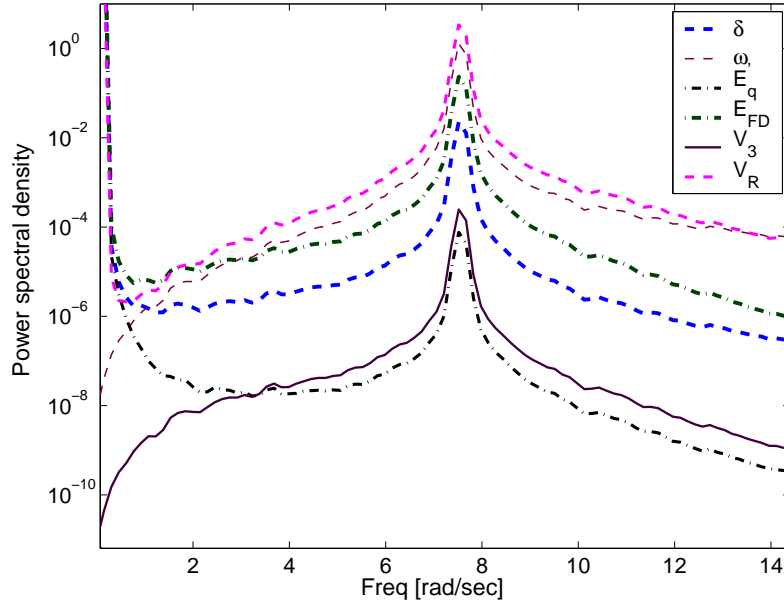


Figure 4.4: Power spectral densities of the states of the single generator connected to an infinite bus system. The bifurcation parameter was set to  $K_A = 185$ . Band-limited AWGN of zero mean and  $(0.000032)^2$  power was added to  $P_m$ .

that assigns the participation factors of system states in the critical mode as will be discussed in Section 6.2). The simulations of this model were conducted using the software package PSAT [16]. For values of the load on bus 5 close to 4.0 pu, the linearization of the system at the operating point has two complex conjugate pair of eigenvalues close to the imaginary axis,  $\lambda_{1,2} = -0.17665 \pm j8.184$  and  $\lambda_{3,4} = -0.3134 \pm j1.7197$ . As the load on bus 5 is increased further, the pair  $\lambda_{3,4}$  approaches the imaginary axis, while the other pair  $\lambda_{1,2}$  changes only slightly. For example, when the load at bus 5 is 4.4 pu,  $\lambda_{1,2} = -0.18231 \pm j8.0978$  and  $\lambda_{3,4} = -0.04602 \pm j2.1151$ . Increasing the load on bus 5 beyond 4.5 pu causes the pair  $\lambda_{3,4}$  to cross the imaginary axis from left to right.

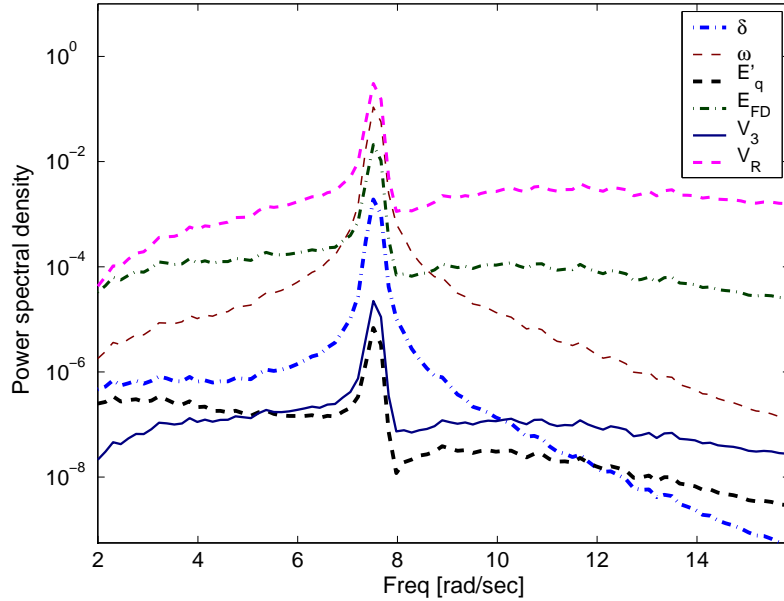


Figure 4.5: Power spectral densities of the states of the single generator connected to an infinite bus system. The bifurcation parameter was set to  $K_A = 185$ . Band-limited AWGN of zero mean and  $(0.000032)^2$  power was added to  $V_{ref}$ .

From the values of the ISPFs calculated for this system, we found that both of the critical modes have higher participation when the probe signal is applied to  $P_{m_3}$ , the mechanical power of generator number 3. Also, we found that these modes have high participation in the field voltage of the exciters. Therefore, in the following simulations, the probe signal is added to  $P_{m_3}$  and the power spectral densities of the field voltages of the three exciters (i.e.,  $E_{fd_i}, i = 1, 2, 3$ ) are monitored. Table 4.6 shows input-to-state participation factors for the 3-machine nine-bus system (partial listing) when the load at bus 5 is 4.4 pu. Figure 4.9 and Figure 4.10 show the power spectral densities of  $E_{fd_i}, i = 1, 2, 3$  when the load on bus 5 ( $P_{L_5}$ ) is 4.0 pu and 4.4 pu, respectively. It is clear from Figure 4.9 that when the load on bus 5 is

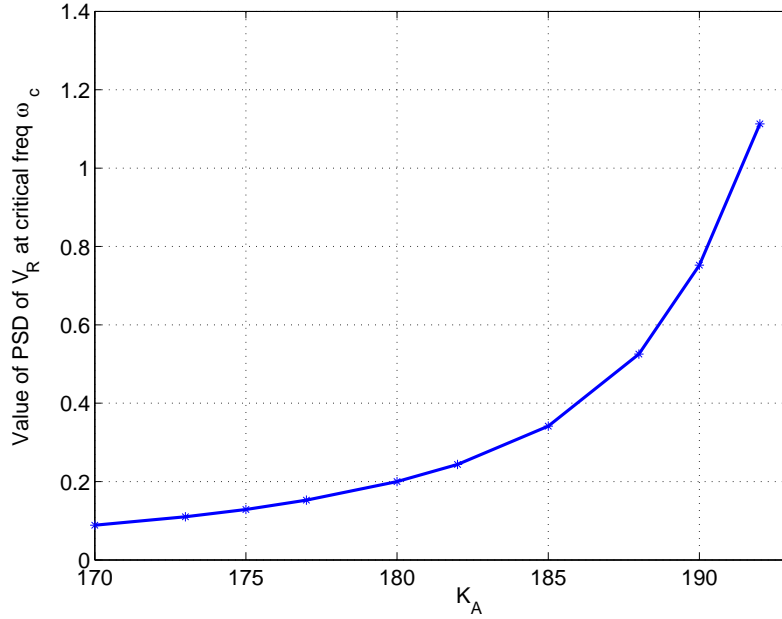


Figure 4.6: Variation of the peak value of the power spectral density of  $V_R$  as a function of the bifurcation parameter  $K_A$ . Band-limited AWGN of zero mean and  $(0.000032)^2$  power was added to  $P_m$ .

4.0 pu, the spectrum has two peaks at 0.28 Hz and 1.3 Hz. These two frequencies correspond to the complex eigenvalues  $\lambda_{3,4}$  and  $\lambda_{1,2}$ , respectively. Note that the peak at 1.3 Hz that corresponds to the pair of complex eigenvalues  $\lambda_{1,2}$  is higher than the peak at 0.28 Hz. However, when the load at bus 5 is increased to 4.4 pu, the peak at 0.28 Hz becomes much larger than the one at 1.3 Hz (see Figure 4.10), which is an indicator that an instability is being approached. Figure 4.11 shows the power spectral density of  $E_{fd1}$  for three values of  $P_{L5}$ : 4.0 pu, 4.25 pu and 4.4 pu.

Next, we consider using IOPFs to decide which is the best output to measure. Table 4.7 shows partial listings of the IOPFs when the load at bus 5 is 4.4

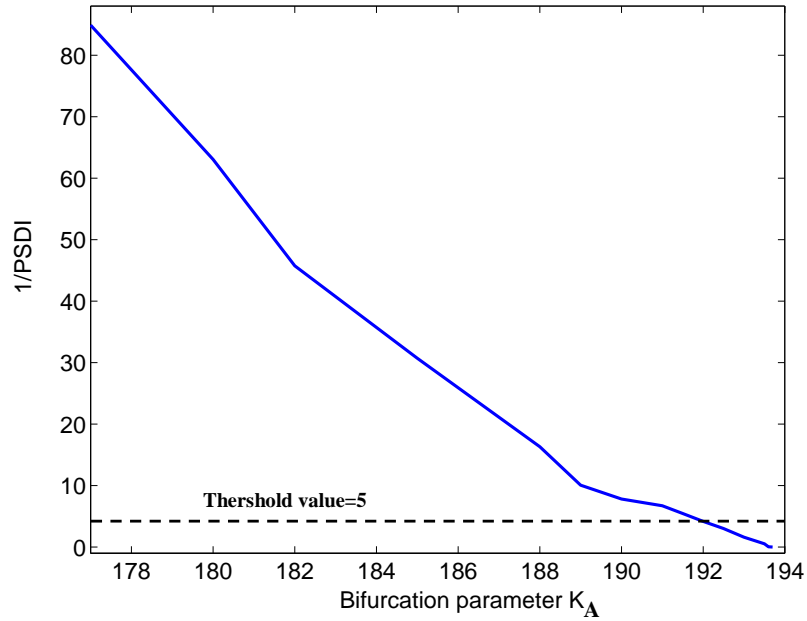


Figure 4.7: Plot of the inverse of the power spectral density index of  $\omega$  versus the bifurcation parameter  $K_A$ . The threshold value is equal to 5.

pu. The values listed correspond to cases where the probe signal is applied to one of the mechanical powers of the generators  $\{P_{m_1}, P_{m_2}, P_{m_3}\}$  and one of the outputs  $\{V_5, V_6, V_7, Q_{14}, Q_{39}, Q_{27}\}$  is measured.  $\{V_5, V_6, V_7\}$  are voltages at buses  $\{5, 6, 7\}$ , respectively and  $\{Q_{14}, Q_{39}, Q_{27}\}$  are reactive powers flowing between buses  $\{(1, 4), (3, 9), (2, 7)\}$ , respectively. Figure 4.12 shows the power spectral density for state  $E_{fd_1}$  and outputs  $Q_{14}$  and  $Q_{27}$ . The load value is 4.4 pu. The noise is added to  $P_{m_3}$ , the mechanical power of generator number 3. It is clear from the figure that IOPFs can be used to aid in the selection of signals to monitor the system other than signals of state variables.

Parameters	Machine 1	Machine 2	Machine 3
$H(sec)$	23.64	6.4	3.01
$x_d(pu)$	0.146	0.8958	1.3125
$x'_d(pu)$	0.0608	0.1198	0.1813
$x_q(pu)$	0.0969	0.8645	1.2578
$x'_q(pu)$	0.0969	0.1969	0.25
$T'_{do}(sec)$	8.96	6.0	5.89
$T'_{qo}(sec)$	0.31	0.535	0.6

Table 4.4: Three-generator nine-bus power system: machine data.

Parameters	$K_A$	$T_A(sec)$	$K_E$	$T_E(sec)$	$K_F$	$T_F(sec)$
	20	0.2	1.0	0.314	0.063	0.35

Table 4.5: Three-generator nine-bus power system: exciter data.

Input noise added to	States measured					
	$E_{fd_1}$	$E_{fd_2}$	$E_{fd_3}$	$\omega_1$	$\omega_2$	$\omega_3$
$P_{m_1}$	3.0017	2.6973	2.1357	0.0033	0.0028	0.0031
$P_{m_2}$	2.6113	2.3465	1.858	0.0029	0.0024	0.0027
$P_{m_3}$	4.7816	4.2967	3.4022	0.0052	0.0044	0.0049
$V_{ref_1}$	0.0155	0.014	0.0111	0.0000169	0.0000143	0.000016
$V_{ref_2}$	0.0233	0.021	0.0166	0.0000255	0.0000215	0.00002409
$V_{ref_3}$	0.0475	0.0427	0.0338	0.0000519	0.000043	0.000049

Table 4.6: Input-to-state participation factors for the 3-machine nine-bus system (partial listing). The load at bus 5 is 4.4 pu.

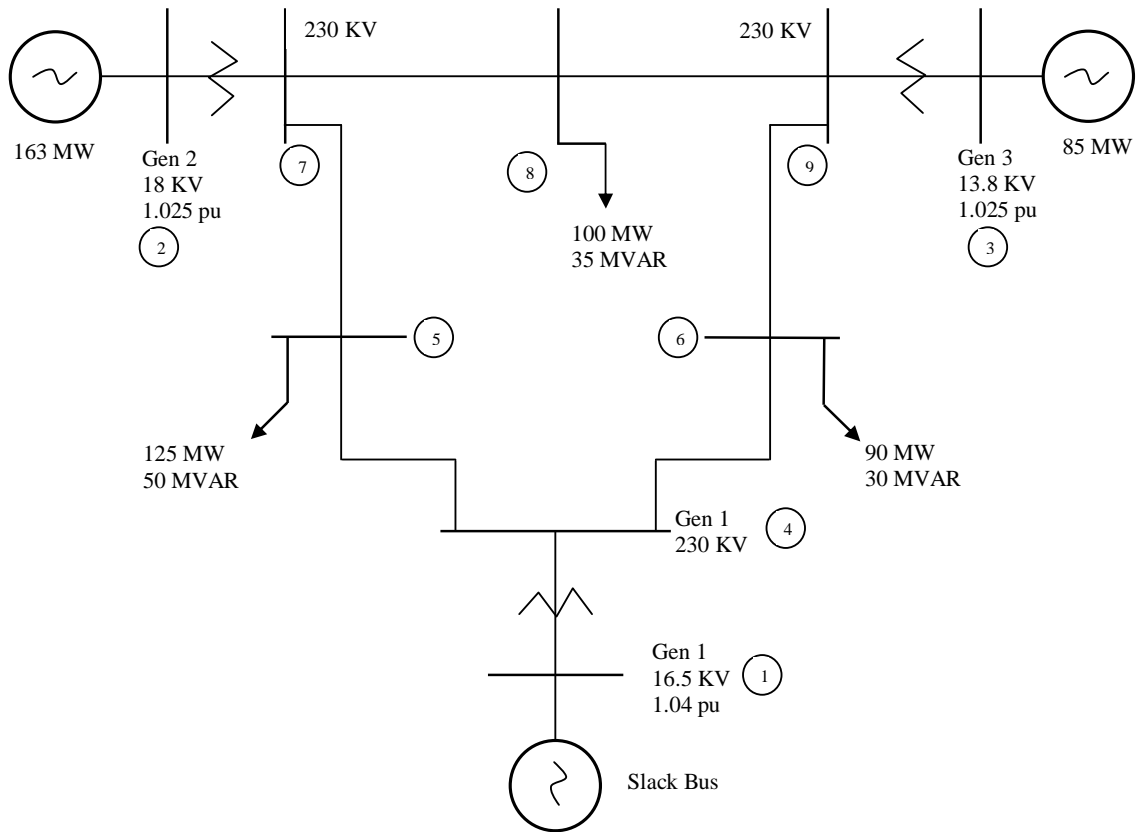


Figure 4.8: WSCC 3-machine, 9-bus system.

Input noise added to	Outputs measured					
	$V_5$	$V_6$	$V_7$	$Q_{14}$	$Q_{39}$	$Q_{27}$
$P_{m_1}$	0.8255	0.6490	0.6922	4.2022	0.9882	1.4460
$P_{m_2}$	0.7182	0.5646	0.6021	3.6557	0.8597	1.2579
$P_{m_3}$	1.3152	1.0339	1.1027	6.6948	1.5743	2.3037
$V_{ref_1}$	0.0043	0.0034	0.0036	0.0218	0.0051	0.0075
$V_{ref_2}$	0.0064	0.0050	0.0054	0.0327	0.0077	0.0112
$V_{ref_3}$	0.0131	0.0103	0.0110	0.0666	0.0157	0.0229

Table 4.7: Input-to-output participation factors for the 3-machine nine-bus system (partial listing). The load at bus 5 is 4.4 pu.

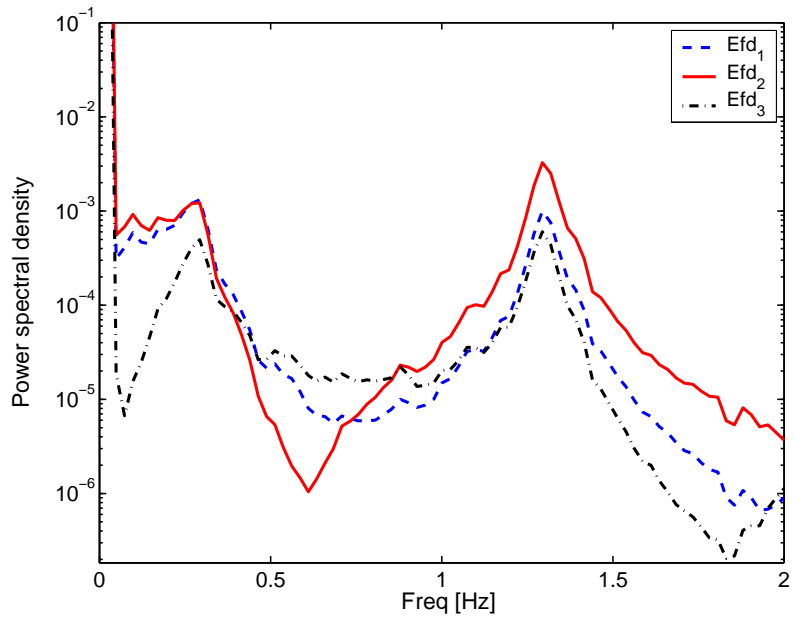


Figure 4.9: Power spectral densities of the states  $E_{fd_1}$ ,  $E_{fd_2}$  and  $E_{fd_3}$ . The load on bus 5 was used as a bifurcation parameter. The load value is 4.0 pu. Band-limited AWGN of zero mean and 0.05 power was added to  $P_{m_3}$ , the mechanical power of generator number 3.

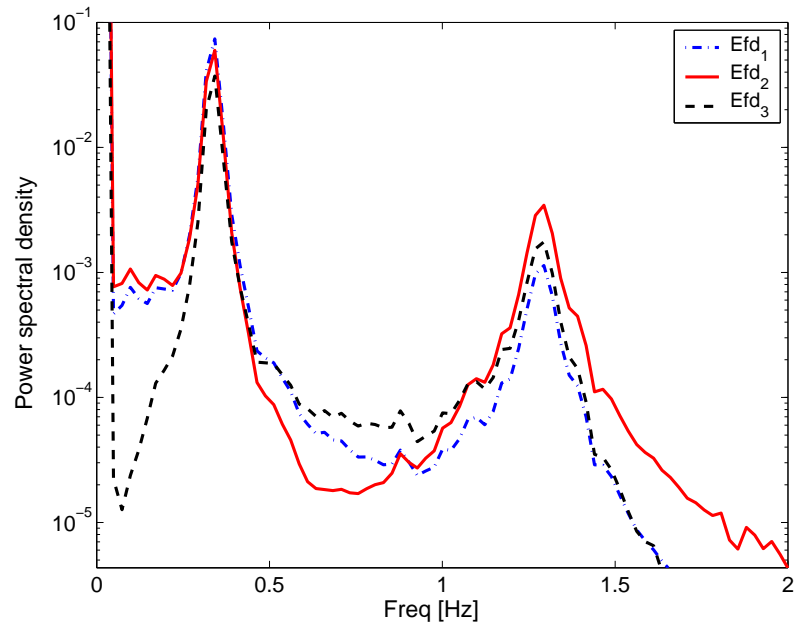


Figure 4.10: Power spectral densities of the states  $E_{fd_1}$ ,  $E_{fd_2}$  and  $E_{fd_3}$ . The load on bus 5 was used as a bifurcation parameter. The load value is 4.4 pu. Band-limited AWGN of zero mean and 0.05 power was added to  $P_{m_3}$ , the mechanical power of generator number 3.

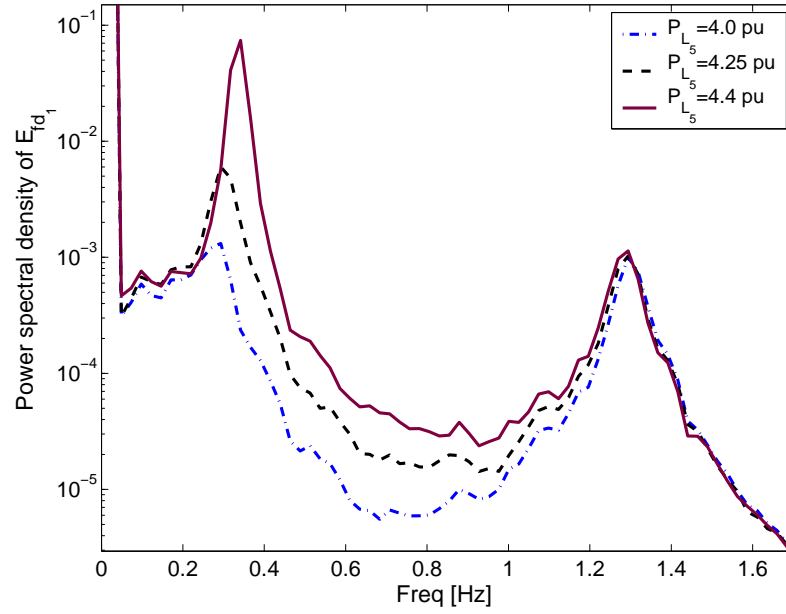


Figure 4.11: Power spectral density of  $E_{fd1}$  for three values of  $P_{L5}$  (the load on bus 5):  $P_{L5} = 4.0$  pu (dash-dotted line),  $P_{L5} = 4.25$  pu (dashed line) and  $P_{L5} = 4.4$  pu (solid line). Band-limited AWGN of zero mean and 0.05 power was added to  $P_{m3}$ , the mechanical power of generator number 3.

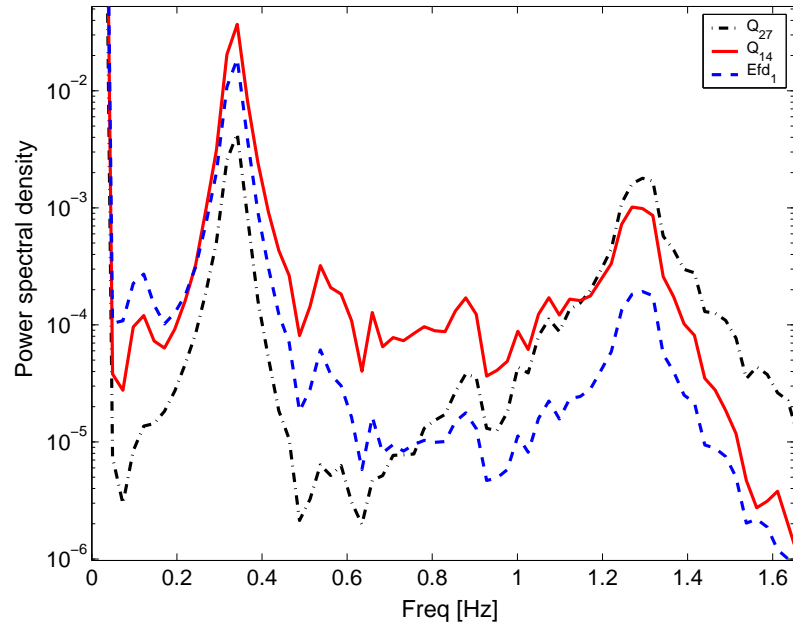


Figure 4.12: Power spectral densities of the state  $E_{fd_1}$  and outputs  $Q_{14}$  and  $Q_{27}$ . The load on bus 5 was used as a bifurcation parameter. The load value is 4.4 pu. Band-limited AWGN of zero mean and 0.05 power was added to  $P_{m_3}$ , the mechanical power of generator number 3.

## Chapter 5

# Participation Factor Assignment Using Eigenvector Assignment-Based Feedback Control

In this chapter, we develop state feedback control to assign modal participation factors for systems nearing instability using eigenvector assignment-based techniques. We focus on assigning participation factors for state variables within a predefined group of state variables, where the group can be any subvector of the state vector, or could consist of all system states. A procedure for computing the desired closed-loop right eigenvector(s) (based on a given desired closed-loop participation factors) is presented.

This chapter proceeds as follows. In Section 5.2, the algorithms for assigning participation factors of system states in a mode associated with a single real eigenvalue approaching zero are presented. In Section 5.3, the case of assigning

participation factors for systems with an open-loop mode associated with a pair of conjugate complex eigenvalues approaching the imaginary axis is discussed.

## 5.1 Introduction

The goal of the control effort is not to shift the eigenvalue(s) associated with a mode that is approaching the imaginary axis (denoted as the critical mode). Rather, the goal is to assign the participation factors of a predefined group of states in the critical mode. We would typically desire that some of these participation factors be small, and possibly that others be relatively large so that the energy in the mode affects these physical states more than the “protected” ones. This could be viewed as using some states, which could be associated with devices inserted into the system, as vibration absorbers that tend to shield the most valued parts of the system from the instability especially in its initial stages.

The feedback control will be designed to only change the closed-loop right eigenvector(s) associated with the critical mode. The remaining closed-loop right eigenvectors (associated with the remaining eigenvalues of the system) will be kept the same as their open-loop values.

We address two cases, first the case of assigning participation factors of states in a mode associated with a single real eigenvalue approaching zero, and second the case of assigning participation factors of states in a mode associated with a pair of conjugate complex eigenvalues approaching the imaginary axis.

Consider the closed-loop *LTI* system

$$\dot{x}(t) = (A + BF)x(t) \quad (5.1)$$

associated with an open-loop system

$$\dot{x}(t) = Ax(t) + Bu(t) \quad (5.2)$$

to which a state feedback  $u(t) = Fx(t)$  is applied.

In Chapter 4, it has been shown that noisy precursors can be used as a warning signal indicating that a system is operating dangerously close to instability. This warning signal can be used to trigger some control system as the one presented in this chapter. The objective will be to move the system to a safer operating condition in the sense that the “high-value” vulnerable parts of the system are more “protected”.

Minimizing the participation factors of a high-value group of states in the critical mode implies that some other group of states will experience higher magnitudes of participation factors in the critical mode. Deciding which group of states will be seen as “*low-value*” is based on system conditions and operators experience.

To avoid confusion, we will denote the group of high-value and low-value states as the control group states. Also, we will arrange the system states such that high-value states are followed by low-value states followed by the rest of the system states. Based on the number of states in the control group and the number of system inputs  $m$ , assigning participation factor associated with a critical mode

can be divided into two cases, (i) when  $n_{ng} \leq m$ , and (ii) when  $n_{ng} > m$ , where  $n_{ng}$  is the number of states in the control group. In the first case, we will show that exact assignment of participation factors in the control group is possible. In the second case, an optimal solution will be sought as the freedom of exact assignment is limited by the number of system inputs (which is less than the number of states in the control group).

## 5.2 Participation Factor Assignment: Case of Real Eigenvalue Approaching Zero

In this section, we develop feedback control algorithms for assigning participation factors of states in a mode associated with a single real eigenvalue approaching zero. Such a mode is considered critical in the sense that it is associated with the possibility of the system losing stability. Indeed, in such cases, the system would typically undergo some type of stationary bifurcation at the critical parameter values where the zero eigenvalue is actually attained. Next, we show how to compute the desired closed-loop right eigenvector  $r^{i'd}$  based on a given (desired) specification of the closed-loop participation factors. Note that the superscript ( $'$ ) is used to denote closed-loop quantities.

### 5.2.1 Computing desired closed-loop right eigenvector $r^{i'd}$

The desired closed-loop  $i$ -th right eigenvector  $r^{i'd}$  can be written as

$$r^{i'd} := \begin{bmatrix} r^s \\ r^{ns} \\ r^{nc} \end{bmatrix},$$

where,  $r^s \in \mathbb{R}^{n_s}$ ,  $r^{ns} \in \mathbb{R}^{n_{ns}}$ ,  $r^{nc} \in \mathbb{R}^{n-(n_s+n_{ns})}$  represent vectors of components of  $r^{i'd}$  corresponding to high-value, low-value and uncontrolled states, respectively.  $\{n_s, n_{ns}, n_{nc}\}$  represent the number of high-value, low-value and uncontrolled states, respectively. The high-value and low-value states form a control group. Let  $n_{ng} = n_s + n_{ns}$  be the number of control group states.

The case of zero closed-loop participation factors of high-value states in mode  $i$  is straightforward and can be achieved by setting  $r^s = 0$  and  $r^{ns} = e \in \mathbb{R}^{n_{ns}}$  where  $e$  is a column vector of nonzero elements (to avoid zero participation). The remaining  $(n - n_{ng})$  components are left unspecified (unconstrained).

Next, we consider the general case of nonzero closed-loop participation factors. Let the desired closed-loop participation factors of the control group states  $\{x_2, \dots, x_{n_{ng}}\}$  in mode  $i$  be given in terms of the closed-loop participation factor of state  $x_1$  (first state of the group), i.e., let  $z_k$ ,  $k = 2, \dots, n_{ng}$  be the desired ratio between the closed-loop participation factor of state  $x_k$  and that of state  $x_1$ . Next, we state a proposition that focuses on solving this participation factor assignment problem in the case where we only desire to attain a certain ratio of closed-loop

participation factors for two states. The proposition shows how to compute the ratio between components of the closed-loop right eigenvector  $r^{i'}$  (associated with the real  $i$ -th eigenvalue  $\lambda_i$ ) to achieve a given (desired) ratio between the closed-loop participation factors of two states  $\{x_k, x_j\}$  in mode  $i$ .

**Proposition 5.1** *Consider a linear time-invariant system (5.1–5.2) with the goal of achieving a desired ratio  $z$  between the closed-loop participation factors of any two states  $\{x_k, x_j\}$  in the  $i$ -th mode (viewed as the critical mode). It is possible to achieve this desired ratio through state feedback without changing any right eigenvector except for  $r^i$ . Moreover, this is achieved by assigning the  $k$ -th and  $j$ -th components  $\{r_k^{i'}, r_j^{i'}\}$  of the closed-loop  $i$ -th right eigenvector such that their ratio is  $\frac{z}{l_k^i/l_j^i}$ , where  $l_k^i, l_j^i$  are the  $k$ -th and  $j$ -th components of the open-loop  $i$ -th left eigenvector, respectively.*

**Proof:** See Appendix A.1.

For the general case where more than two participation factors are to be assigned, let  $z_k, k = 2, \dots, n_{ng}$  be the desired ratio between the closed-loop participation factor of state  $x_k$  and that of state  $x_1$ . The first  $n_{ng}$  components of the closed-loop  $i$ -th right eigenvector should be selected such that the ratio between the  $k$ -th component and the first component is  $\frac{z_k}{l_k^i/l_1^i}$ , for  $k = 2, \dots, n_{ng}$ . The remaining  $(n - n_{ng})$  components are unspecified (unconstrained).

### 5.2.2 Feedback control design: exactly assignable case

In this case, the number of states in the control group (formed of high-value and low-value states) is less than or equal to the number of inputs  $m$ , i.e.,

$$n_{ng} = n_s + n_{ns} \leq m.$$

Recall the main assumption of the assignment problem, that is, the controller should not change any open-loop eigenvalue or any open-loop right eigenvector except the eigenvector associated with mode  $i$ . Saying that, observe that for all open-loop pairs  $(\lambda_j, r^j)$ ,  $\{j = 1, 2, \dots, n, j \neq i\}$ , conditions (1) and (2) of Proposition 2.1 are trivially satisfied. Moreover, by definition,  $r^j$  lies in the null space of  $(\lambda_j I - A)$ , and hence in the span of  $N_{\lambda_j}$  (satisfying condition (3) of the Proposition). Therefore, according to Proposition 2.1, there exists a feedback gain matrix  $F$  such that all open-loop pairs  $(\lambda_j, r^j)$ ,  $\{j = 1, 2, \dots, n, j \neq i\}$  can be kept invariant from their original, uncontrolled values. Next we recall the steps to compute the state feedback gain matrix  $F$  given in Section 2.3.1 with appropriate modifications to solve the assignment problem beforehand.

#### Steps to compute $F$

1. Using the procedure given in Section 5.2.1, compute the desired vectors  $r^s, r^{ns}$  of components of the  $i$ -th closed-loop right eigenvector  $r^{i'}$  (to be exactly assigned) corresponding to high-level and low-level states, respectively.

2. Form a column vector  $e \in \mathbb{R}^{m-n_g}$  of nonzero elements.

3. Compute  $k$  to satisfy

$$\begin{bmatrix} r^s \\ r^{ns} \\ e \end{bmatrix} = \tilde{N}_{\lambda_i} k \quad (5.3)$$

where  $\tilde{N}_{\lambda_i}$  is the  $m \times m$  matrix of the first  $m$  rows of  $N_{\lambda_i}$  (defined in (2.19)) associated with the first  $m$  states.<sup>1</sup> The closed-loop right eigenvector  $r^{i'}$  is then given by

$$r^{i'} = N_{\lambda_i} k$$

4. Let

$$w^i = -M_{\lambda_i} k,$$

where  $M_{\lambda_i}$  is given by (2.19). Construct the real matrices  $W \in \mathbb{R}^{m \times n}$  and  $V \in \mathbb{R}^{n \times n}$

$$\begin{aligned} W &= [0 \ \dots \ 0 \ w^i \ 0 \ \dots \ 0] \\ V &= [\dots \operatorname{Re}\{r^j\} \ \operatorname{Im}\{r^j\} \ \dots \ r^{i'} \ \dots \ r^q \ \dots] \end{aligned}$$

where  $r^j$  and  $r^q$  represent open-loop right eigenvectors associated with complex and real eigenvalues, respectively.

---

<sup>1</sup>In case  $\tilde{N}_{\lambda_i}$  is singular, a state from the control group has to be replaced by a state from outside the group and test again for the singularity of the new  $\tilde{N}_{\lambda_i}$ .

5. The feedback gain matrix  $F$  is given by

$$F = WV^{-1}.$$

## Numerical example

Consider an example of a linear time-invariant system (5.2) ([23], pp. 108), where

$$A = \begin{bmatrix} 0 & 1 & 0 & 0 \\ 0 & -1.89 & 0.39 & -5.555 \\ 0 & -0.034 & -2.98 & 2.43 \\ 0.035 & -0.0011 & -0.99 & -0.21 \end{bmatrix} \quad \text{and} \quad B = \begin{bmatrix} 1 & 0 \\ 0.76 & -1.6 \\ -0.95 & -0.032 \\ 0.03 & 0 \end{bmatrix}. \quad (5.4)$$

The system's four eigenvalues are  $\{-0.1051, -1.4811 \pm 0.6239i, -2.0127\}$ . Since the eigenvalue  $\{-0.1051\}$  is the closest to the origin, let us focus on its associated participation factors for assignment through feedback. The open-loop participation factors of system states  $\{x_1, x_2, x_3, x_4\}$  in the first mode are  $\{1.1492, -0.0653, 0.0403, -0.1241\}$ , respectively. The ratio between the participation factors of  $\{x_1, x_2\}$  is  $-17.6$ , i.e., the participation of  $x_1$  in the first mode is much higher than the participation of state  $x_2$ . Suppose it is desired to reduce the ratio between the participation factors of  $\{x_1, x_2\}$  to 0.5 (i.e., it is desired to push the participation of the second state in the first mode to be twice that of the participation of the first

state). The right modal matrix  $R$  of the open-loop system is

$$R = \begin{bmatrix} 0.9934 & -0.4738 + 0.1996i & -0.4738 - 0.1996i & 0.4447 \\ -0.1044 & 0.8262 & 0.8262 & -0.8951 \\ 0.0314 & -0.1738 + 0.0881i & -0.1738 - 0.0881i & -0.0221 \\ 0.0357 & -0.0730 + 0.0990i & -0.0730 - 0.0990i & -0.0213 \end{bmatrix}.$$

The open-loop left eigenvector components  $l_1^1, l_2^1$  are  $\{1.1568, 0.6258\}$ , respectively.

Thus the design ratio for  $r_1^{1'}/r_2^{1'}$  should be  $0.5/(1.1568/.6258) = 0.2705$ . Applying the steps above to compute the feedback gain matrix  $F$  yields

$$F = \begin{bmatrix} 0.5280 & 0.2857 & 0.5846 & -1.5851 \\ 0.1578 & 0.0854 & 0.1748 & -0.4738 \end{bmatrix}$$

The closed-loop system matrix  $A_c = A + BF$  is given by

$$A_c = \begin{bmatrix} -0.5280 & 0.7143 & -0.5846 & 1.5851 \\ -0.1488 & -1.9705 & 0.2253 & -5.10850 \\ 0.5067 & 0.2401 & -2.4190 & 0.90900 \\ 0.0192 & -0.0097 & -1.0075 & -0.1624 \end{bmatrix}. \quad (5.5)$$

The eigenvalues of  $A_c$  are the same as the open-loop eigenvalues (as expected), and the closed-loop right modal matrix  $R'$  is

$$R' = \begin{bmatrix} 0.2457 & -0.4738 + 0.1996i & -0.4738 - 0.1996i & 0.4447 \\ 0.9083 & 0.8262 & 0.8262 & -0.8951 \\ 0.0152 & -0.1738 + 0.0881i & -0.1738 - 0.0881i & -0.0221 \\ -0.3382 & -0.0730 + 0.0990i & -0.0730 - 0.0990i & -0.0213 \end{bmatrix}.$$

The closed-loop participation factors are  $\{0.1389, 0.2778, 0.0095, 0.5738\}$ . Note that the participation of  $x_1$  in the first mode is half that of  $x_2$  (as desired). Also note that, although the desired goal was met, state  $x_2$  is not the state having the highest participation in the first mode. State  $x_4$  is the one having the highest closed-loop participation although it was not the one with the highest open-loop participation. Thus, the exact assignment methodology can precisely assign participation factors among the states in the control group but has no authority over the participation factors for states outside the control group.

### 5.2.3 Feedback control design: not exactly assignable case

In this case,

$$n_{ng} = n_s + n_{ns} > m.$$

Let the desired closed-loop participation of the control group states  $\{x_2, \dots, x_{n_{ng}}\}$  in mode  $i$  be given in terms of the closed-loop participation factor of state  $x_1$  (first state of the group), i.e., let  $z_k$ ,  $k = 2, \dots, n_{ng}$  be the desired ratio between the closed-loop participation factor of state  $x_k$  and that of state  $x_1$ . Generally, the freedom in specifying components of the closed-loop eigenvectors is limited by the number of system inputs  $m$  as noted by Liu and Paton [23]. Thus, it is not possible to exactly assign the desired  $r^{i'd}$  (computed in Section 5.2.1) to achieve the specified ratios  $z_k$ ,  $k = 2, \dots, n_{ng}$ . Instead, a *best possible* choice for an achievable eigenvector is made. Recall the expression to compute the best achievable vector  $r^{i'a}$  and the

corresponding coefficient vector  $k$  (given in (2.26)–(2.27)),

$$k = (N_{\lambda_i}^T N_{\lambda_i})^{-1} N_{\lambda_i}^T r^{i'd} \quad (5.6)$$

$$r^{i'a} = N_{\lambda_i} (N_{\lambda_i}^T N_{\lambda_i})^{-1} N_{\lambda_i}^T r^{i'd}. \quad (5.7)$$

Construction of the feedback gain matrix  $F$  is straightforward following steps (4) and (5) in Section 5.2.2.

#### 5.2.4 Feedback control design: “sacrificial” case

In this case, no prior specifications on the closed-loop participation factors are given except that it is required that the participation factors of the low-value states be maximized with respect to the rest of the system states. Thus, the low-value states will be “sacrificed” to “protect” the rest of the system states (including the high-value states). A trivial assumption is

$$n - n_{ns} \geq m,$$

otherwise, it would be possible to assign zeros to all participation factors of system states except the low-value ones to achieve infinite relative participation of low-value states with respect to the rest of the system states. The proposed setting is to maximize the ratio between the norms of two vectors. The entries of the two vectors are those of the closed-loop participation factors of low-value states and the rest of the system states, respectively. Next, we show the setup of the optimization problem.

For simplicity of notation, the letter  $i$  used as a subscript with the critical eigenvalue, or used as a superscript with the right/left eigenvector associated with the critical mode, is omitted whenever it is clear from the context. The subscripts  $ns$  and  $t$  are used to denote quantities that are a function of low-value and rest-of-the-system states respectively. Also, the states are reordered such that low-value states come first followed by the rest of the system states.

The closed-loop  $i$ -th right eigenvector can be written as:

$$\begin{aligned} r' &= \begin{bmatrix} r'^{ns} \\ r'^t \end{bmatrix} \\ &= \begin{bmatrix} N_{\lambda_{ns}} \\ N_{\lambda_t} \end{bmatrix} k \end{aligned} \quad (5.8)$$

where,  $N_{\lambda_{ns}}$  and  $N_{\lambda_t}$  are the matrices formed of the rows of  $N_\lambda$  associated with low-value and the rest of the system states, respectively. Define column vectors  $P_{ns}$  and  $P_t$  of closed-loop participation factors of low-value states and the rest of the system states, respectively,

$$\begin{aligned} P_{ns} &:= [p'_1 \ \dots \ p'_{ns}]^T \\ P_t &:= [p'_{ns+1} \ \dots \ p'_n]^T \end{aligned}$$

where, the closed-loop participation factor of state  $q$  in the real eigenvalue  $i$ ,  $p'_{qi} = l_q^{i'} r_q^{i'}$ , can be written in terms of open-loop quantities and  $r_q^{i'}$  as (see (A.2) in Appendix A)

$$p'_{qi} = \frac{|R|}{|R'|} l_q^i r_q^{i'}$$

Define diagonal matrices  $L_{ns}$  and  $L_t$  as

$$L_{ns} = \begin{bmatrix} l_1^i & & & \\ & l_2^i & & \\ & & \ddots & \\ & & & l_{ns}^i \end{bmatrix} \quad \text{and} \quad L_t = \begin{bmatrix} l_{ns+1}^i & & & \\ & l_{ns+2}^i & & \\ & & \ddots & \\ & & & l_n^i \end{bmatrix},$$

respectively. Using (5.8),  $P_t$  and  $P_{ns}$  can be written as

$$P_{ns} = \frac{|R|}{|R'|} L_{ns} N_{\lambda_{ns}} k, \quad (5.9)$$

$$P_t = \frac{|R|}{|R'|} L_t N_{\lambda_t} k \quad (5.10)$$

respectively. The solution to the optimization problem is to find the coefficient vector  $k$  that maximizes the ratio between the norms of the two vectors  $\{P_{ns}, P_t\}$ .

The statement of the problem is

$$\max Q := \frac{P_{ns}^T P_{ns}}{P_t^T P_t} \quad (5.11)$$

$$\text{subject to } k^T k = 1$$

where  $(\cdot)^T$  indicates taking the transpose of a matrix or a vector. Using (5.9)–(5.10),

the objective function  $Q$  in (5.11) can be written as

$$Q = \frac{k^T N_{\lambda_{ns}}^T L_{ns}^T L_{ns} N_{\lambda_{ns}} k}{k^T N_{\lambda_t}^T L_t^T L_t N_{\lambda_t} k}$$

Denote  $N_{\lambda_{ns}}^T L_{ns}^T L_{ns} N_{\lambda_{ns}}$  and  $N_{\lambda_t}^T L_t^T L_t N_{\lambda_t}$  as  $G$  and  $H$  respectively. The objective

function  $Q$  can be rewritten in terms of matrices  $G$  and  $H$  as

$$Q = \frac{k^T G k}{k^T H k}$$

It is clear that  $G$  and  $H$  are symmetric matrices. If  $H$  is not positive definite, we may select  $k$  to drive the denominator of this objective function to zero. This would be the best case for our design; the participation factors of the low-value states in the mode  $i$  will be infinite relative to the participation factors of the rest of the system states. More likely, however, is the case in which  $H$  is of full rank. In this case,  $H$  will have a well-defined matrix square root ( $H^{1/2} = L_t N_{\lambda t}$ ), and the maximum value of the objective function  $Q$  in (5.11) is equal to the maximum eigenvalue of

$$E := H^{-1/2}GH^{-1/2}. \quad (5.12)$$

The associated principal direction of  $Q$ , which we may denote as  $v_{max}$ , determines  $k$  via

$$k = H^{-1/2}v_{max}$$

Therefore, it is possible to analytically find a coefficient vector  $k$  that solves the optimization problem. Knowing the optimal coefficient vector  $k_{opt}$ , the closed-loop right eigenvector  $r^{i'}$  can be computed using (5.8). Construction of the feedback gain matrix  $F$  is straightforward following steps (4) and (5) in Section 5.2.2.

## Numerical example

In this example, we revisit the example given in Section 5.2.2. Recall that the system has an eigenvalue equal to  $\{-0.1051\}$  and it is the closest eigenvalue to the origin. We focus on the case where states  $\{x_1, x_2\}$  are the high-value states while

states  $\{x_3, x_4\}$  are the low-value ones. No prior specifications on the closed-loop participation factors are given except that it is required that the participation factors of the low-value states be maximized with respect to the rest of the system states (high-value states in this example). Since the number of high-value states is two and the system has two inputs, one might think that a “good” solution is to exactly assign zeros to the closed-loop participation factors of states  $\{x_1, x_2\}$ . This is not possible as the rank of  $N_{\lambda_t}$  (matrix formed of the rows of  $N_\lambda$  associated with the high-value states) is two, i.e., no coefficient vector  $k$  can be found to assign zeros to the closed-loop participation factors of states  $\{x_1, x_2\}$  in the first mode. Thus, our objective is to assign the closed-loop participation factors of the system states to maximize the ratio of the participation factors of states  $\{x_3, x_4\}$  to states  $\{x_1, x_2\}$ .

Recall that open-loop participation factors of system states  $\{x_1, x_2, x_3, x_4\}$  in mode one ( $\lambda_i = -0.1051$ ) are  $\{1.1492, -0.0653, 0.0403, -0.1241\}$ , respectively. The ratio between the norms of the vectors of open-loop participation factors of states  $\{x_3, x_4\}$  and  $\{x_1, x_2\}$  is 0.0129. Computing matrix  $E$  in (5.12) yields

$$E = \begin{bmatrix} 1.0437 & 1.8279 \\ 1.8279 & 3.2066 \end{bmatrix}$$

The eigenvalues of  $E$  are  $\{0.0013, 4.249\}$ , and therefore, the maximum attainable value of the objective function  $Q$  is 4.249. The corresponding coefficient vector  $k_{opt}$  that achieves that value is  $[0.5107 \ 0.8598]^T$ . Computing the feedback gain matrix

$F$  yields

$$F = \begin{bmatrix} 0.5998 & 0.3245 & 0.6641 & -1.8007 \\ 0.1793 & 0.0970 & 0.1985 & -0.5383 \end{bmatrix}$$

The closed-loop participation factors of system states  $\{x_1, x_2, x_3, x_4\}$  in mode one are  $\{0.0015, 0.3244, 0.0053, 0.6687\}$ , respectively. The ratio between the norms of the vectors of closed-loop participation factors of states  $\{x_3, x_4\}$  and  $\{x_1, x_2\}$  is 4.249. This result shows a  $\{4.249/0.0129\} \simeq 329$ -fold increase between open-loop and closed-loop cases.

### 5.3 Participation Factor Assignment: Case of Eigenvalue Pair Approaching Imaginary Axis

In this section, we develop a state feedback control for assigning participation factors for systems nearing another form of instability. The approaching instability studied here is Hopf bifurcation, where a pair of complex conjugate eigenvalues cross the imaginary axis. Let  $\{\lambda_i, \lambda_{i+1} = \lambda_i^*\}$  be the pair of complex eigenvalues approaching the imaginary axis. As in the case of real eigenvalue approaching imaginary axis given in Section 5.2, the goal pursued by the control effort is to achieve a prescribed set of ratios between the norms of closed-loop participation factors of states in a group denoted as the control group. This will be done without affecting any eigenvalues or any right eigenvectors except those right eigenvectors associated with

mode  $i$ . Next, we show how to compute the desired closed-loop right eigenvectors  $\{r^{i'd}, r^{i+1'd}\}$  based on a given (desired) specification of the closed-loop participation factors.

### 5.3.1 Computing desired closed-loop right eigenvectors

$$\{r^{i'd}, r^{i+1'd} = r^{i'd*}\}$$

The same notation used in Section 5.2.1 to specify different components of the desired closed-loop right eigenvector  $r^{i'd}$  will be adopted here, i.e.,

$$r^{i'd} := \begin{bmatrix} r^s \\ r^{ns} \\ r^{nc} \end{bmatrix},$$

where,  $r^s \in \mathbb{C}^{n_s}$ ,  $r^{ns} \in \mathbb{C}^{n_{ns}}$ ,  $r^{nc} \in \mathbb{C}^{n-(n_s+n_{ns})}$  represent vectors of components of  $r^{i'd}$  corresponding to high-value, low-value and uncontrolled states, respectively.  $\{n_s, n_{ns}, n_{nc}\}$  represent the number of high-value, low-value and uncontrolled states, respectively. The high-value and low-value states form a control group. Let  $n_{ng} = n_s + n_{ns}$  be the number of control group states.

The case of zero closed-loop participation factors of high-value states in mode  $i$  is straightforward and it can be achieved by setting  $r_s = 0$  and  $r_{ns} = e \in \mathbb{C}^{n_{ns}}$  where  $e$  is a column vector of elements with nonzero norms (to avoid zero participation). The remaining  $(n - n_{ng})$  components are unspecified (unconstrained).

For the general case of nonzero closed-loop participation factors, let the

desired norms of the closed-loop participation factors of the control group states  $\{x_2, \dots, x_{n_{ng}}\}$  in mode  $i$  be given in terms of the norm of the closed-loop participation factor of state  $x_1$  (first state of the group), i.e., let  $z_k$ ,  $k = 2, \dots, n_{ng}$  be the desired ratio between the norm of the closed-loop participation factor of state  $x_k$  and that of state  $x_1$ . Next, we show how to write the closed-loop participation factor of the  $j$ -th state  $x_j$  in mode  $i$  in terms of the closed-loop right eigenvector  $r^{i'}$ . Recall that

$$p'_{ji} = l_j^{i'} r_j^{i'} \quad (5.13)$$

Denote by  $R'$  the matrix of closed-loop right eigenvectors

$$R' = \begin{bmatrix} r_1^1 & \dots & r_1^{i'} & r_1^{i'^*} & \dots & r_1^n \\ \vdots & \vdots & \vdots & \vdots & \vdots & \vdots \\ r_j^1 & \dots & r_j^{i'} & r_j^{i'^*} & \dots & r_j^n \\ \vdots & \vdots & \vdots & \vdots & \vdots & \vdots \\ r_n^1 & \dots & \underbrace{r_n^{i'}}_{r^{i'}} & \underbrace{r_n^{i'^*}}_{r^{i+1'}} & \dots & r_n^n \end{bmatrix}$$

where  $r^{i'}$  and  $r^{i+1'} = r^{i'^*}$  are the only closed-loop eigenvectors that are different from their corresponding open-loop values. The  $j$ -th component of the  $i$ -th closed-loop left eigenvector  $l_j^{i'}$ , which lies in the  $i$ -th row and  $j$ -th column of the matrix of closed-loop left eigenvectors  $L'$  ( $L' = R'^{-1}$ ), is given by:

$$l_j^{i'} = \frac{(-1)^{j+i}}{\det\{R'\}} \det\{M_{ij}\}, \quad (5.14)$$

where  $M_{ij}$  ( $M_{ij} \in \mathbb{C}^{(n-1) \times (n-1)}$ ) is the matrix that results from removing the  $j$ -th row and the  $i$ -th column of  $R'$ , i.e.,

$$M_{ij} = \begin{bmatrix} r_1^1 & \cdots & r_1^{i-1} & r_1^{i' *} & r_1^{i+2} & \cdots & r_1^n \\ \vdots & \vdots & \vdots & \vdots & \vdots & \vdots & \vdots \\ r_{j-1}^1 & \cdots & r_{j-1}^{i-1} & r_{j-1}^{i' *} & r_{j-1}^{i+2} & \cdots & r_{j-1}^n \\ r_{j+1}^1 & \cdots & r_{j+1}^{i-1} & r_{j+1}^{i' *} & r_{j+1}^{i+2} & \cdots & r_{j+1}^n \\ \vdots & \vdots & \vdots & \vdots & \vdots & \vdots & \vdots \\ r_n^1 & \cdots & r_n^{i-1} & \underbrace{r_n^{i' *}}_{r^{i+1'}} & r_n^{i+2} & \cdots & r_n^n \end{bmatrix}$$

Let

$$Q_j := [(-1)^{i+1}|C_{i1}| \cdots (-1)^{i+j-1}|C_{i(j-1)}| \underbrace{0}_{j\text{-th}} (-1)^{i+j}|C_{ij}| \cdots (-1)^{i+n-1}|C_{i(n-1)}|]^T$$

where matrices  $C_{im}$  ( $C_{im} \in \mathbb{C}^{(n-2) \times (n-2)}$ ) are formed by removing the  $m$ -th row and  $i$ -th column of  $M_{ij}$ , ( $m = 1, \dots, n-1$ ). The determinant of  $M_{ij}$  can now be obtained by cofactor expansion along the  $i$ -th column, yielding an expression in terms of  $r^{i+1'} = r^{i' *}$  and  $Q_j$ :

$$\det\{M_{ij}\} = r^{i'H} Q_j \quad (5.15)$$

where  $(\cdot)^H$  indicates taking the Hermitian, or complex conjugate transpose, of a matrix or vector. Using (5.13)–(5.15), the closed-loop participation factor  $p'_{ji}$  in (5.13) can be written as

$$p'_{ji} = \left\{ \frac{(-1)^{j+i}}{\det\{R'\}} \right\} \cdot \{r^{i'H} Q_j\} \cdot r_j^{i'} \quad (5.16)$$

Recall from (2.22) that  $r^{i'}$  can be written as

$$r^{i'} = N_\lambda k$$

for some vector  $k \in \mathbb{C}^m$  and  $N_\lambda$  defined as given in (2.18). Using that,  $p'_{ji}$  can be expressed as

$$p'_{ji} = \left\{ \frac{(-1)^{j+i}}{\det\{R'\}} \right\} \cdot \{k^H N_\lambda^H Q_j\} \cdot N_{\lambda_j} k \quad (5.17)$$

where  $N_{\lambda_j}$  is the  $j$ -th row of  $N_\lambda$ . To simplify the expression in (5.17), denote by  $\Theta_j$  the  $m \times m$  matrix

$$\Theta_j := N_\lambda^H Q_j N_{\lambda_j}. \quad (5.18)$$

Equation (5.17) now becomes

$$p'_{ji} = \frac{(-1)^{j+i}}{\det\{R'\}} \cdot k^H \Theta_j k \quad (5.19)$$

Note that square matrix  $\Theta_j$  ( $\Theta_j \in \mathbb{C}^{(m \times m)}$ ) is singular and of rank one.

Next, we state a proposition that focuses on solving this participation factor assignment problem in the case where we only desire to attain a certain ratio of closed-loop participation factors for two states. The proposition shows how to compute the  $i$ -th closed-loop right eigenvector  $r^{i'}$  (associated with the complex  $i$ -th eigenvalue  $\lambda_i$ ) to achieve a given (desired) ratio between the norms of closed-loop participation factors of two states  $\{x_j, x_l\}$  in mode  $i$ .

**Proposition 5.2** *Consider a linear time-invariant system (5.1–5.2), with the goal of achieving a desired ratio  $z$  between the norms of the closed-loop participation*

factors of any two states  $\{x_j, x_l\}$  in the critical mode “ $i$ .” Suppose that the matrices  $\{\Theta_j, \Theta_l\}$  don’t have the same null space. (Recall that matrices  $\{\Theta_j, \Theta_l\}$  are given by (5.18).) Then, it is possible to achieve the desired ratio  $z$  of participation factors without affecting any right eigenvectors except those associated with mode  $i$ .

**Proof:** See Appendix A.2.

Thus, according to Proposition 5.2, it is likely to find vectors  $k^j, j = 2, \dots, n_{ng}$  that solve for all desired ratios  $z_j, j = 2, \dots, n_{ng}$ . Despite that, it might be impossible to find a single vector  $k$  that simultaneously solves for all desired ratios  $z_j, j = 2, \dots, n_{ng}$ . A candidate coefficient vector  $k_{cad}$  could be a weighted sum of the computed  $k^j$ ’s that solves for the  $z_j$ ’s. Those weights can be chosen based on the most desired ratios. If for example, the ratios are equally desired, then the candidate vector  $k_{cad}$  is simply the average of the computed  $k^j$ ’s.

### 5.3.2 Feedback control design: exactly assignable case

Unlike exactly assignable cases discussed in Section 5.2.2 for systems with a real eigenvalue approaching zero, the cases discussed in this section are limited. Two cases are discussed, case (a) where we only desire zero closed-loop participation of high-value states (of dimension less than number of inputs  $m$ ) in mode  $i$ , and case (b) where we only desire to attain certain ratio between norms of closed-loop participation factors for two states only. The feedback control design follows a similar approach to the one given for the real eigenvalue case except for some minor

changes.

Recall the main assumption of the assignment problem, that is, the controller should not change any open-loop eigenvalue or any open-loop right eigenvector except the eigenvectors  $(r^i, r^{i+1} = r^{i*})$  associated with mode  $i$ . Saying that, the same argument presented in the real eigenvalue case holds, i.e., according to Proposition 2.1, there exist a feedback gain matrix  $F$  such that all open-loop pairs  $(\lambda_j, r^j)$ ,  $\{j = 1, 2, \dots, n, j \neq \{i, i + 1\}\}$  can be kept invariant from their original, uncontrolled values. Next we recall the steps to compute the state feedback gain matrix  $F$  given in Section 2.3.1 with the appropriate modifications to solve the assignment problem beforehand.

### Steps to compute $F$ : case (a)

1. Set  $r^s$  (vector of closed-loop right eigenvector components corresponding to high-value states) to zeros.
2. Form a column vector  $e \in \mathbb{C}^{m-n_s}$  of elements of nonzero norms.
3. Compute  $k$  to satisfy

$$\begin{bmatrix} r^s \\ e \end{bmatrix} = \tilde{N}_{\lambda_i} k$$

where  $\tilde{N}_{\lambda_i}$  is the  $m \times m$  matrix of the first  $m$  rows of  $N_{\lambda_i}$  (defined in (2.18)) associated with the first  $m$  states.<sup>2</sup> The closed-loop right eigenvector  $r^{i'}$  is

---

<sup>2</sup>In case  $\tilde{N}_{\lambda_i}$  is singular, see footnote in page 81.

then given by

$$r^{i'} = N_{\lambda_i} k$$

4. Let

$$w^i = -M_{\lambda_i} k.$$

Construct the real matrices  $W \in \mathbb{R}^{m \times n}$  and  $V \in \mathbb{R}^{n \times n}$

$$W = [0 \dots 0 \operatorname{Re}\{w^i\} \operatorname{Im}\{w^i\} 0 \dots 0]$$

$$V = [\dots \operatorname{Re}\{r^j\} \operatorname{Im}\{r^j\} \dots \operatorname{Re}\{r^{i'}\} \operatorname{Im}\{r^{i'}\} \dots r^q \dots]$$

where  $r^j$  and  $r^q$  represent open-loop right eigenvectors associated with complex and real eigenvalues, respectively.

5. The feedback gain matrix  $F$  is given by

$$F = WV^{-1}.$$

### Steps to compute $F$ : case (b)

1. Using the result stated in Proposition 5.2, compute the coefficient vector  $k$  that achieves the desired ratio of participation factors between two states.

The closed-loop right eigenvector  $r^{i'}$  is then given by

$$r^{i'} = N_{\lambda_i} k$$

2. Follow steps (4) and (5) of the procedure to compute  $F$  given for case (a) above.

### 5.3.3 Feedback control design: not exactly assignable case

This case involves the assignment of closed-loop participation factors of more than two states. Assuming the existence of solution vectors  $k^j$ ,  $j = 2, \dots, n_{ng}$  that solve for all desired ratios  $z_j$ ,  $j = 2, \dots, n_{ng}$ , a candidate coefficient vector  $k_{cad}$  is a weighted sum of the computed  $k^j$ 's that solves for the  $z_j$ 's (as discussed in Section 5.3.1). The weights are chosen based on system's operation and operator's experience. The closed-loop right eigenvector  $r^{i'}$  is given by

$$r^{i'} = N_{\lambda_i} k_{cad}.$$

Construction of the feedback gain matrix  $F$  is straightforward following steps (4) and (5) of the procedure to compute  $F$  given for case (a) of the exactly assignable case. Next, we present a numerical example of participation factor assignment involving more than two states.

#### Numerical example

The example in Section 5.2.2 is revisited but with a slight modification. The system considered here has an extra input, i.e., the input matrix  $B$  has an extra column,

$$B = \begin{bmatrix} 1 & 0 & 2 \\ 0.76 & -1.6 & -5 \\ -0.95 & -0.032 & 3 \\ 0.03 & 0 & 2.8 \end{bmatrix}.$$

As noted in the example in Section 5.2.2, The system's four eigenvalues are  $\{-0.1051, -1.4811 \pm 0.6239i, -2.0127\}$ . For the mode associated with the pair of complex conjugate eigenvalues (eigenvalues 2 and 3), let us focus on its associated participation factors for assignment through feedback. The open-loop participation factors of system states  $\{x_1, x_2, x_3, x_4\}$  in that mode are  $\{-0.0446 - 0.1059i, 0.0129 + 0.1872i, 0.3868 - 1.1663i, 0.6449 + 1.0850i\}$ , respectively. The norms of the open-loop participation factors are  $\{0.1149, 0.1877, 1.2287, 1.2621\}$ . Suppose that three states  $\{x_1, x_2, x_4\}$  are selected to form the control group with state  $x_4$  chosen as the high-value state and states  $\{x_1, x_2\}$  are the low-value ones. The open-loop participation ratios are  $\frac{|p_{12}|}{|p_{42}|} = 0.0910$  and  $\frac{|p_{22}|}{|p_{42}|} = 0.1487$ . Note that the open-loop participation of the high-value state  $x_4$  is higher than the participation of the low-value states  $\{x_1, x_2, x_4\}$  in the second (and third) mode.

Suppose it is desired to assign the participation of states  $\{x_1, x_2, x_4\}$  to achieve the following desired ratios between norms of closed-loop participations:  $z_1^d = \frac{|p'_{12}|}{|p'_{42}|} = 1.2$  and  $z_2^d = \frac{|p'_{22}|}{|p'_{42}|} = 2.24$ . Using the procedure given in the proof of Proposition 5.2 (see Appendix A), the coefficient vectors  $\{k^1, k^2\}$  that separately solve for the desired ratios  $\{z_1^d, z_2^d\}$ , respectively, are

$$\begin{aligned} k^1 &= [0.3299 \quad -0.1856 + 0.3824i \quad 0.8452 + 0.3967i]^T, \\ k^2 &= [0.3531 \quad -0.1558 + 0.3824i \quad 0.7623 + 0.3967i]^T \end{aligned}$$

Choosing  $k_{cad}$  to be the average of  $\{k^1, k^2\}$  yields,

$$k_{cad} = [0.3415 \quad -0.1707 + 0.3824i \quad 0.8037 + 0.3967i]^T$$

Table 5.1 shows the different possibly achievable closed-loop ratios  $\{z_1, z_2\}$  for different coefficient vectors  $\{k^1, k^2\}$  and for the candidate vector  $k_{cad}$ .

	$z_1 = \frac{ p'_{12} }{ p'_{42} }$	$z_2 = \frac{ p'_{22} }{ p'_{42} }$
$k^1$	1.20	1.84
$k^2$	1.45	2.24
$k_{cad}$	1.31	2.02

Table 5.1: Closed-loop ratios  $\{z_1, z_2\}$  for coefficient vectors  $\{k^1, k^2, k_{cad}\}$ . The desired closed-loop ratios are  $\{z_1^d = 1.2, z_2^d = 2.24\}$ .

## Chapter 6

# Application to Electric Power Networks

In this chapter, we apply the results obtained in Chapter 5 on participation factor assignment for LTI systems to an example from electric power networks. The system (at equilibrium) is operating close to instability where a pair of complex eigenvalues is close to the imaginary axis. Modal analysis of linearized model of that network is performed. Generators highly affected by the critical mode are identified. State feedback control is applied to assign the participation factors of a group of the state variables to protect high-value generating units.

This chapter proceeds as follows. In Section 6.2, Western System Coordinating Council (WSCC) 3-generator, 9-bus power system model, is examined. This system has a critical electrical mode associated with the system exciters. A state feedback control is designed for assigning closed-loop participation factors. The goal fulfilled is to trade the risk of participation in the critical mode between a *high-value* generator and the other generators in the system denoted as *low-value* generators.

In Section 6.3, remarks on the use of state feedback in power networks are given.

## 6.1 Introduction

For small disturbance analysis in electric power networks, the participation factor of a mode in a state can be interpreted, from the view point of probability, as the participation “risk”. Larger norm of participation factor of a state in a particular mode means it has more effect on and will be more affected by this mode. It may be desirable that the participation factor of a particular state variable be reduced in some critical system modes. This desire is based on the fact that the higher the magnitude of participation factor the higher the tendency of such state to be affected in a serious way by an impending (or true) instability. In power systems operation, nuclear units, for example, are regarded as high value subsystems. Reducing participation factors of these units in some critical mechanical and/or electrical mode would reduce the risk of premature tripping, as well as alleviate the effect on these units of a troublesome mode being excited.

## 6.2 Three-Generator Nine-Bus Power System

In this section, we revisit the Western System Coordinating Council (WSCC) 3-generator, 9-bus power system model, studied for monitoring impending instabilities in Section 4.2.3 (see Figure 4.8 for the line diagram). In this model, a subcritical

Hopf bifurcation occurs as the load on bus 5 is increased beyond 4.5 pu [33]. It is observed that the critical modes associated with the pair of complex conjugate eigenvalues closest to the imaginary axis are the electrical ones associated with the exciter. The system is composed of three synchronous generators equipped with three identical IEEE-type I exciters. A fourth order model is used to capture the dynamics of the synchronous generator:

$$\begin{aligned}\dot{\delta} &= \Omega_b(\omega - 1) \\ \dot{\omega} &= (T_m - T_e - D(\omega - 1))/M \\ \dot{e}'_q &= (-f_s(e'_q) - (x_d - x'_d)i_d + v_f^*)/T'_{d0} \\ \dot{e}'_d &= (-e'_d + (x_q - x'_q)i_q)/T'_{q0},\end{aligned}$$

where the subscripts  $d$  and  $q$  refer to the direct and quadrature axes, respectively.  $f_s(\cdot)$  captures the saturation characteristic of the synchronous generator. The electrical power is

$$P_e = (v_q + r_a i_q)i_q + (v_d + r_a i_d)i_d$$

and current link is described by the equations:

$$\begin{aligned}0 &= v_q + r_a i_q - e'_q + (x'_d - x_1)i_d \\ 0 &= v_d + r_a i_d - e'_d + (x'_q - x_1)i_q\end{aligned}$$

The exciter is depicted in Figure 6.1 and described by the following equations:

$$\begin{aligned}
 \dot{v}_m &= (V - v_m)/T \\
 \dot{v}_{r1} &= (K_a(V_{ref} - v_m - v_{r2} - \frac{K_f}{T_f}v_f) - v_{r1})/T_a \\
 v_r &= \begin{cases} v_{r1} & \text{if } v_{r\min} \leq v_{r1} \leq v_{r\max} \\ v_{r\max} & \text{if } v_{r1} > v_{r\max}, \\ v_{r\min} & \text{if } v_{r1} < v_{r\min}. \end{cases} \\
 \dot{v}_{r2} &= -(\frac{K_f}{T_f}v_f + v_{r2})/T_f \\
 \dot{v}_f &= -(v_f(1 + S_e(v_f)) - v_r)/T_e
 \end{aligned} \tag{6.1}$$

The generators and excitors data are given in Section 4.2.3. Details of loads and

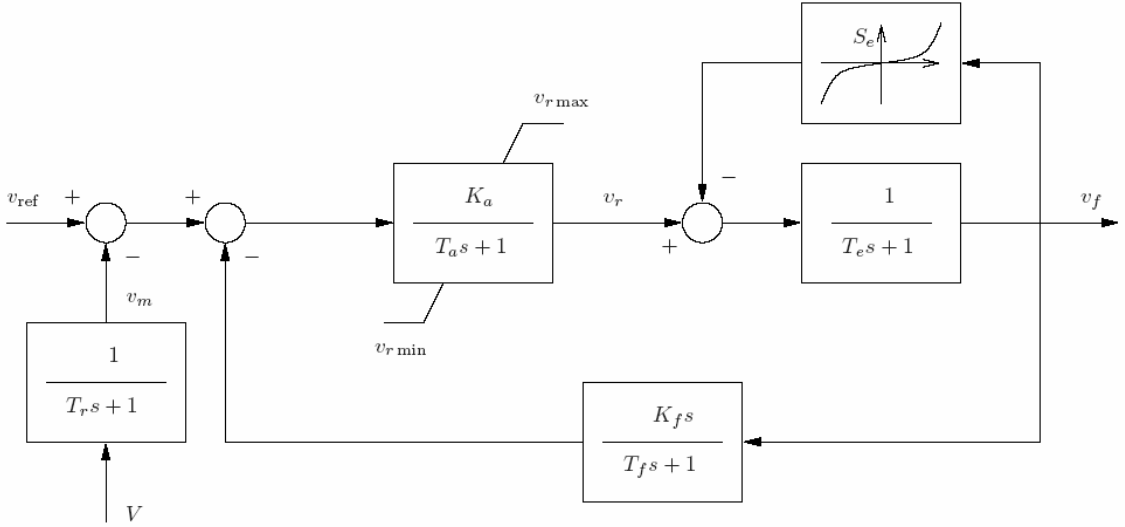


Figure 6.1: Exciter for the three-generator, nine-bus system.

transmission lines can be found in [33]. The system has 24 states arranged as follows:

$$x(t) = [\delta_1 \ \omega_1 \ e'_{q1} \ e'_{d1} \ v_{m1} \ v_{r11} \ v_{r21} \ v_{f1} \ \dots]^T.$$

When the load at bus 5 is 4.4 pu, the linearization of the system at the operating point has a complex conjugate pair of eigenvalues  $\lambda_{\{i,i+1\}} = -0.04602 \pm j2.1151$ . This is the pair of complex conjugate eigenvalues closest to the imaginary axis. Denote the mode associated with that pair of eigenvalues as the critical mode. Computing the participation factors of system states in that mode reveals that states representing  $q$ -axis transient voltage,  $e'_q$ , are the states with the highest participation in the critical mode. Table 6.1, shows the states having the highest open-loop participation factors in the critical mode. Note that, the norms of the participation factors were divided by the sum of the norms of the participation factors to get more sense out of the numbers for comparison.

State	$ r_q^i $	$\angle r_q^i$	$ p_{qi}  = \frac{ r_q^i }{\sum_{k=1}^n  r_k^i }$
$e'_{q3}$	0.0108	66.802	0.19887
$e'_{q1}$	0.0189	34.437	0.14365
$e'_{q2}$	0.0230	43.401	0.09643
$e'_{d1}$	0.0339	9.702	0.07081
$e'_{d2}$	0.0323	5.327	0.05138
$v_{r21}$	0.0481	-59.185	0.05207
$v_{r22}$	0.0433	-55.0678	0.07031

Table 6.1: The states with the highest norms of open-loop participation factors in the critical mode associated with  $\lambda_{\{i,i+1\}} = -0.04602 \pm j2.1151$ . The load at bus 5 is 4.4 pu.

Observe that  $e'_{q3}$ ,  $q$ -axis transient voltage of the third generator, is the state with the highest participation in the critical mode indicating that the third gen-

erator is the most affected generator by the critical mode. Assume that the third generator is a high-value generator (nuclear unit for example). We would like to lower the participation of this generator in the critical mode to alleviate any undesirable effects that may possibly occur if the critical mode is excited. The critical mode of the system can be revealed from the time domain simulation by applying a 2% perturbation to the initial condition of the  $q$ -axis transient voltage of generator 2 ( $e_{q_2}^0$ ) while keeping the rest of the states at their equilibrium values. The resulting  $q$ -axis transient voltage of generators 1, 2, and 3 are shown in Figure 6.2. From Figure 6.2, it is obvious that after short-time transients of the three generators, a poorly damped mode with frequency around 0.33 Hz can be detected (note the sustained oscillations). This is consistent with that the critical mode is associated with a pair of eigenvalues with frequency of 0.3337 Hz. Note also how the 3 states reacts differently to the perturbation.  $e'_{q_3}$ , for example, is the most affected followed by  $e'_{q_2}$  followed by  $e'_{q_1}$ . This is expected from the values of the norms of the participation factors of the  $q$ -axis transient voltage states in the critical mode (see Table 6.1).

The open-loop ratios between the norms of the participation factors of states  $\{e'_{q_1}, e'_{q_2}\}$  and state  $e'_{q_3}$  are  $\{0.7223, 0.4849\}$ , respectively. Suppose it is desired that the closed-loop ratios between the norms of the participation factors of states  $\{e'_{q_1}, e'_{q_2}\}$  and state  $e'_{q_3}$  are  $\{z_{13} = 2.92, z_{23} = 2.03\}$ , respectively. Particularly, we need to trade the risk of participation in the critical mode between the third generator (high-value generator) and the other two generators (low-value generators) of the

system. Next, we design a state feedback control to assign the system participation factors in the critical mode to fulfil the goal mentioned above.

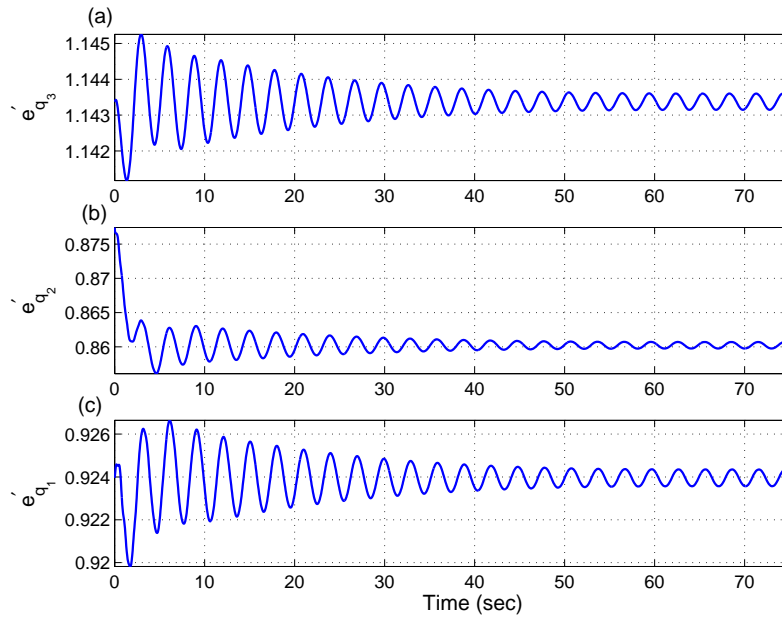


Figure 6.2: Open-loop response for a perturbation of 2% in the initial condition of the  $q$ -axis transient voltage of generator 2 ( $e_{q_2}^0$ ) of the WSCC 3-gen., 9-bus power system. (a)  $e'_{q_3}$ , (b)  $e'_{q_2}$  and (c)  $e'_{q_1}$ .

### 6.2.1 Feedback control design

Recall the procedure for the control design given in Section 5.3.3. We have two desired ratios  $\{z_{13}, z_{23}\}$  relating the closed-loop norms of the participation factors of  $q$ -axis transient voltage states,  $e'_{q_k}$ ,  $k = 1, 2, 3$ , to achieve. The control action will take place through the the reference input of the exciter connected to each generator. The input matrix  $B$  is a matrix of dimension  $(24 \times 3)$  of zeros except at

entries (14, 1), (18, 2) and (22, 3) corresponding to input  $v_{ref}$  of generators 1, 2 and 3, respectively (see (6.1)). The nonzero entries are identical and equal to  $\frac{K_a}{T_a} = 100$ . Using the procedure given in the proof of Proposition 5.2 (see Appendix A), the coefficient vectors  $\{k^1, k^2\}$  that separately solve for the desired ratios  $\{z_{13}, z_{23}\}$ , respectively, are

$$\begin{aligned} k^1 &= [0.2753 + 0.1238i \quad 0.5075 - 0.4070i \quad 0.1508 - 0.5426i]^T, \\ k^2 &= [0.2347 - 0.0288i \quad 0.6427 - 0.1942i \quad -0.0374 - 0.5528i]^T. \end{aligned}$$

Choosing  $k_{cad}$  to be the average of  $\{k^1, k^2\}$  yields,

$$k_{cad} = [0.2550 + 0.0475i \quad 0.5751 - 0.3006i \quad 0.0567 - 0.5477i]^T.$$

Table 6.2 shows the different possibly achievable closed-loop ratios for different coefficient vectors  $\{k^1, k^2\}$  and for the candidate vector  $k_{cad}$ .

	$z_{13}$	$z_{23}$
$k^1$	2.92	1.227
$k^2$	1.9425	2.03
$k_{cad}$	2.4314	1.6341

Table 6.2: Closed-loop ratios  $\{z_{13}, z_{23}\}$  for coefficient vectors  $\{k^1, k^2, k_{cad}\}$ . The desired closed-loop ratios are  $\{z_{13} = 2.92, z_{23} = 2.03\}$ .

Table 6.3 shows the states having the highest closed-loop participation factors in the critical mode. As expected, the participation of the  $q$ -axis transient voltage state of generator 3 in the critical mode is reduced, and it is not the state with the

State	$ p_{qi}  = \frac{ l_q^i  r_q^i }{\sum_{k=1}^n  l_k^i  r_k^i }$
$e'_{q3}$	0.0864
$e'_{q1}$	0.20754
$e'_{q2}$	0.13934
$e'_{d1}$	0.07036
$e'_{d2}$	0.04882
$v_{r12}$	0.05019
$v_{r21}$	0.07605

Table 6.3: The states with the highest norms of closed-loop participation factors in the critical mode associated with  $\lambda_{\{i,i+1\}} = -0.04602 \pm j2.1151$ . The load at bus 5 is 4.4 pu.

highest participation in the critical mode. Time domain simulations of this model were conducted using PSAT [16]. Figures 6.3-6.5 show the different time response of the  $q$ -axis transient voltage states,  $\{e'_{q1}, e'_{q2}, e'_{q3}\}$ , for a 2% perturbation to the initial condition of the  $q$ -axis transient voltage of generator 2 ( $e_{q2}^0$ ) before and after control. The Figures show the improvement in the response of the high-value state  $e'_{q3}$  of the third machine and the effects of increased participation in the critical mode of the low-value states  $\{e'_{q1}, e'_{q2}\}$  of the first and second machine, respectively.

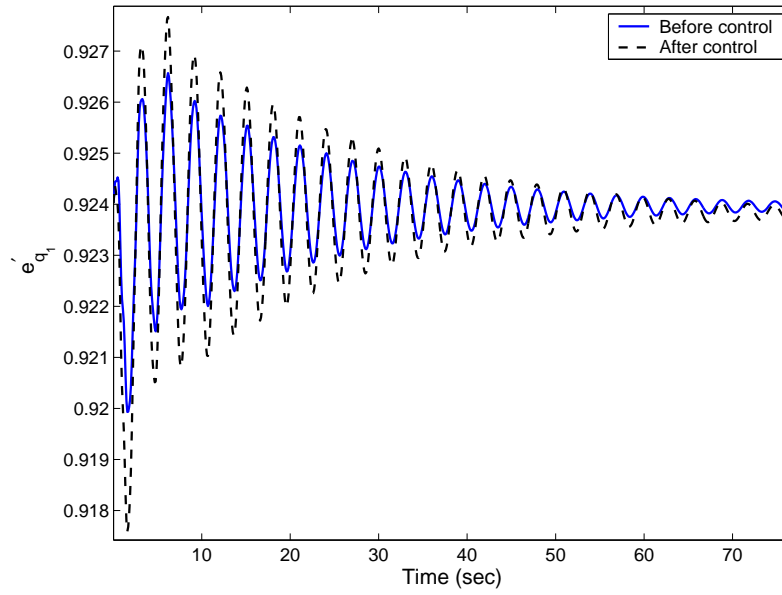


Figure 6.3: Plot of  $q$ -axis transient voltage of generator 1 ( $e'_{q1}$ ) versus time for a perturbation of 2% in the initial condition of the  $q$ -axis transient voltage of generator 2 ( $e'_{q2}$ ) before and after control.

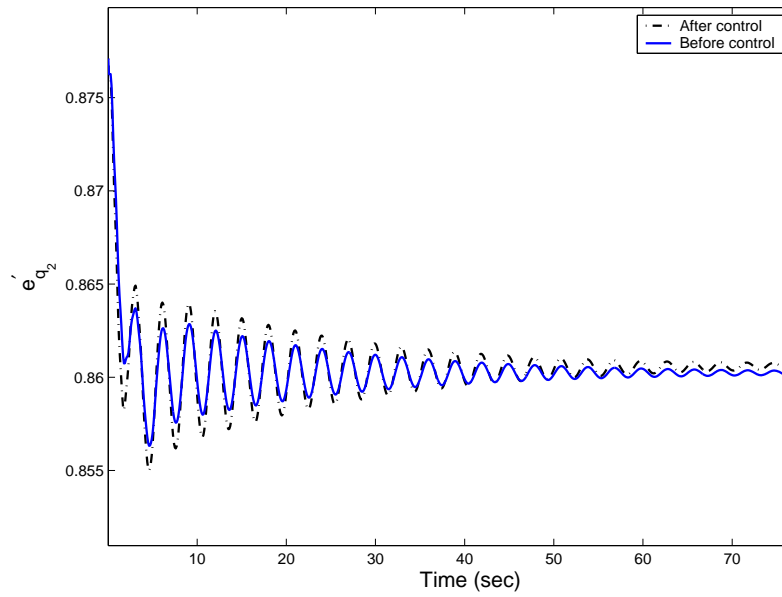


Figure 6.4: Plot of  $q$ -axis transient voltage of generator 2 ( $e'_{q_2}$ ) versus time for a perturbation of 2% in the initial condition of the  $q$ -axis transient voltage of generator 2 ( $e'_{q_2}$ ) before and after control.

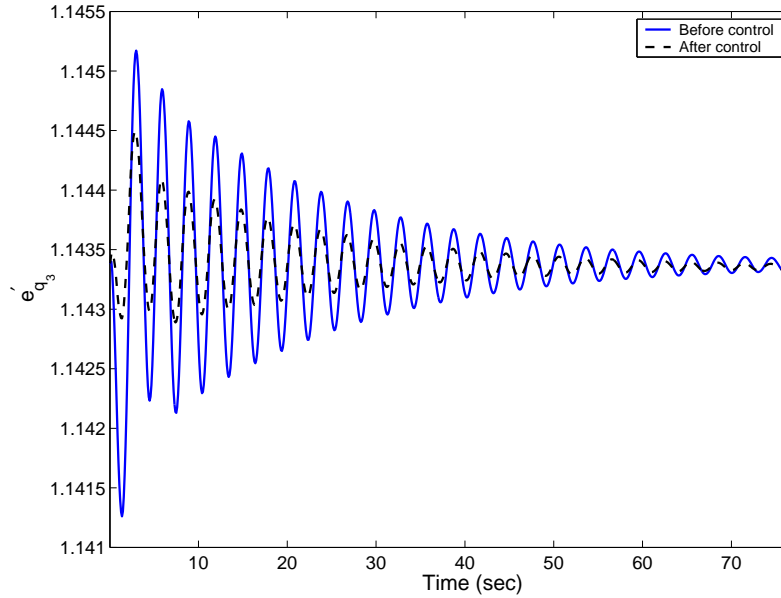


Figure 6.5: Plot of  $q$ -axis transient voltage of generator 3 ( $e'_{q_3}$ ) versus time for a perturbation of 2% in the initial condition of the  $q$ -axis transient voltage of generator 2 ( $e''_{q_2}$ ) before and after control.

### 6.3 Remarks on Use of State Feedback in Power Networks

The work in this chapter assumes access to the system state vector for purposes of feedback control. There are several ways to deal with this assumption from a practical perspective. One approach is to use a dynamic observer to calculate the state vector from available output measurements. Another approach is to calculate a state feedback control and then approximate it by an output feedback controller. The third approach is to actually make real-time state measurements available, and this is a real possibility in light of recent technological developments in real-time

phasor measurements [45]. As noted by Phadke [45], synchronized phasor measurements provide the first real possibility of providing a dynamic state estimator. Using such measurements, it is possible for the substations to provide a continuous stream of phasor data to the control center. In this way, a state vector estimate that follows the system dynamics can be constructed. With normal dedicated communication circuits, a continuous data stream of one phasor measurement every 2-5 cycles (33.3 - 83.33 msec) can be sustained. Considering that typical power system dynamic phenomena fall in the frequency range of 0-2 Hz, it is possible to observe power system dynamic phenomena in real-time with high fidelity at the control center.

## Chapter 7

# Conclusions and Future Directions

### 7.1 Conclusions

In this dissertation, we have developed monitoring and control systems to improve the performance of systems that are sometimes required to operate at the edge of their stability envelopes. Our main contributions are as follows:

- We used the concept of modal participation factors extensively in this work, and generalized the concept in several directions. In particular, we introduced output participation factors and input-to-output participation factors.
- A signal-based approach for real-time detection of impending instability in nonlinear systems was considered. The main idea pursued involves using a small additive white Gaussian noise as a probe signal and monitoring the spectral density of one or more measured states or outputs for certain signatures of impending instability. Input-to-state and input-to-output participation fac-

tors were introduced as tools to aid in selection of locations for probe inputs and states or outputs to be monitored, respectively. Since these participation factors are model-based, the work presented combines signal-based and model-based ideas toward achieving a robust methodology for instability monitoring. We also introduced a proximity index to help assess closeness to instability based on power spectral density measurement.

- We also introduced the problem of participation factor assignment by feedback, and made important progress on this problem. Feedback algorithms were developed for assigning modal participation factors using eigenvector assignment-based techniques. The goal is to reduce the interaction between a selected group of states (*high-value group*) and an undesirable mode. In particular, we addressed two cases, first the case of a mode associated with a single real eigenvalue approaching zero (*Stationary bifurcation*), and second the case of a mode associated with a pair of conjugate complex eigenvalues approaching the imaginary axis (*Hopf bifurcation*). A novel procedure for computing the desired closed-loop right eigenvector(s) associated with the critical mode (based on given constraints on the desired closed-loop participation factors) was presented
- We applied our results to a well-studied electric power network, the WSCC 3-generator, 9-bus network. As expected, participation factor assignment has a clear effect on the relative time domain responses of system states.

## 7.2 Future Directions

Among the many open problems of interest are the following:

- More work is needed on generalized participation factors and on participation factor assignment by state and output feedback. Particularly, the problem of finding a definition for participation of outputs in modes that reduces to the original state participation when the output is simply one of the states is yet to be solved. Unlike state participation problem that has identical expressions for participation of modes in states and states in modes, the output participation problem is quite different and an expression for participation of outputs in modes is not expected to be the same as the expression proposed for participation of modes in outputs in Chapter 3.
- A particularly challenging problem involves detection not only nearness to instability, but also detecting the severity of the impending instability from the point of view of nonlinear system behavior. For example, an oscillatory instability can be of the hunting type, in which small amplitude oscillations occur, or it can be divergent, resulting in complete loss of operation. Although this can be determined using analytical models using known methods of bifurcation analysis, it is not known how this can be achieved using a signal-based approach.
- Another direction involves studying use of other probe signals besides AWGN.

Examples include periodic signals, chaotic signals covering an appropriate frequency range, and colored noise signals. The relative advantages and disadvantages of the various probe signals should be considered. In this regard, connections to past work in real-time probing of power systems and aircraft dynamics should be studied. In research aircraft, for example, it is common to use “chirp” signals to probe the aircraft for its stability properties in various parts of its flight envelope.

## Appendix A

# Proof of Propositions 5.1 and 5.2

## A.1 Proof of Proposition 5.1

The matrix of closed-loop right eigenvectors  $R'$  is given by

$$R' = [r^1 \ \dots \ r^{i'} \ \dots \ r^n],$$

where  $r^{i'}$  (associated with the real eigenvalue  $\lambda_i$ ) is the only closed-loop right eigenvector affected by the control law. The matrix of closed-loop left eigenvectors  $L' = R'^{-1}$  is given by

$$L' = [l^{1'T} \ \dots \ l^{i'T} \ \dots \ l^{n'T}]^T.$$

The closed-loop  $i$ -th left eigenvector  $l^{i'}$  is given by

$$l^{i'} = \frac{1}{\det\{R'\}} [c_{i1} \ \dots \ c_{ik} \ \dots \ c_{in}],$$

where the  $c_{ik}$ 's,  $k = 1, 2, \dots, n$ , represent matrix cofactors, i.e.,

$$c_{ik} = (-1)^{k+i} \cdot \det\{M_{ik}\},$$

where  $M_{ik}$  is the matrix of dimension  $(n-1)$  that is obtained by eliminating the  $k$ -th row and the  $i$ -th column of  $R'$ . Since the only change to the open-loop right modal matrix  $R$  is to the components of its  $i$ -th column  $r^i$ , the  $c_{ik}$ 's,  $k = 1, 2, \dots, n$  are only function in open-loop left eigenvectors  $l^q$ 's,  $q = 1, \dots, n$ ,  $q \neq i$ . Therefore, the  $k$ -th component of the closed-loop  $i$ -th left eigenvector  $l^{i'}$  can be written in terms of the  $k$ -th component of the open-loop  $i$ -th left eigenvector  $l_k^i$  as

$$l_k^{i'} = \frac{\det\{R\}}{\det\{R'\}} l_k^i. \quad (\text{A.1})$$

Using (A.1), the closed-loop participation factor of state  $k$  in mode  $i$  is reduced to

$$\begin{aligned} p'_{ki} &= l_k^{i'} r_k^{i'} \\ &= \frac{\det\{R\}}{\det\{R'\}} l_k^i r_k^{i'} \end{aligned} \quad (\text{A.2})$$

Next, we use (A.2) to write the desired ratio  $z$  between the closed-loop participation factors of states  $\{x_k, x_j\}$  in mode  $i$  as

$$z = \frac{p'_{ki}}{p'_{ji}} = \frac{l_k^{i'} r_k^{i'}}{l_j^{i'} r_j^{i'}} \quad (\text{A.3})$$

$$= \frac{l_k^i r_k^{i'}}{l_j^i r_j^{i'}}, \quad (\text{A.4})$$

Therefore, to achieve the desired ratio  $z$ , the closed-loop right eigenvector components  $r_k^{i'}$ ,  $r_j^{i'}$  should be chosen such that  $\frac{r_k^{i'}}{r_j^{i'}} = \frac{z}{l_k^i/l_j^i}$ . ■

## A.2 Proof of Proposition 5.2

The closed-loop participation factor of the  $j$ -th state  $x_j$  in mode  $i$  in terms of the closed-loop right eigenvector  $r^{i'}$  is given by (see (5.13)):

$$p'_{ji} = \frac{(-1)^{j+i}}{\det\{R'\}} \cdot k^H \Theta_j k \quad (\text{A.5})$$

The ratio between the norms of the closed-loop participation factors of two states  $\{x_j, x_l\}$  in the critical mode “ $i$ ” is:

$$\frac{|p'_{ji}|}{|p'_{li}|} = \frac{|l_j^{i'}| |r_j^{i'}|}{|l_l^{i'}| |r_l^{i'}|} \quad (\text{A.6})$$

$$= \frac{|k^H \Theta_j k|}{|k^H \Theta_l k|}, \quad (\text{A.7})$$

where matrices  $\{\Theta_j, \Theta_l\}$  are given by (5.18). Matrices  $\{\Theta_j, \Theta_l\} (\in \mathbb{C}^{m \times m})$  are singular and of rank one. The goal is to find a coefficient vector  $k (\in \mathbb{C}^m)$  that achieves a desired ratio  $z$  between the norms of the closed-loop participation factors of the two states  $\{x_j, x_l\}$  in the critical mode “ $i$ ,” i.e., find  $k$  that solves:

$$\begin{aligned} \frac{|p'_{ji}|}{|p'_{li}|} &= \frac{|k^H \Theta_j k|}{|k^H \Theta_l k|} \\ &= z. \end{aligned} \quad (\text{A.8})$$

In general, if there are any solutions other than 0, one would expect the solutions to form a variety of codimension 1 in  $\mathbb{C}^m$ . If we can find some  $k^0$  for which the right side of (A.8) is less than  $z$  and some  $k^1$  for which it is greater than  $z$ , then there is a solution  $k$ ,

$$k = t k^0 + (1 - t) k^1, \quad 0 < t < 1. \quad (\text{A.9})$$

The squares of the norms in (A.8) are quartic polynomials in  $t$ . Solving these quartic polynomials for  $t$ , we can find  $k$  that solves for the desired ratio. One possible choice of  $k^0$  is a vector that lies in the null space of  $\Theta_j$  and not in the null space of  $\Theta_l$  (in this case, the right side of (A.8) is equal to zero). One possible choice of  $k^1$  is a vector that lies in the null space of  $\Theta_l$  and not in the null space of  $\Theta_j$  (in this case, the right side of (A.8) is equal to infinity). Note that this is always possible providing that the assumption on matrices  $\{\Theta_j, \Theta_l\}$  of Proposition 5.2 holds. Knowing  $t$ , the coefficient vector  $k$  that solves for the desired ratio  $z$  can be computed using (A.9). ■

## Appendix B

### Table of Symbols

Symbol	Meaning
$\det\{A\}$ or $ A $	determinant of $A$
$\operatorname{Re}\{v\}$	Real part of $v$
$\operatorname{Im}\{v\}$	Imaginary part of $v$
$A^T, x^T$	transpose of matrix $A$ , vector $x$
$A^*, x^*$	conjugate of matrix $A$ , vector $x$
$A^H, x^H$	conjugate transpose of matrix $A$ , vector $x$
$ a $	absolute value (magnitude, if $a$ is complex) of $a$
$\ x\ $	norm of vector $x$
$e^j$	$j$ -th unit vector ( $j$ -th entry is 1; 0 otherwise)
$\mathbb{R}^n(\mathbb{C}^n)$	real (complex) $n$ -dim. space
$\mathbb{R}^{m \times n}(\mathbb{C}^{m \times n})$	real (complex) $m \times n$ matrices

## Bibliography

- [1] F. L. Pagola, I. J. Perez-Arriaga and G. C. Verghese, “On sensitivities, residues and participations: Applications to oscillatory stability analysis and control,” *IEEE Transactions on Power Systems*, Vol. 4, No. 1, pp. 278–285, Feb. 1989.
- [2] I. J. Perez-Arriaga, G. C. Verghese and F. C. Schweppe, “Selective modal analysis with applications to electric power systems, Part I: Heuristic introduction,” *IEEE Transactions on Power Apparatus and Systems*, Vol. 101, No. 9, pp. 3117–3125, Sep. 1982.
- [3] P. Kundur, *Power System Stability and Control*. McGraw Hill, New York, 1994.
- [4] C. L. DeMarco, “Design of predatory generation control in electric power systems,” *Thirty-First Annual Hawaii International Conference on System Sciences HICSS*, Vol. 3, pp. 32–38, Jan. 1998.
- [5] E. Abed, A. Tesi and H. Wang, “Control of bifurcation and chaos,” in *The Control Handbook*, (CRC Press), 1996.

- [6] E. H. Abed and J. H. FU, “Local feedback stabilization and bifurcation control, I. Hopf bifurcation,” *Systems and Control Letters*, Vol. 7, pp. 11–17, February 1986.
- [7] E. H. Abed and J. H. FU, “Local feedback stabilization and bifurcation control, II. stationary bifurcation,” *Systems and Control Letters*, Vol. 8, pp. 467–473, May 1987.
- [8] A.N. Andry, E.Y. Shapiro and J.C. Chung, “Eigenstructure Assignment for Linear Systems,” *IEEE Trans. on Aerospace and Electronic Systems*, Vol. 19, No. 5, pp. 711–729, Sept. 1983.
- [9] L. C. P. da Silva, Y. Wang, V. F. da Costa and W. Xu, “Assessment of generator impact on system power transfer capability using modal participation factors,” *IEE proceedings on Generation, Transmission and Distribution*,” Vol. 149, No. 5, pp. 564–570, Sept. 2002.
- [10] Y. Y. Hsu, C. L. Chen, “Identification of Optimum Location of Stabilizer Applications Using Participation Factors,” *IEE Proceedings on Generation, Transmission and Distribution*,” Vol. 134, pp. 238–44, May 1987.
- [11] I. J. Perez-Arriaga, L. Rouco, F. L. Pagola and J. L. Sancha, “The role of participation factors in reduced order eigenanalysis of large power systems,”

- IEEE International Symposium on Circuits and Systems*, Vol. 927, pp. 923–927, June 1988.
- [12] H. O. Wang, E. H. Abed, and M. A. Hamdan, “Bifurcation, chaos, and crises in voltage collapse of a model power system,” *IEEE transactions on Circuits and Systems- I: Fundamental Theory and Applications*, Vol. 41, No. 4, pp. 294–302, March 1994.
- [13] P. Huang and Y. Hsu, “Eigenstructure assignment in a longitudinal power system via excitation control,” *IEEE transactions on Power Systems*, Vol. 5, No. 1, pp. 96–102, Feb. 1990.
- [14] E. H. Abed and P. P. Varaiya, “Nonlinear oscillations in power systems,” *International J. Electrical Power and Energy Systems*, Vol. 6, No. 1, pp. 37–43, Jan. 1984.
- [15] E. H. Abed, D. Lindsay and W. A. Hashlamoun, “On participation factors for linear systems,” *Automatica*, Vol. 36, No. 10, pp. 1489–1496, Oct. 2000.
- [16] F. Milano, “Power System Analysis Toolbox Documentation for PSAT,” version 1.3.0, 2004 (available online at <http://www.power.uwaterloo.ca/~fmilano/>).
- [17] B. C. Moore, “On the flexibility offered by state feedback in multivariable systems beyond closed loop eigenvalue assignment,” *IEEE Trans. on Automatic*

*Control*, pp. 689–692, Oct. 1976.

- [18] M. A. Hassouneh, H. Yaghoobi and E. H. Abed, “Monitoring and control of bifurcations using probe signals,” in *Dynamics, Bifurcations and Control*, Lecture Notes in Control and Information Sciences, Vol. 273, F. Colonius and L. Gruene, Eds., Berlin: Springer Verlag, pp. 51–65, 2002.
- [19] J. F. Hauer and M. J. Beshir, “Dynamic performance validation in the western power system,” *Association of Power Exchanges*, Kananaskis, Alberta, Oct. 2000.
- [20] C. G. Verghese, I. J. Perez-Arriaga and F. C. Schweppe, “Measuring state variable participation for selective modal analysis,” *IFAC symposium on digital control*, New Delhi, India.
- [21] M.A. Hassouneah, M. S. Saad and E. H. Abed, “Signal-Based Instability Monitoring of Electric Power Systems,” *16th IFAC World Congress*, Prague, Czech Republic, 2005.
- [22] E. H. Abed, M.A. Hassouneah and M. S. Saad, “Instability monitoring and control of power systems,” *Applied Mathematics for Restructured Electric Power Systems*, J. H. Chow, F. F. Wu and J. A. Momoh, Eds., Springer, pp. 159–178, 2005.

- [23] G. P. Liu and R. J. Patton, *Eigenstructure Assignment for Control System Design*. Wiley, New York, 1998.
- [24] C. W. Helstrom, *Probability and Stochastic Processes for Engineers*, Second Edition, Macmillan, 1991.
- [25] T. Kim and E. H. Abed, "Closed-loop monitoring systems for detecting impending instability," *IEEE Trans. Circuits and Systems-I: Fundamental Theory and Applications*, Vol. 47, No. 10, pp. 1479–1493, Oct. 2000.
- [26] N. Martins and L. T. G. Lima, "Determination of suitable locations for power system stabilizers and static VAR compensators for damping electromechanical oscillations in large scale power systems," *IEEE Transactions on Power Systems*, Vol. 5, No. 4, pp. 1455–1469, Nov 1990.
- [27] E. H. Abed, H. O. Wang and R. C. Chen, "Stabilization of period-doubling bifurcations and implications for control of chaos," *Physica D*, Vol. 70, pp. 154–164, Jan 1994.
- [28] C. A. Canizares, S. Corsi and M. Pozzi, "Modeling and implementation of TCR and VSI based FACTS controllers," in Technical Report AT-UCR 99/595, ENEL Ricerca, Milan, Italy, Dec 1999.
- [29] Z. Feng, V. Ajjarapu and D. J. Maratukulam, "A comprehensive approach for

- preventive and corrective control to mitigate voltage collapse,” *IEEE Trans. on Power Systems*, Vol. 15, No. 2, pp. 791–797, May 2000.
- [30] T. Kim, *Noisy Precursors for Nonlinear System Instability with Application to Axial Flow Compressors*. Ph.D. thesis, University of Maryland, College Park, 1997.
- [31] I. Genc, H. Schattler and J. Zaborszky, “Clustering the bulk power system with applications towards hopf bifurcation related oscillatory instability,” *Electric Power Components and Systems*, Vol. 33, No. 2, pp. 181–198, Feb 2005.
- [32] V. M. I. Genc, “Hopf Bifurcation Related Coherent Oscillations in Electric Power Systems with a Clustered Texture,” Ph.D. Dissertation, Washington University, Saint Louis, MO, Dec 2001.
- [33] P. W. Sauer and M. P. Pai, *Power System Dynamics and Stability*, Prentice Hall, New Jersey, 1998.
- [34] G. C. Verghese, I. J. Perez-Arriaga and F. C. Schweppe, “Selective modal analysis with applications to electric power systems, Part II: The dynamic stability problem,” *IEEE Trans. Power Apparatus and Systems*, Vol. 101, No. 9, pp. 3126–3134, Sep. 1982.
- [35] N. Mithulananthan, C.A. Canizares, J. Reeve and G.J. Rogers, “Comparison

- of PSS, SVC, and STATCOM Controllers for Damping Power System Oscillations,” *IEEE Transactions on Power Systems*, Vol. 18, No. 2, pp. 786–792, May 2003.
- [36] H. Ghasemi, C. A. Canizares and A. Moshref, “Oscillatory stability limit prediction using stochastic subspace identification,” *IEEE Transactions on Power Systems*, Vol. 21, No. 2, pp. 736–745, May 2006.
- [37] K. Wiesenfeld, “Noisy precursors of nonlinear instabilities,” *Journal of Statistical Physics*, Vol. 38, No. 5-6, pp. 1071–1097, 1985.
- [38] K. Wiesenfeld, “Virtual Hopf phenomenon: A new precursor of period doubling bifurcations,” *Physical Review A*, Vol. 32, Sep. 1985.
- [39] C. Jeffries and K. Wiesenfeld, “Observation of noisy precursors of dynamical instabilities,” *Physical Review A*, Vol. 31, pp. 1077–1084, 1985.
- [40] H. Yaghoobi and E. H. Abed, “Optimal actuator and sensor placement for modal and stability monitoring,” *Proceedings of the American Control Conference*, pp. 3702–3707, San Diego, CA, June 1999.
- [41] H. Yaghoobi, *Stability Monitoring and Control of Nonlinear Systems Susceptible to Oscillatory Bifurcations*. Ph.D. thesis, University of Maryland, College Park, 2000.

- [42] J. Lu, H. D. Chiang and J. S. Thorp, “Eigenstructure assignment by decentralized feedback control,” *IEEE Transactions on Automatic Control*, Vol. 38, No. 4, pp. 587–594, April 1993.
- [43] J. F. Hauer and J. G. DeSteese, “A Tutorial on Detection and Characterization of Special Behavior in Large Electric Power Systems,” Pacific Northwest National Laboratory Richland, Washington 99352, July 2004.
- [44] C. Canizares, “Voltage stability assessment: Concepts, practices and tools,” Technical Report SP101PSS, Institute for Electrical and Electronic Engineers, 2002.
- [45] A. G. Phadke, “Synchronized phasor measurements in power systems,” *IEEE Computer App. in Power*, Vol. 6, pp. 10–15, April 1993.